The Role and Regulation of Quinol Oxidase in Rhizobium Etli

Zachary Ryan Lunak
Marquette University

THE ROLE AND REGULATION OF QUINOL OXIDASE IN *RHIZOBIUM ETLI*

by

Zachary Lunak, B.S., M.S.

A Dissertation Submitted to the Faculty of the Graduate School,
Marquette University,
in Partial Fulfillment of the Requirements for
the Degree of Doctor of Philosophy

Milwaukee Wisconsin

May 2015

ABSTRACT
THE ROLE AND REGULATION OF QUINOL OXIDASE IN *RHIZOBIUM ETLI*

Zachary Lunak, B.S., M.S.

Marquette University, 2015

Aerobic bacteria typically respire by delivering electrons to oxygen via cytochrome *c* oxidases. In addition, many bacteria can respire by transferring electrons to oxygen via quinol oxidases. Exactly why bacteria contain quinol oxidases when they already have cytochrome *c* oxidases is unclear. In particular, the Cyo quinol oxidase, encoded by *cyoABCD*, is widespread among the dominant bacterial groups but its specific role is unknown. *Rhizobium etli* CFN42 provides an aerobic respiratory model in which Cyo can be directly compared to cytochrome *c* oxidases within the same organism.

Mutants of the terminal oxidases in *R. etli* were constructed and their ability to grow in different physiological conditions was examined. The *cyo* mutant had noticable growth defects in low oxygen, low pH and low iron conditions. Furthermore, the *cyo* gene in the wild type was significantly up-regulated in these conditions. Conversely, in slow-growth conditions, such as stationary growth or growth in certain carbon sources, *cyo* was significantly down-regulated. A respiratory mutant, in which Cyo is the only viable terminal oxidase, had clear phenotypic defects in these conditions due to the regulation of *cyo*. Examination of the 5' promoter region of *cyo* revealed multiple DNA binding sites for the transcription factor, ActR of the ActSR 2-component system. An *actSR* mutant was constructed and had significantly lower levels of *cyo* expression in all physiological conditions tested.

The results suggest Cyo is important for growth and adaptation to low oxygen conditions, low pH, and low iron conditions in *R. etli*. Having an oxidase that enables the bacterium to aerobically respire in these conditions is of great benefit for bacteria, in particular soil bacteria that have to frequently adjust to adverse environmental conditions. Interestingly, each of these conditions would theoretically lead to higher quinol:quinone ratios in the cell. The activity of the transcriptional activator of *cyo*, ActSR, has been linked to the redox state of quinone in other bacteria, where quinone has been shown to inhibit ActSR activity. Altogether, the results indicate that the quinol:quinone ratio in the cell may be an important cue for Cyo utilization and expression.

ACKNOWLEDGEMENTS

Zachary Lunak, B.S., M.S.

I would first like to thank my advisor, Dr. Dale Noel. His enthusiasm towards my work and willingness to develop me as an independent researcher is greatly appreciated. I am grateful to have had him as both a mentor and friend.

I would like to acknowledge my committee: Dr. James Maki, Dr. James Anderson, Dr. Krassimira Hristova, and Dr. Rosemary Stuart for their suggestions and constructive criticisms regarding this research.

Many thanks to the past members of the Noel lab. I would particularily like to thank Dr. Tiezheng Li, for being a good role model as a graduate student and a great companion in the lab.

Without the support of my wife, Jordan, I do not believe I would have been able to complete this work. Her flexibility and understanding during this process is much appreciated. Thank you.

TABLE OF CONTENTS

LIST OF FIGURES

LIST OF TABLES

LIST OF ABBREVIATIONS

Abs	absorbance
ActR	DNA binding protein, response regulator, RegA
ActS	sensor kinase of ActSR 2 component system, RegB
ActSR	2-component regulatory system, RegBA
Amp	ampicillin
BacS	bacteroid specific protein, putative phasin
CFU	colony forming units
Cm	chloramphenicol
Cta	cytochrome *c* oxidase, encoded by *ctaCDGE*
CoxM_P	cytochrome *c* oxidase, encoded by *coxMNOP*
Cyd	quinol oxidase encoded by *cydAB*
Cyo	qucinol oxidase, encoded by *cyoABCD*
Cyt	cytochrome
Fbc	bc1 complex, ubiquinol-cytochrome *c* oxidoreductase
FixN_P	cytochrome *c* oxidase, encoded by *fixNOQP*
Fnr	fumarate and nitrate reductase regulatory protein
Gm	Gentamicin
HCO	heme-copper oxidase
Km	Kanamycin
OD	optical density
NifA	activator of the RpoN sigma factor induced at low oxygen
PCR	polymerase chain reaction
RpoE	Extracellular sigma factor
RpoH	Sigma32 type factor
RpoN	Sigma54 type factor
RT-qPCR	reverse transcriptase quantitative PCR

Sm	streptomycin
Sp	spectinomycin

CHAPTER ONE: INTRODUCTION

Aerobic bacteria are metabolically diverse and many of them can generate energy in a variety of physiological conditions. Presumably an important aspect of their metabolic diversity is their ability to aerobically respire through a variety of quinol oxidases and/or cytochrome *c* oxidases. These terminal oxidases differ in their affinity for oxygen, proton-pumping ability and transcriptional regulation. The question remains whether terminal oxidases are redundant or if they have evolved to have defined physiological roles. Increasing evidence suggests oxidases are preferentially expressed in certain conditions to ensure efficient growth and energy production. Knowing how all oxidases are regulated and their physiological roles can provide an even better understanding of how bacteria adapt to their surrounding environments. Although the Cyo quinol oxidase, encoded by *cyoABCD*, is widespread among the abundant proteobacteria and firmicutes, few studies have been devoted to this enzyme. Much of what is known about this quinol oxidase has been concluded from studies done in *E. coli*, which lacks cytochrome *c* oxidases. The physiological role and regulation of Cyo has yet to be fully investigated in organisms that already contain a variety of cytochrome *c* oxidases. *Rhizobium etli* CFN42 provides an aerobic respiratory model in which Cyo can be investigated in the context of cytochrome *c* oxidases within the same organism.

A. Terminal Oxidases

Terminal oxidases are the enzymes that catalyze oxygen reduction during aerobic respiration. There are two types of terminal oxidases: quinol oxidases and cytochrome *c* oxidases (**Table 1**, **Fig. 1**). Cytochrome *c* oxidases catalyze electron transfer from

cytochrome *c* to oxygen. Prior to this reaction, cytochrome *c* is reduced by quinol through the action of ubiquinol-cytochrome *c* oxidoreductase (Fbc), also known as the bc1 complex. Quinol oxidation is a key branch point in aerobic respiration. Electrons from quinol flow either through the aforementioned Fbc or directly to oxygen via quinol oxidases.

Oxidase	Alternate Names	Encoded Operon	Reported K_m Values	Classification	Substrate
Cyo	Cyt O, BO quinol oxidase	*cyoABCD*	200 nM (D'Mello *et al.*, 1995)	HCO A-type	Quinol
Cyd	Cyt D, BD quinol oxidase	*cydBD*	3-8 nM (D'Mello *et al*., 1996)	bd-type	Quinol
Cta	Cyt *c* oxidase, aa3	*ctaCDGE*	Unknown	HCO A-type	Cyt *c*
FixN_P	Cbb, cbb3	*fixNOQP*	7 nM (Preisig *et al.*, 1996)	HCO C-type	Cyt *c*

Table 1: Common terminal oxidases in aerobic respiration.
Cyt = cytochrome, HCO = Heme-copper oxidase. For the reported K_m values, the reference is in parentheses.

Initial studies of terminal oxidases were focused on determining which oxidases were present in bacteria. Biochemical and genetic tools were used to determine subunit architecture, substrate utilization, expression analysis, heme-content and in some cases oxygen affinity (Poole & Cooke, 2000). From these studies, terminal oxidases are often classified into two different families: heme-copper oxidases (HCO) and bd-type oxidases. Besides containing copper in their metallic centers, HCO's activity results in higher proton translocation thereby producing more energy than bd-type oxidases (Morris & Schmidt, 2013).

Terminal oxidases are typically classified by their apparent Km for oxygen. The bo-type quinol oxidase (Cyo), encoded by *cyoABCD*, and the aa3-type cytochrome *c* oxidase (Cta) are classified as low-affinity "A-type" HCO's utilized at higher oxygen concentrations. Conversely, the cbb3-type cytochrome *c* oxidase (FixN_P), encoded by *fixNOQP* (*ccoNOQP* in some organisms), is classified as a high-affinity "C-type" HCO utilized at lower oxygen conditions. The bd-type quinol oxidase (Cyd), encoded by *cydAB*, is also considered a high-affinity oxidase utilized at lower oxygen conditions (García-Horsman *et al*., 1994; Morris & Schmidt, 2013).

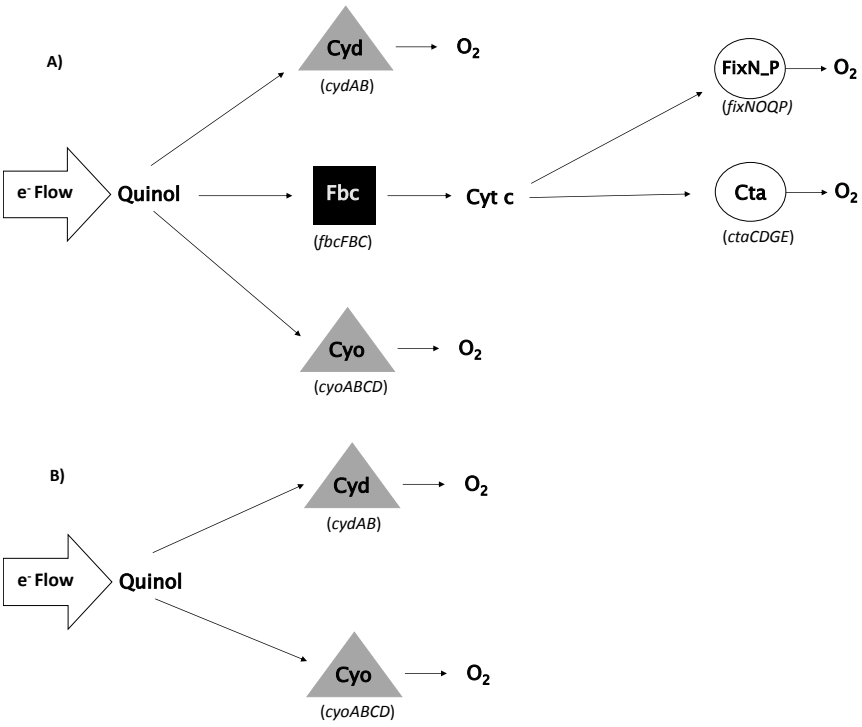

Figure 1: Potential terminal branches of aerobic respiratory chains in bacteria. A). Electrons from quinol to oxygen can be transferred through Fbc (square) leading to a variety of cytochrome *c* oxidases (circles), such as FixN_P and Cta. Independent of the Fbc pathway, bacteria can transfer electrons directly from quinol to oxygen via quinol oxidases (triangles), such as Cyo and Cyd. Genetic operons that encode each of the enzymes are in parentheses. **B)** *E. coli* aerobic respiratory chains.

The HCO's typically have 4 subunits (I-IV). Subunits I and II are essential for catalytic activity. Subunit I contains copper and heme, and is similar between all HCO's (García-Horsman *et al*., 1994). It is responsible for binding and transferring electrons to oxygen (**Fig. 2**). The difference between quinol oxidases and cytochrome *c* oxidases is within subunit II. Subunit II of cytochrome *c* oxidases, such as Cta, contains copper and is responsible for the binding of cytochrome *c*. On the other hand, subunit II of quinol oxidases, such as Cyo, lacks copper and binds quinol instead of cytochrome *c*. Therefore, subunit II is used to differentiate whether an operon encodes a quinol oxidase or cytochrome *c* oxidase based on homology. At this point, the exact biochemical function of subunits III and IV of the oxidases are unknown.

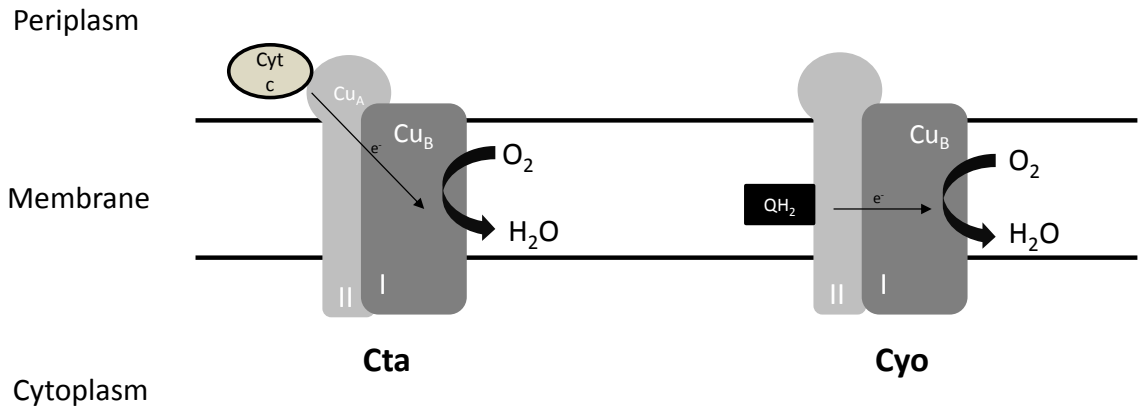

Figure 2: Schematic of subunit architecture and substrates between cytochrome *c* oxidase (Cta) and quinol oxidase (Cyo).

B. Transcriptional regulation of bacterial terminal oxidases

Bacterial genes are often regulated at the level of transcription. In order for bacterial cells to initiate transcription, the RNA polymerase contains a sigma factor that recognizes the promoter sequence in the DNA. The housekeeping sigma70 factor (also known as RpoD or SigA) transcribes most of the genes that are essential in growing cells (Balleza *et al*., 2009). Bacteria also contain additional sigma factors (e.g., RpoE, RpoH, RpoN) that each recognize different DNA promoter sequences to transcribe genes often involved in different environmental stresses, such as heat-shock, osmotic stress and starvation. Most often, additional transcription factors are needed to allow the recognition of the promoter sequence and sigma factor. Transcription factors typically bind to the DNA either promoting the interaction between the promoter sequence and sigma factor (activators) or preventing the interaction between the promoter sequence and sigma factor (repressors).

Because oxygen is a substrate for all terminal oxidases, it is a common cue in how terminal oxidases are regulated (Bueno *et al*., 2012). Some transcription factors, such as Fnr (fumarate and nitrate reductase), sense oxygen directly. Fnr proteins form an active dimer conformation in the absence of oxygen, at which they bind to a consensus DNA binding site (TTGAT-N4-ATCAA) in upstream promoter regions of target genes (Kiley & Beinert, 1999; Körner *et al*., 2003). The high affinity FixN_P oxidase is commonly regulated by Fnr proteins in many organisms to ensure it is up-regulated exclusively at low oxygen (Bueno *et al*., 2012).

Some oxidases are regulated by transcription factors that sense oxygen indirectly based on the redox state of certain molecules. An example is the RegBA two-component system in *Rhodobacter capsulatus*. In this case, RegB is a sensor kinase that autophosphorylates upon activation and transfers the phosphate group to the DNA-binding protein RegA (Elsen *et al*., 2004; Wu & Bauer, 2008). The phosphorylated RegA then binds to downstream gene targets either activating or repressing gene expression.

The initial RegB autophosphorylation activity is greatly influenced by the redox state of quinone (**Fig. 3a**). Although quinone and quinol both bind with RegB with equal affinity, only quinone inhibits the autophosphorylation activity of RegB (Wu & Bauer, 2010). Thus, a higher quinol:quinone ratio in the cell leads to higher RegBA activity. Independently of the binding of quinone/quinol, the redox state of a conserved cysteine (Cys) residue can also influence the autophosphorylation activity of RegB (Wu *et al*., 2013). The oxidation of Cys promotes an inactive conformation of RegB (**Fig. 3b**). Conversely, a protonated Cys residue promotes an active RegB. Whether the oxidized state of Cys or the binding of quinone/quinol has a greater impact on RegB activity in vitro or in vivo has yet to be determined.

The RegBA two-component system is widespread among rhizobia and other α-proteobacteria (ActSR in *Sinrohizobium meliloti*, RegSR in *Bradyrhizobium japonicum*, PrrBA in *Rhodobacter sphaeroides*). These homologous systems appear to have similar function, given that the operons can complement one another between species (Emmerich *et al*., 2000a, Elsen *et al*., 2004; Wu & Bauer, 2008). For many bacteria, it is an important global regulator for both low and high oxygen environments, and adaptation to

acidic conditions (Qian & Tabita, 1996; Tiwari *et al*., 1996; Bauer *et al*., 1998; Torres *et al*., 2014).

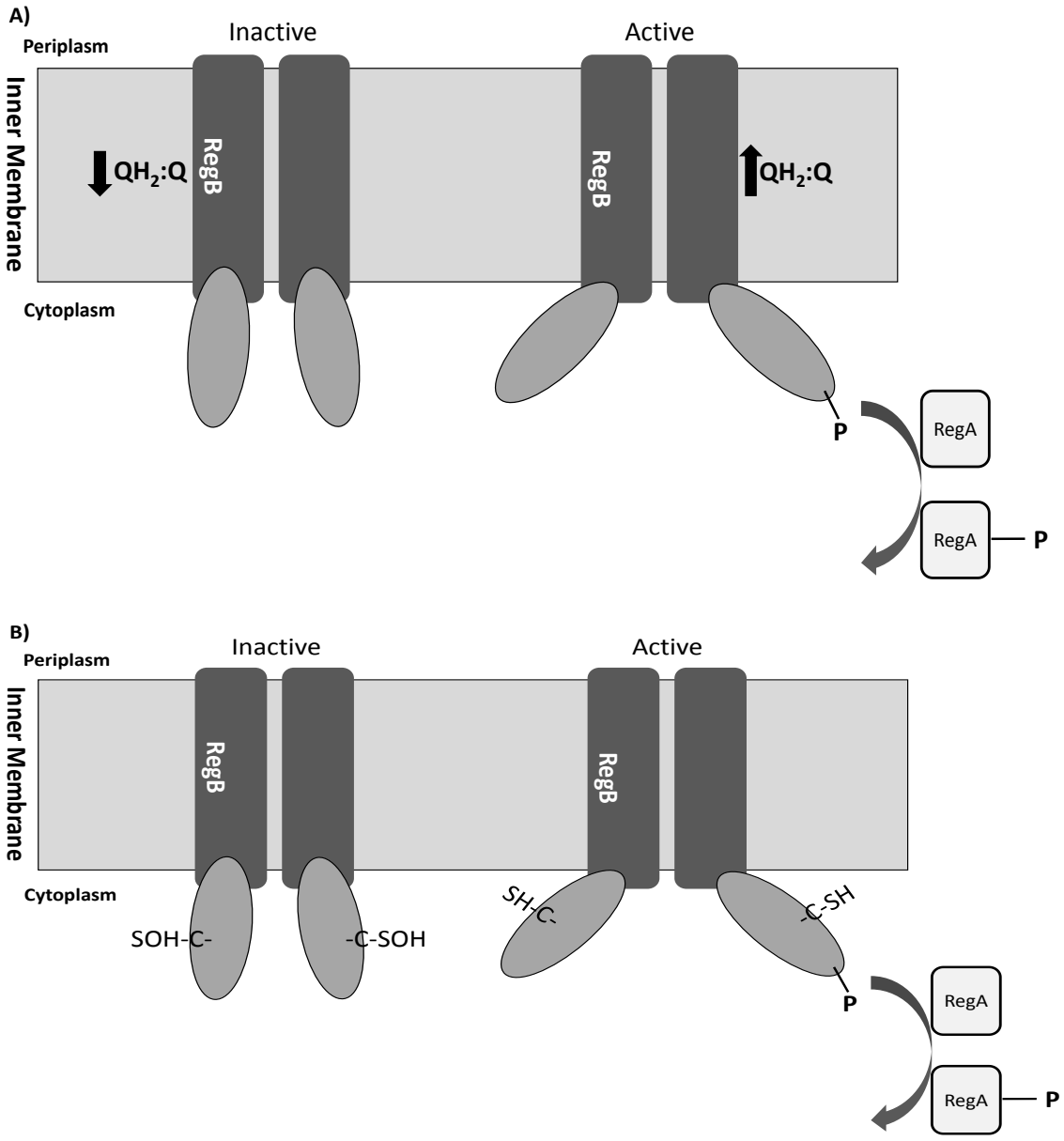

Figure 3: Models for redox sensing by RegBA two-component system in *R. capsulatus*. A) The impact of quinone:quinol (QH_2:Q) on RegB activity. Binding of quinol (QH_2) leads to an active conformation of RegB, whereas binding of quinone (Q) leads to an inactive conformation. **B**) An oxidized Cys residue leads to an inactive conformation whereas the protonated Cys leads to an active conformation.

C. Cyo quinol oxidase

Much research has been devoted to high-affinity oxidases, FixN_P and Cyd, regarding their regulation and functional roles in aerobic physiology. Comparatively, very little is known about the other respiratory oxidases present in bacteria. This has left a large gap in knowledge of how all terminal oxidases are integrated physiologically into aerobic respiration. For instance, the Cta and Cyo oxidases are classified together as low-affinity oxidases utilized at high oxygen concentrations, giving the impression that these oxidases are redundant. Yet these enzymes use different substrates (**Fig. 2**) and the affinity has yet to be reported for Cta. Basic research of these enzymes is needed to completely understand how oxidases are integrated into aerobic physiology.

Cyo is of particular interest because it is widespread among aerobic bacteria, but surprisingly little study has been devoted to its role in the cell. Much of what is known about Cyo physiology has been concluded from studies done in *E. coli*, where Cyo is utilized at higher oxygen concentrations and Cyd is utilized at lower oxygen concentrations (D'Mello *et al.*, 1995; D'Mello *et al*., 1996; Tseng *et al.*, 1996). However, *E.coli* doesn't contain an Fbc or cytochrome *c* oxidases (**Fig. 1b**). Therefore, the regulation and utilization of Cyo may be much different in bacteria that contain a functional Fbc pathway (**Fig. 1a**).

Rhizobium etli CFN42, like all rhizobia, contain both quinol oxidases and cytochrome *c* oxidases (Delgado *et al*., 1998). This enables a direct comparison between quinol oxidases and cytochrome *c* oxidases, for instance Cta and Cyo, within the same

organism. Much of what is known about aerobic respiration in *R. etli* is limited to the necessary components involved in the symbiosis with the legume, *Phaseolus vulgaris*. The development of symbiosis requires bacterial infection of the roots via infection threads, during which legumes form a nodule. The bacteria then proliferate within plant cells and began fixing nitrogen allowing for vigorous plant growth. This developmental process requires the bacteria to grow while adjusting to lowering oxygen levels. Oxygen concentrations may be as high as 250 µM in the free soil, whereas in the infected plant cells the oxygen concentration is below 50 nM (Poole & Cooke, 2000).

D. Possible roles for Cyo

Although the regulation of Cyo has been studied very little, there are a few observations in the literature leading to possible insights into Cyo's function in the presence of cytochrome *c* oxidases. As opposed to *E. coli*, studies in different rhizobial species have indicated Cyo to be important for growth or transcriptionally upregulated in microaerobic conditions in culture. In *S. meliloti*, using a DNA microarray and transcriptional fusion respectively, it was shown *cyo* is transcriptionally up-regulated (2-4 fold) at lower oxygen concentrations (1-2%) (Trzebiatowski *et al*., 2001; Bobik *et al*., 2006). In *B. japonicum*, a mutation in Cyo's homologue (*coxWXYZ*) had a growth defect at low oxygen conditions in chemolithotrophic conditions (Surpin and Maier, 1998). In addition, a *cyo* mutant in *R. etli* had a growth defect when streaked on plates in low oxygen (Landeta *et al*., 2011).

Other physiological cues, independent of oxygen, reportedly also have an impact on *cyo* expression in *Pseudomonas* species. During stationary-phase in aerobic

conditions, *cyo* expression levels are lower compared to exponential phase in both *P. putida* and *P. aeruginosa* (Morales *et al*., 2006; Kawakami *et al*., 2010). On the other hand, the expression of *cyo* is upregulated in *P. aeruginosa* under iron-depleted conditions (Kawakami *et al*., 2010). Given that the Fbc pathway contains more proteins that functionally require iron (Fbc and cytochrome c) compared to the Cyo respiratory pathway, it has been suggested that Cyo is a preferred respiratory option in low-iron conditions (Arai, 2011).

Although these observations have provided insights into the physiological role for Cyo, the findings are fragmented between studies of different organisms. A more complete picture of how Cyo is integrated into aerobic physiology is needed. For instance, whether Cyo is necessary and how *cyo* is transcriptionally regulated in the aforementioned physiological conditions is unknown at this point.

E. Aims

The goal of this dissertation was to provide a foundation for understanding the physiological role of Cyo in bacteria that already contained cytochrome *c* oxidases. *Rhizobium etli* CFN42 was used as a model organism; it contains a combination of both terminal oxidase types. Using genetic and molecular tools, the following aims were designed to provide a framework for how Cyo is integrated into aerobic physiology:

Chapter 2: To determine the oxygen concentrations in which Cyo is utilized.

Chapter 3: To determine the major transcription factor involved in regulating *cyo*.

Chapter 4: To determine the impact of growth on Cyo utilization and expression.

CHAPTER TWO: THE O_2 CONCENTRATION IN WHICH CYO IS UTILIZED

A. Introduction

Bacteria have remarkable adaptability to environmental changes, such as fluctuations in oxygen concentration. Presumably, an important aspect of coping with variation in oxygen concentration is that aerobic bacteria have a variety of cytochrome and quinol oxidases (**Table 1**, **Fig. 1a)**. Because oxygen is a substrate for these terminal oxidases, oxygen is expected to be a major factor in how each of these oxidases are regulated and utilized within bacteria. In this work, *Rhizobium etli* CFN42 was used as a model organism. Like other rhizobia, *R. etli* contains both terminal oxidase types. This enables the ability to compare quinol oxidases and cytochrome *c* oxidases within the same organism.

Much of what is known about aerobic respiration in *R. etli* is limited to the necessary components for nitrogen fixation during the symbiosis with the legume, *Phaseolus vulgaris*. The development of symbiosis requires bacterial infection of the roots via infection threads, during which legumes form a nodule. The bacteria then proliferate within plant cells and begin fixing nitrogen allowing for vigorous plant growth. This developmental process requires the bacteria to grow while adjusting to lowering oxygen levels. Oxygen concentrations may be as high as 250 μM in the free soil, whereas in the infected plant cells the oxygen concentration is below 50 nM (Poole & Cooke, 2000). It has been well established that the high-affinity FixN_P oxidase is necessary for nitrogen fixation (Delgado *et al.*, 1998). How the other oxidases in *R. etli*, such as Cyo, are utilized and regulated in *R. etli* CFN42 is unclear. Mutants, with altered levels of Cyo, have been isolated and examined in the symbiosis (Soberón *et al.*, 1989;

Soberón *et al.*, 1990). However, to our knowledge these mutations are either not in the *cyo* genes, or they have not been genetically defined.

In this chapter, the oxygen conditions in which Cyo was utilized in liquid culture were determined. As a start, the ability of a *cyo* mutant to grow at various oxygen concentrations in comparison to other oxidase mutants was analyzed. Next, the activity of *cyo* promoter was measured at various oxygen conditions. Lastly, the impact of *cyo* mutation on symbiosis with *P. vulgaris* was examined.

B. The predicted aerobic respiratory branches of *R. etli* CFN42

The genome nucleotide sequence of *R. etli* CFN42 has been determined (Gonzalez *et al*., 2006). With BLAST (Altschul *et al*., 1990) searches, the terminal oxidases encoded by the genome of this strain were determined (**Fig. 4**). The only quinol oxidase revealed in this way was a potential Cyo quinol oxidase, encoded by contiguous *cyoABCD* genes. On the other hand, the *R. etli* CFN42 genome revealed sequences for several cytochrome *c* oxidases: FixN_P (two copies), Cta, and an alternative aa3-oxidase (CoxM_P), encoded by *coxMNOP*. Two additional operons that encode putative cytochrome *c* oxidases were also revealed in the genome, RHE_CH00981-85 and RHE_PB00063-66. Based on these oxidases present in the genome, the aerobic respiratory chains in *R. etli* CFN42 were predicted (**Fig. 5**).

C. Sequence-directed oxidase mutant construction

To gain insight into the physiological function of the oxidases, strains were constructed with mutations in the essential subunits I and/or II of the oxidases using antibiotic-resistance cassettes. The *fixN_P* mutant, strain CFNx641, was one previously constructed by Girard *et al*. (2000). In this strain both *fixNOQP* operons have been mutated. An *fbc* mutant, previously isolated in the lab, was also studied. This mutant carries a Tn5 in the iron-sulfur cluster gene, *fbcF* (Rosado and Noel, unpublished). Despite repeated attempts, a double mutant (*fbc/cyo*) was not attained. Specific mutations in RHE_CH00981-85 and RHE_PB00063-66 putative cytochrome *c* oxidases were not constructed.

D. Quinol Oxidase activity of the wild type and mutants

To confirm that the *cyo* genes encoded active proteins and that Cyo was the only quinol oxidase present under aerobic conditions in *R. etli* CFN42, the quinol oxidase activity was measured in the wild type (CE3), *fbc* (CE119), and *cyo* (CE574) mutants during exponential growth (**Fig. 6**). Quinol oxidase activity was undetectable in the Cyo^- mutant, supporting the notion that Cyo is the only quinol oxidase present under these conditions. Addition of the wild-type *cyoA* gene, pZL34 (pFAJ1708:*cyoA*), restored activity similar to that of wild-type. The *fbc* mutant had increased quinol oxidase activity compared to the wild type.

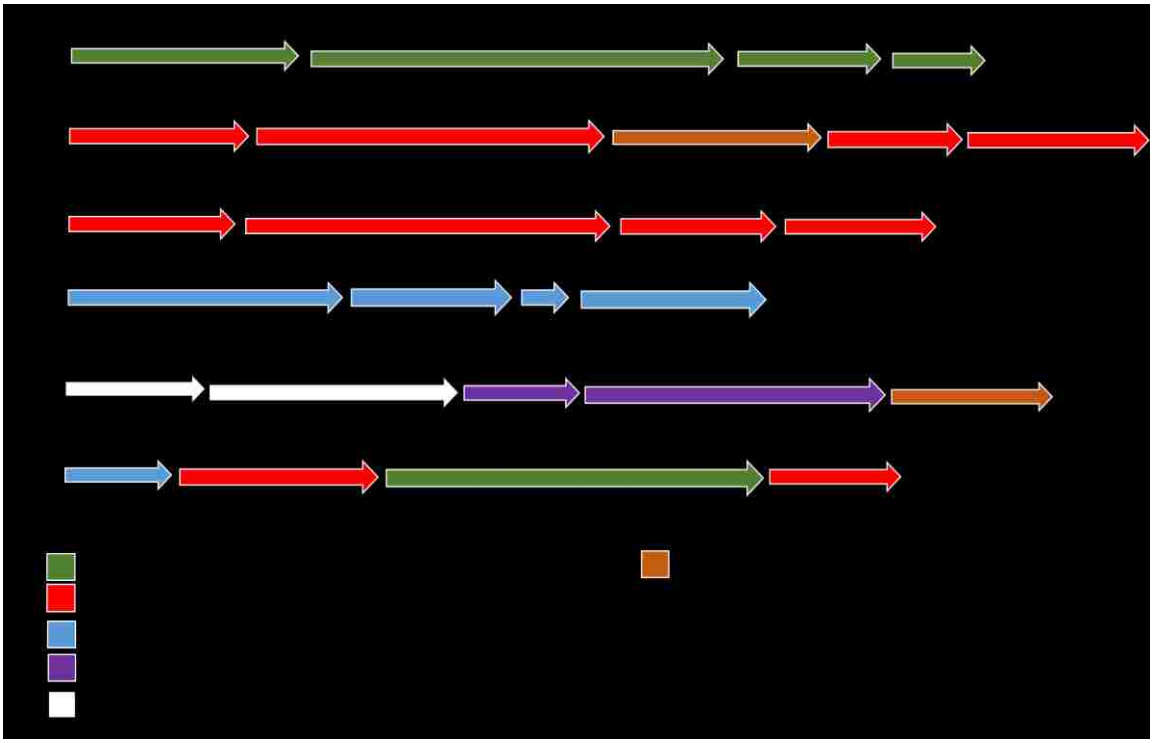

Figure 4: Putative oxidase operons in *R. etli* CFN42. The genes are color-coded to indicate which heme-type cytochrome *c* oxidase or quinol oxidase they appear to encode. In parentheses is the putative subunit of the oxidase in which the gene encodes (I, II, III, or IV). **(A)** *cyoABCD* operon, located on plasmid E, encoding a bo-type quinol oxidase. **(B)** *ctaCDGE* operon, located on the chromosome, encoding an aa3-type cytochrome *c* oxidase. *cta*B encodes a protoheme farnesyl transferase. Subunit IV is not encoded in this operon. There is a putative gene for aa3-type subunit IV located on the chromosome (RHE_CH03614). **(C)** *coxMNOP* operon encoding an aa3-type cytochrome *c* oxidase located on the chromosome. **(D)** *fixNOQP* operon encoding a bb3-type cytochrome *c* oxidase located on both plasmid F and plasmid D. **(E)** RHE_CH00985-81 operon, located on the chromosome, seemingly encoding a ba3-type cytochrome *c* oxidase. Closest matches to CH00985-984 appear to encode cytochrome *c* oxidase proteins that are not specifically associated with certain heme-types. CH00981 sequence suggests it encodes a cytochrome *c* protein. **(F)** RHE_PB00063-66, located on plasmid B, may encode an oxidase that contains a variety of heme-type subunits. Sequence suggests that this putative oxidase contains a quinol-oxidase encoding subunit I, whereas its subunit II seemingly encodes a cytochrome *c* oxidase subunit II. In either quinol or cytochrome *c* oxidases, subunit I contains copper and is responsible for the binding and delivering electrons to oxygen. Therefore, subunit II is used to differentiate between quinol oxidases and cytochrome *c* oxidases (García-Horsman, *et al*., 1994). In cytochrome *c* oxidases, subunit II contains copper and is responsible for the binding and receiving electrons from cytochrome *c*. In quinol oxidases, subunit II lacks copper and is responsible for binding and receiving electrons from ubiquinol. Therefore, we attribute RHE_PB00063-66 sequence to a potential cytochrome *c* oxidase.

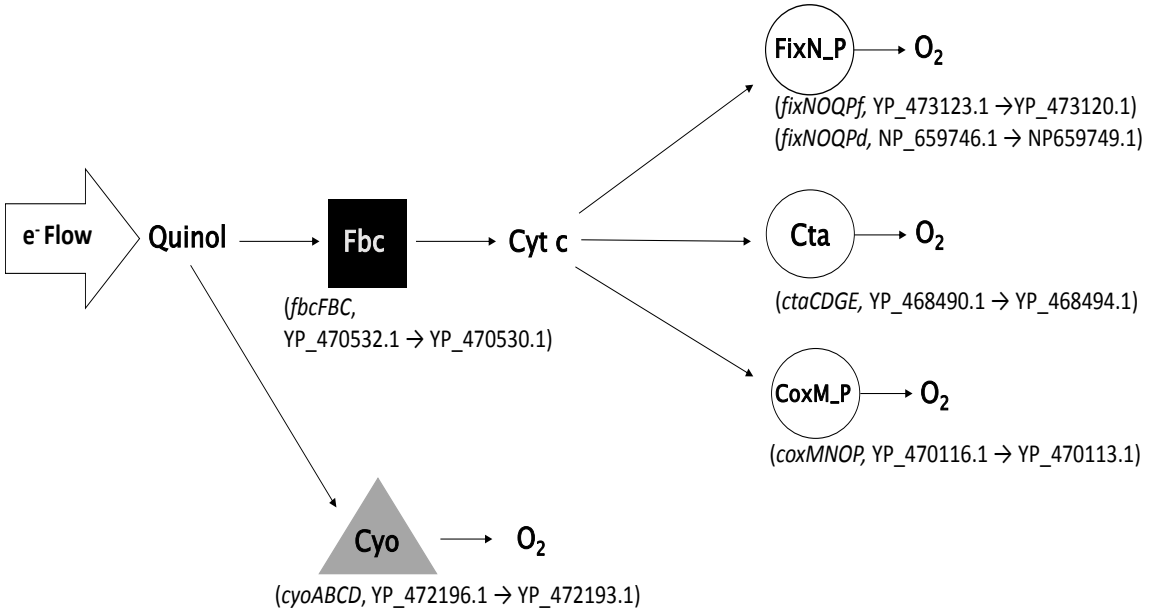

Figure 5: The predicted aerobic respiratory chains of *R. etli* CFN42. Electrons from quinol to oxygen can be transferred through Fbc (square) ultimately leading to cytochrome *c* oxidases (circles): FixN_P, Cta, and CoxM_P. Independent of the Fbc pathway, *R. etli* can transfer electrons directly from quinol to oxygen via Cyo (triangle). In parentheses, below each of the oxidases and Fbc complex, are the indicated operons that encode each of the oxidases followed by their NCBI reference numbers of the encoded proteins. Not included in the diagram are two putative cytochrome *c* oxidases, RHE_CH00981-85 and RHE_PB00063-66.

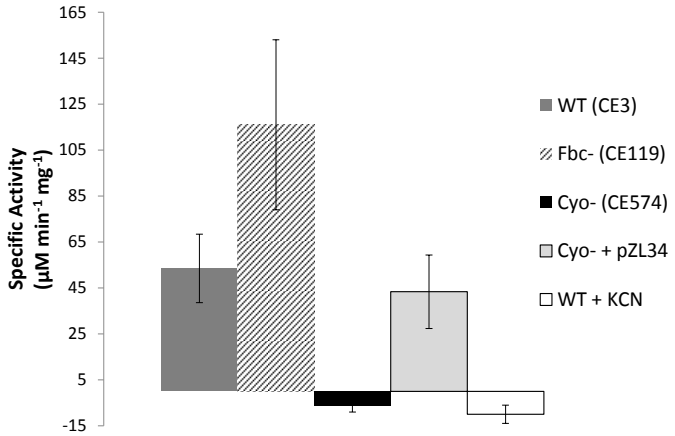

Figure 6: Quinol oxidase activities of solubilized membranes. Strains were grown in aerobic conditions in 250 ml of TY media in 500 ml Erlenmeyer flasks, and solubilized membranes were prepared as described in Methods. The addition of KCN depleted the activity in all strains. Reaction mixtures with no substrate (quinol) and no membranes were used as separate negative controls (data not shown) that gave no apparent quinol oxidase activity. Mean values and standard deviations (error bars) were calculated from measured activities from three separate experiments and cultures.

E. Growth at varying oxygen concentrations

To determine the growth of mutants at low oxygen, the headspace in sealed batch cultures was adjusted to 1% or 0.1% oxygen. To ensure low oxygen conditions had been met, a bacteroid specific protein, BacS (Jahn *et al.*, 2003), was used as a physiological biomarker. BacS is a protein that is regulated by NifA, and is expressed only at low oxygen conditions. As the oxygen concentration was lowered, the amount of BacS increased (**Fig. 7a**). In general, growth was monitored by measuring the O.D. of the cultures. However, to assess whether O.D. was a valid indicator of growth, c.f.u. was measured in some cases as well. It was determined at low oxygen (0.1%) that an increase of O.D. corresponded with an increase in c.f.u. (**Fig. 7b**).

As expected, the growth of the high-affinity *fixN_P* mutant was deficient in low oxygen conditions (**Fig. 8a,b**). The *fbc* mutant was defective similarly to the *fixN_P* mutant in low oxygen conditions. Unexpectedly, the *cyo* mutant was the strain that had the longest lag phase compared to the wild type and other respiratory mutants in both 1% and 0.1% conditions (**Fig. 8a,b**). This effect was alleviated after transferring the wild-type copy of *cyoA* into the *cyo* mutant background (**Fig. 8d**). Furthermore, a *cyo/fixN_P* mutant (CE583) was unable to grow in the 0.1% condition, whereas the single *cyo* or *fixN_P* mutant recovered to grow after a delay (**Fig. 8a**). The *fbc* mutant, presumably completely dependent on Cyo activity, not only suffered less delay but sustained its growth at 0.1% comparably to the *cyo* mutant, which could use FixN_P. The *cta* (CE598) and *coxM_P* (CE582) mutants displayed growth similar to the wild type at low oxygen conditions (data not shown).

In fully aerobic conditions, the *cta* mutant reproducibly had a slight growth defect (**Fig. 8c**). The *fbc* mutant had a similar growth defect compared to the *cta* mutant at high oxygen conditions.

A)

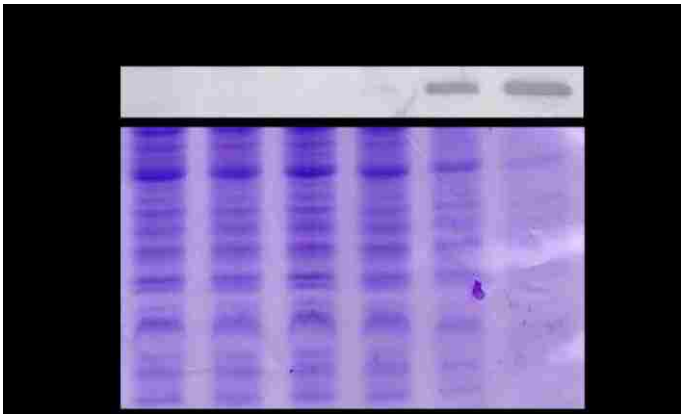

B)

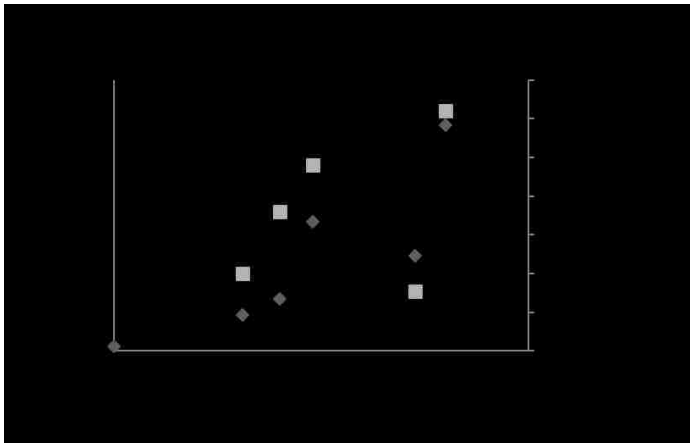

Figure 7: Validating growth at low oxygen. A) Use of BacS to indicate when decreased headspace oxygen concentrations caused a known cellular response to low oxygen. Strain CE3 cells were harvested after full growth under various oxygen conditions (21% to 0.1%). Cell pellets were extracted at 100°C in SDS gel-loading buffer and subjected to SDS-gel electrophoresis in 15% polyacrylamide. The lower panel shows protein staining of gel lanes loaded with cells grown at the respective oxygen conditions. The arrow indicates where BacS (15 kD) would run on the SDS-PAGE, although it was undetectable by the Coomasie staining in all lanes. The upper panel is the corresponding western blot incubated with polyclonal antiserum raised against BacS protein. **B)** The O.D. and corresponding c.f.u./ml of a wild-type culture grown at low oxygen (0.1%).

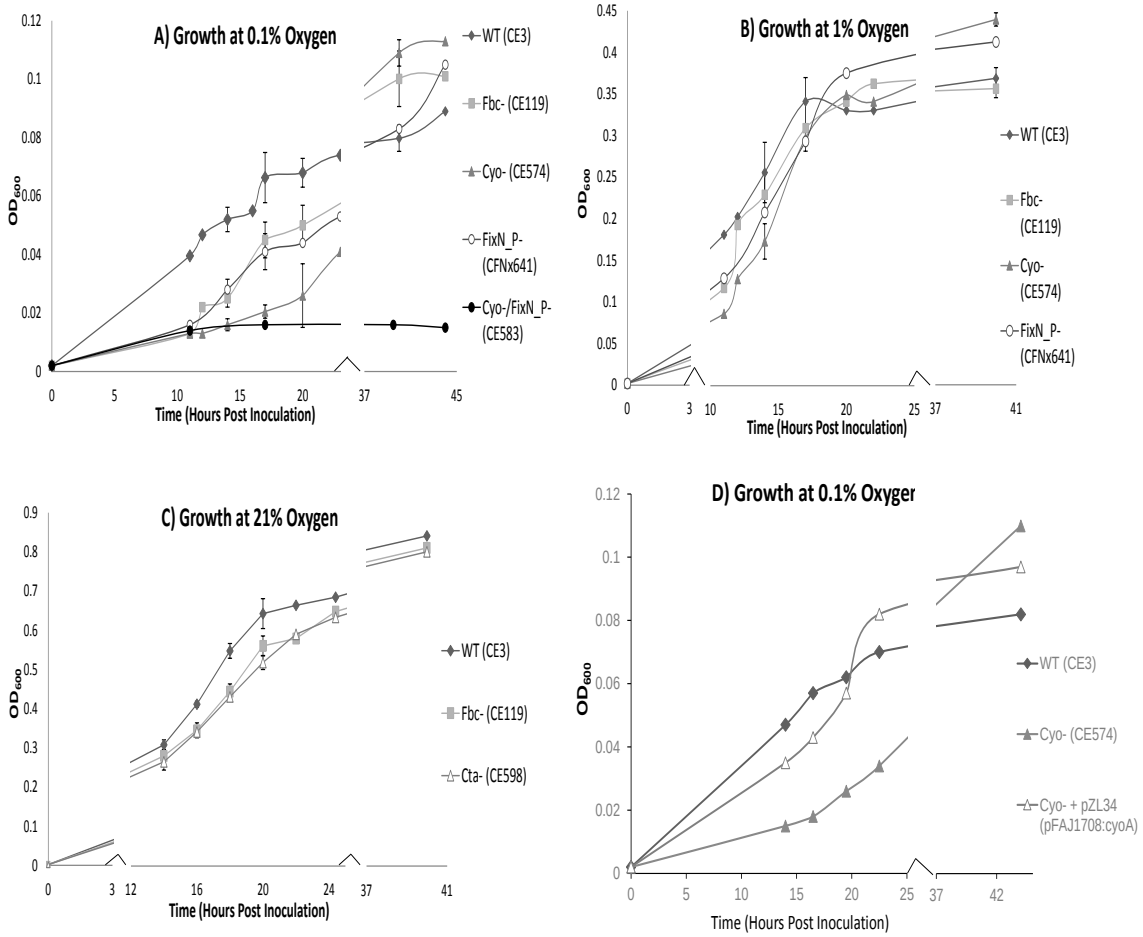

Figure 8: Growth Curves at 0.1% oxygen (A), 1.0% oxygen (B) and 21% oxygen (C). Strains were initially grown in TY liquid under a gas phase with 21% oxygen. At full growth they were sub-cultured 1:200 into 5 ml of TY liquid in 60 ml serum vials. As described in Methods, nitrogen and air were added to the headspaces in the vials above the liquid to give the indicated concentrations of oxygen. Growth was followed by measuring the optical density (OD) at 600 nm. Error bars indicate standard deviation from at least three separate experiments. **(D)** Complementation of *cyo* mutant at low oxygen (0.1%).

F. *cyo* expression at various oxygen concentrations

A transcriptional fusion containing the promoter region of *cyo* and the *lacZ* reporter (P*cyo:lacZ*) was used to analyze *cyo* expression at various oxygen concentrations ranging from 0.1% to 21% oxygen in the wild type (**Fig. 9a**). Expression of *cyo* gradually increased as oxygen was lowered, peaking at 1-2.5% oxygen. The beta-galactosidase activity was approximately 2.5-fold higher from cells grown at 1% oxygen compared to 21% oxygen conditions. As oxygen concentration was further lowered to 0.1%, the expression decreased even though analysis of mutant growth had shown a more obvious importance of Cyo at 0.1% oxygen. *cyo* expression at 1% and 21% was investigated more closely using RT-qPCR, which showed *cyo* to be up-regulated approximately 5-fold at 1% oxygen compared to fully aerobic conditions. Depicted in **Fig. 9b** is data from one of the RT-qPCR experiments performed. Furthermore, the quinol oxidase activity in the wild type was greatly increased at 1% compared to 21% oxygen (**Fig. 9c**).

G. Impact of *cyo* mutant on development of symbiosis

To analyze the symbiotic role of Cyo, nodules harboring the wild type were compared to nodules harboring the *cyo* mutant. Although *cyo* and wild-type nodules displayed nitrogenase activity the same day (8 days post inoculation, DPI), nodules harboring the *cyo* mutant had significantly less activity compared to the wild type (**Fig. 10a**).

As a more direct measure of infection, the bacterial content inside nodules was examined by tagging the bacteria with the *gus* gene (**Fig. 10b**), assuming that the

intensity of GUS staining was proportional to the bacterial content inside the nodule. The GUS activities of the studied *gus*-tagged strains were equivalent in cells grown in TY liquid at various oxygen conditions (**Fig. 10c**). At early DPI (6-7) the staining of nodules harboring the *gus*-tagged wild type (CE426) was more intense compared to the nodules harboring the *gus*-tagged *cyo* mutant (CE607). By 8 DPI, the *cyo* nodules had comparable staining to the wild type.

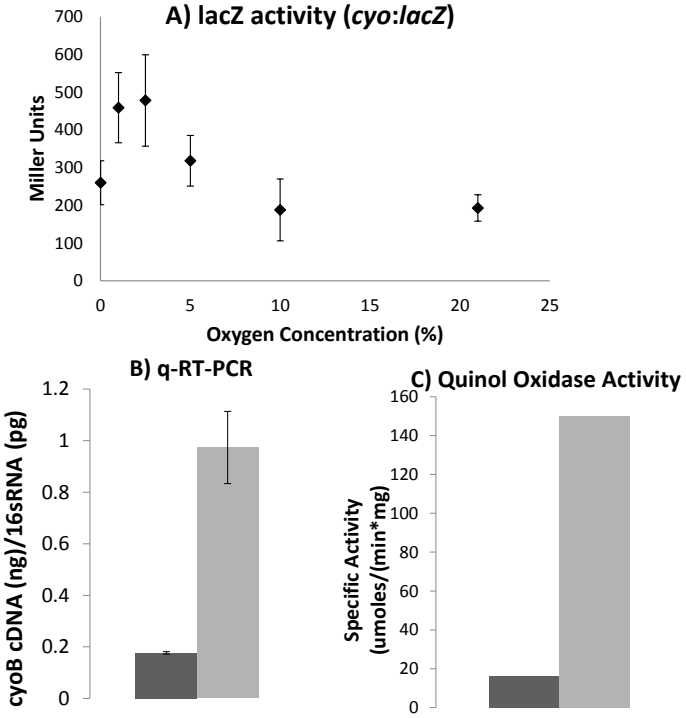

Figure 9: Cyo expression at varying oxygen concentrations. Protein, RNA, and membranes were all extracted from cells in exponential phase. **A)** Beta-galactosidase activity of wild type cells carrying the transcriptional fusion plasmid, pZL39 (*cyoA:lacZ*). Mean values and standard deviations (error bars) were calculated from three or more separate lacZ assays from two different cultures. **B)** RT-qPCR of *cyoB*. RNA was extracted and converted into cDNA using the reverse gene-specific primer. cDNA was then quantified by qPCR. The amount of *cyoB* cDNA (ng) was then normalized to the amount of *16sRNA* cDNA (pg) from the original RNA sample. Means and standard deviations (error bars) were calculated from three separate qPCR assays. C) Specific quinol oxidase activity of wild type solubilized membranes. Wild type cells were grown in 6 separate 120 ml serum vials containing 10 ml of TY media. These cultures were pooled together and the membranes were prepared and solubilized as described in Methods. Note: In these experiments, growth was in serum vials not in Erlenmeyer flasks as described in Fig. 6.

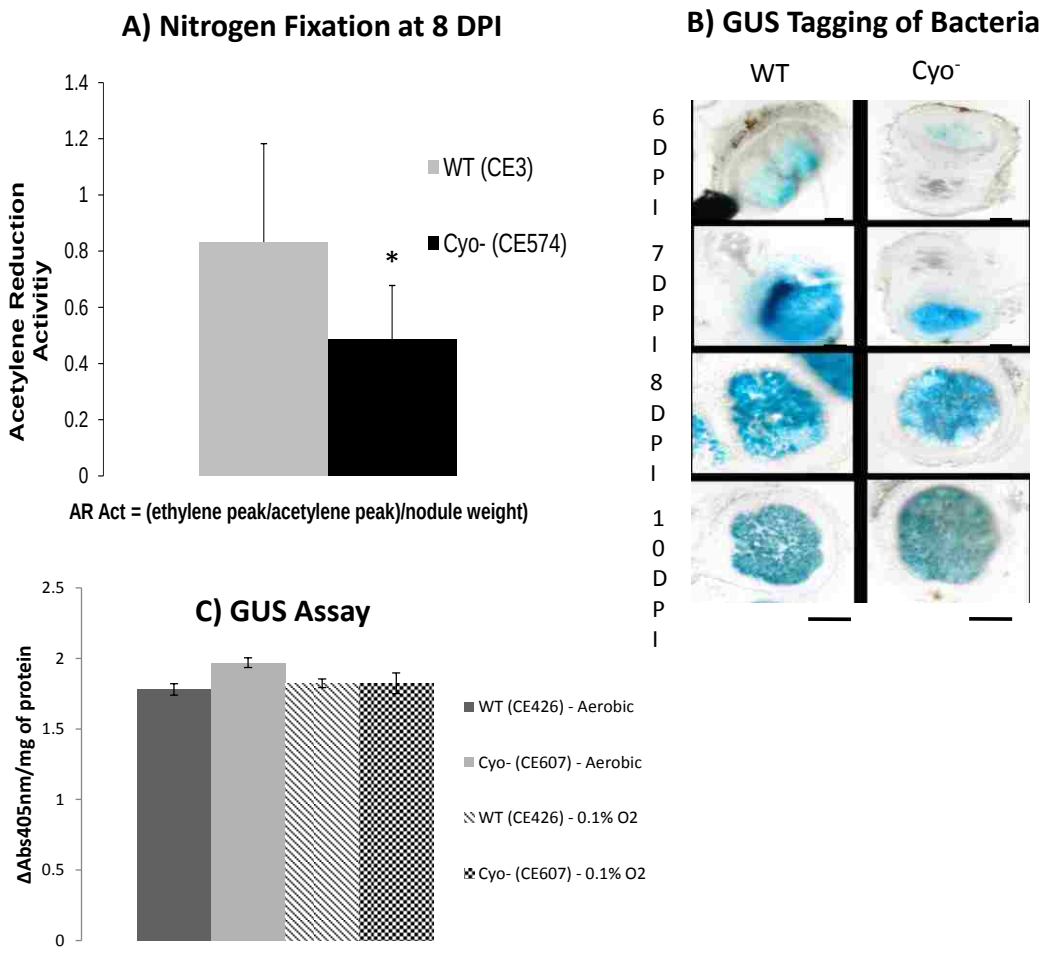

Figure 10: Impact of *cyo* mutant on early development of symbiosis, A) The nitrogenase activity of intact nodulated roots whose nodules harbored wild type or Cyo⁻ at 8 days post inoculation (DPI). Error bars indicate standard deviations (N=8, P<0.05). **B)** Gus-staining of nodules harboring *gus*-tagged wild type (CE426) and *gus*-tagged Cyo⁻ mutants (CE607) at different DPI. The *gusA* gene was constitutively expressed at equivalent levels (in TY culture) in both strains at low (0.1%) and high (21%) oxygen conditions. Therefore, staining reflects the relative density of bacterial cells. The scale bar in the lower right corner in each picture represents 500 µm. **C)** Gus activity of cells that carry the constitutive *gus* gene after low oxygen (0.1%) or aerobic (21%) growth. The activity (ΔAbs_{405}) was normalized to protein concentration (measured by the BCA assay, Thermo Scientific).

H. Impact of respiratory mutants in later stages of symbiosis

Beyond 9 DPI, the *cyo* mutant formed mature red nodules and displayed nitrogenase activity similar to that of the wild type (**Fig. 11a,b**). As seen previously in the lab and other studies, nodules harboring the *fbc* mutant formed bright green nodules and the nitrogenase activity was undetectable (Thöny-Meyer *et al.,* 1989; Wu *et al*., 1996). The *fixN_P* mutant formed darker green nodules and consistently had approximately 8% wild-type nitrogenase levels. The single *cta* and *coxM_P* mutants had no obvious symbiotic defects. However, the *cta*/*fixN_P* double mutant formed bright green nodules and nitrogenase activity was undetectable similar to the *fbc* mutant.

I. Discussion

In this chapter we sought to determine the oxygen conditions in which Cyo is utilized in an Fbc-containing organism such as *R. etli* CFN42. This strain is specifically useful for studying Cyo, as inspection of the genome indicated that Cyo is the only terminal oxidase independent of the Fbc pathway. The inability to obtain a double *cyo*/*fbc* mutant in aerobic conditions supports this notion. In addition, quinol oxidase activity was undetectable in the *cyo* mutant under aerobic conditions. On the other hand, the quinol oxidase activity was increased in an *fbc* mutant, as might be predicted, given that Cyo is the only viable respiratory option in this case. These results indicate the quinol oxidase assay is specific for Cyo in *R. etli* CFN42, and presumably enables measuring the activity of Cyo directly in different physiological conditions. However, it is still possible that a cryptic quinol oxidase might be induced under conditions not yet studied.

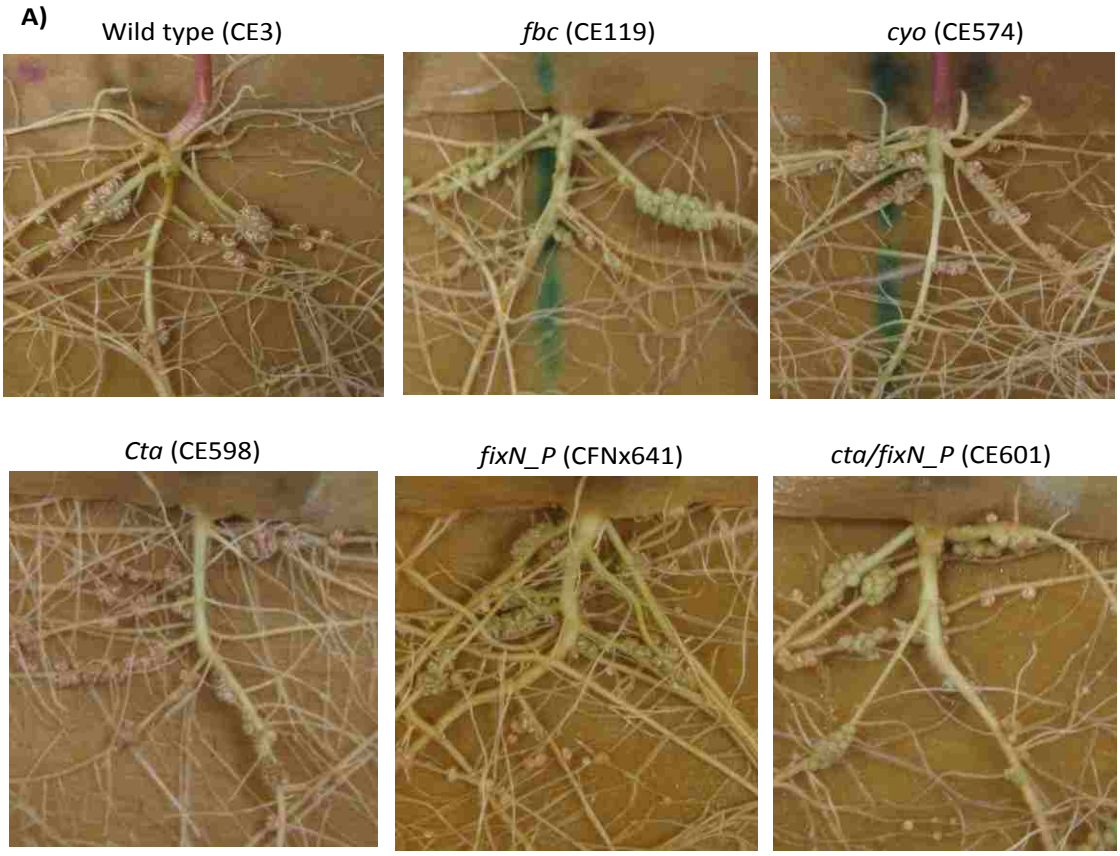

B)

	Wild Type	Δfbc (CE119)	Δcyo (CE574)	ΔfixN_P(CFNx641)	Δcta (CE598)	Δcta/fixN_P (CE601)
Avg AR Activity	1.47	N.D.	1.58	0.0875	1.45	N.D.

Figure 11: Impact of respiratory mutants on mature nodules. A) Pictures of nodules at 20 D.P.I. The strain that the nodules are harboring is indicated above the picture. **B)** The nitrogenase activity of intact nodulated roots whose nodules harbored the indicated strains between 16-20 D.P.I. AR activity was measured by calculating the area of the ethylene peak/acetylene peak from the GC graph. The ratio was then normalized to the nodule weight.

As a start to understanding the oxygen condition in which Cyo is utilized, we analyzed the ability of the *cyo* mutant to grow at low oxygen in comparison to the wild type and other oxidase mutants. Because the inoculant is from an aerobic culture, the results can be interpreted as the bacterium's ability to adapt to a sudden decrease in oxygen concentration. Surprisingly, the *cyo* mutant had the greatest growth defect at low oxygen conditions but no growth defect at high oxygen, even though Cyo is classified as a low-affinity oxidase. This result is supported by a previously reported observation in *R. etli* CFN42 that *cyo* mutants were slow to grow on minimal medium plates in microaerobic conditions compared to the wild type (Landeta *et al*., 2011). In addition, the *fbc* mutant was able to reach a similar ending O.D. as rapidly as the *cyo* at 0.1% oxygen. Interestingly, both *fbc* and *cyo* mutants reproducibly reached an O.D. higher than that of the wild type. The basis for this observation is unknown. These growth results, along with the up-regulation of *cyo* in the wild type, indicate Cyo is utilized and important for adapting to and sustaining growth at low oxygen.

As predicted, the high affinity *fixN_P* mutant had a growth defect at low oxygen and the low-affinity *cta* mutant had a growth defect at high oxygen. The *fbc* mutant had similar growth defects to the *fixN_P* mutant at low oxygen and had similar growth defects to the *cta* mutant in fully aerobic conditions. This is consistent with the literature in that the Fbc pathway terminates with the aa3 oxidase in aerobic conditions and the cbb3 oxidase in microaerobic conditions (Preisig *et al*., 1996; Bott *et al*., 1990). The *coxM_P* mutant did not have a distinct observable growth defect in any of the conditions tested. The two other putative cytochrome *c* oxidases (RHE_CH00981-85 and RHE_PB00063-66) were not specifically addressed in this work.

A potential reason for observing such gross phenotypes associated with Cyo is the fact that *R. etli* CFN42 does not contain the high-affinity Cyd quinol oxidase. However, studies in other rhizobial species have revealed that Cyo may be utilized at lower oxygen conditions regardless of the presence of Cyd. Two separate studies in *Sinorhizobium meliloti,* using a DNA microarray and transcriptional fusion respectively, indicated *cyo* is transcriptionally up-regulated (2-4 fold) at lower oxygen concentrations (1-2%) (Trzebiatowski *et al*., 2001; Bobik *et al*., 2006). In *Bradyrhizobium japonicum*, based on cyanide inhibitor titration patterns of cell membranes, Cyo's homologue (*coxWXYZ*) is predicted to be expressed in microaerobic conditions (1% O_2) (Surpin *et al*., 1996). In addition, a mutation in *coxWXYZ* had a growth defect at low oxygen conditions in chemolithotrophic conditions (Surpin and Maier, 1998). To our knowledge these organisms contain a Cyd quinol oxidase based on BLAST searches. It has yet to be ruled out if absence of Cyd has had an impact on the manner Cyo is utilized and expressed in *R. etli* CFN42. Nevertheless, our results indicate the Cyo and Cta oxidases have distinct physiological roles in regard to oxygen. Based on our growth studies, Cyo allows more capability to respire at lower oxygen concentrations in comparison to the Cta oxidase. Furthermore, it appears that Cyo is capable of functioning in batch culture at 0.1% oxygen as effectively as the FixN_P oxidase.

The symbiotic process from infection to bacteroid differentiation requires *R. etli* to adapt and eventually to respire at very low oxygen concentrations. Based on the results from growth in liquid cultures, it was hypothesized Cyo may have a role during infection, because it is required for the bacterium to grow while adapting to lower levels of oxygen. The onset of nitrogen fixation was initially tested, as it was assumed the more

efficiently the bacterium infected, the faster they would differentiate into bacteroids and fix nitrogen. Although wild-type nodules and *cyo* nodules started to fix nitrogen at the same time, the wild type nodules had significantly more nitrogenase activity compared to the *cyo* nodules at the earliest time investigated. A similar result was reported in *Bradyrhizobium japonicum*, where a mutant defective in Cyo's homologue (*coxWXYZ*) had approximately a 30% decrease in nitrogenase activity (Surpin and Maier, 1999). However, in the present study there was no significant difference in nitrogenase activity after 8 DPI. Using *gus*-tagged bacteria, the results show that there is less bacterial content in early developed *cyo* nodules (6-7 DPI). As nodules matured, the staining was similar between the wild type and *cyo* nodules. Taken together, these results indicate Cyo is advantageous during the early stages of symbiosis and that the Fbc-dependent oxidases are not sufficient to provide optimal bacterial growth during the infection phase.

As seen previously in the lab and in other studies, the *fbc* mutant is completely deficient in nitrogenase activity (Thöny-Meyer *et al.*, 1989; Wu *et* al., 1996). This suggests Cyo is not utilized or not sufficient in the later stages of symbiosis. Assuming that nitrogenase activity is an indicator of aerobic respiration, our results indicate that the FixN_P oxidase accounts for 95% of the respiratory activity and the Cta oxidase accounts for approximately 5%. Based on the literature, one would suggest that Cyo is unable to respire at the low levels of oxygen present in the nodule. However, our results in culture would suggest Cyo performs comparably to FixN_P at low oxygen. It is possible that other regulatory factors are involved during the symbiosis that are not present in the culture conditions.

J) Summary/Conclusions

We propose Cyo is a versatile oxidase that can function at a broad range of oxygen concentrations based on the growth results of the *fbc* mutant, in which it is assumed Cyo is the only functional oxidase. With only slight deficiency in both instances, the *fbc* mutant was able to grow in both fully aerobic and low oxygen conditions. On the other hand, the Cta and FixN_P seem more specialized with respect to oxygen concentrations at which they support growth. The *cyo/fixN_P* mutant was unable to grow at 0.1% oxygen, indicating Cta is unable to function at this oxygen concentration. In fully aerobic conditions, a *cyo/cta* was unattainable indicating the other cytochrome *c* oxidases are not sufficient for growth in fully aerobic conditions. A recent study in another alpha-proteobacterium, *Gluconobacter oxydans*, also indicates Cyo is capable of functioning at a wide-range of oxygen conditions as a *cyo* mutant had a defect in growth and oxygen consumption at both free oxygen and oxygen-limiting conditions (Richhardt *et al.,* 2013). This bacterium is an obligate aerobe yet it does not contain cytochrome *c* oxidases or a high-affinity Cyd quinol oxidase, indicating it may be taking advantage of the versatility of Cyo that we have shown in the present study.

Although it is capable of functioning at a wide range of oxygen concentrations, Cyo may be most important at intermediate oxygen levels. Based on our results, *cyo* expression peaks at approximately 1-2.5%. Perhaps at these concentrations, oxygen is too low for Cta to be adequately effective but not low enough to induce FixN_P. Having an oxidase such as Cyo that is capable of functioning at various oxygen concentrations

would be of great benefit for many bacteria, particularly soil bacteria that have to frequently adjust to wide ranges of oxygen conditions.

CHAPTER THREE: THE TRANSCRIPTIONAL REGULATION OF CYO

A. Introduction

The quinol oxidase, encoded by *cyoABCD*, is wide-spread among proteobacteria and firmicutes. This oxidase (Cyo) is often classified as a low-affinity oxidase utilized in high oxygen based on studies in *E.coli* (García-Horsman *et* al., 1994; Morris & Schmidt, 2013). Conversely, work presented in the previous chapter and other studies in the literature have demonstrated Cyo to be important for growth and adaptation to low oxygen conditions in culture for certain rhizobial species (Surpin & Maier, 1998). In addition, the *cyo* genes have also been shown to be up-regulated in low oxygen in rhizobia (Trzebiatowski *et al*., 2001; Bobik *et al*., 2006). However, the transcriptional regulatory mechanism of how *cyo* is up-regulated at low oxygen is not well understood.

Because oxygen is a substrate for all the terminal oxidases, it is a common factor in how oxidases are regulated (Bueno *et al.*, 2012). Some oxidases can be regulated by transcription factors that sense oxygen directly, such as Fnr proteins. Alternatively, oxidases can be regulated by transcription factors that sense oxygen indirectly based on the redox state of certain molecules. The activity of the two-component system, RegBA, in *Rhodobacter capsulatus,* is regulated in part by the redox state of quinone in the cell and its own cysteine residue as depicted in **Fig. 2**. This two-component system is widespread among bacteria (ActSR in *Sinrohizobium meliloti*, RegSR in *Bradyrhizobium japonicum,* PrrBA in *Rhodobacter sphaeroides*). The homologous proteins appear to have similar function, given that the operons can complement one another between species (Emmerich *et al.,* 2000a, Elsen *et al*., 2004; Wu & Bauer, 2008). The RegSR 2-component system is important for adaptation to low oxygen such as the symbiosis with

legumes and recently has been implicated in denitrification (Bauer *et al*., 1998; Torres *et al.*, 2014). Furthermore, the RegBA homologue in *S. meliloti*, ActSR, is necessary for growth and the induction of genes required for adaptation to low pH conditions (O'Hara *et al*., 1989; Tiwari *et al*., 1996).

In addition to oxygen, iron may be another important cue for Cyo regulation and utilization. The Fbc pathway contains more proteins that functionally require iron (Fbc and cytochrome c) compared to the Cyo respiratory pathway. Therefore, it has been suggested in other bacteria, such as *P. aeruginosa*, that Cyo may be the preferred pathway in lower iron conditions (Arai, 2011). In rhizobia, several regulators are involved in iron-regulated gene expression that bind to conserved iron-control or iron-regulatory elements of target genes (Rudolph *et al*., 2006).

In this chapter, *Rhizobium etli* CFN42 was used as a model organism to determine the major transcription factor involved in regulating *cyo*. Knowing this regulation could provide a better understanding of how this oxidase is integrated into aerobic physiology. As a start, the promoter region of *cyo* was analyzed in silico and revealed multiple putative ActR (RegA, RegR homologue) DNA binding sites. An *actSR* mutant was constructed and the *cyo* expression was examined in various oxygen, pH and iron conditions. Furthermore, the growth of the Δ*actSR* mutant was analyzed in comparison to a *cyo* mutant and *fbc* mutant in these physiological conditions. Lastly, the predicted promoter elements in the 5' promoter region of *cyo* were systematically deleted and their impact on *cyo* expression was examined.

B. 5' upstream sequence of *cyo* and predicted regulatory elements

The genome nucleotide sequence of *R. etli* CFN42 has been determined (Gonzalez *et al.*, 2006). The 5' upstream DNA of the *cyo* operon is depicted in **Fig. 12a**. The promoter region contained a putative Sigma70 promoter (Rámirez-Romero *et al.*, 2006; Soloyvev & Salamov, 2011; de Jong *et al*., 2012) and 4 putative ActR DNA binding sites that aligned with the consensus RegR DNA binding site in *B. japonicum*, $NGNGNCN_{4\text{-}6}GNNNC$ (Emmerich *et* al., 2000b; Lindemann *et al*., 2007; Torres *et al*., 2014). Three of the putative ActR binding sites were in succession 33 base-pairs downstream of the putative Sigma70 promoter (nucleotides 40,188 to 40,130 of the *R. etli* genome sequence). Located 140 base-pairs upstream of the putative promoter was an Fnr anaerobox and another potential ActR DNA binding site (nucleotides 40,387-40.421). This arrangement of the putative ActR DNA binding sites was similar in other *cyo* promoter regions of *S. meliloti* and *R. leguminosarum* (**Fig. 12b,c**). Each of the these strains contained an ActR DNA binding site upstream of the putative Sigma70 promoter and then at least two back-to-back predicted ActR DNA binding sites downstream of the promoter.

C. Mutagenesis of *actSR* and its effect on *cyo* expression at low oxygen

To test whether ActSR regulates *cyo* expression, a strain was constructed by replacing the *actSR* operon with a kanamycin cassette (CE605). The expression of *cyo* was analyzed in this *actSR* mutant at various oxygen conditions using RT-qPCR and a *cyo*:*lacZ* fusion (**Fig. 13a,b**). As seen in the previous chapter, the wild type up-regulates *cyo* at 1% compared to 21% oxygen concentration. In the *actSR* mutant, *cyo* transcript

levels were approximately 8-fold lower compared to wild-type levels at low oxygen (1%). In high oxygen conditions, the expression of *cyo* was decreased in the *actSR* mutant (approximately 2-fold) compared to the wild-type levels. The expression of *cyo* was restored to wild-type levels after transferring the wild-type copy of *actSR*, pZL51, in the *actSR* background.

It is known that *cyo* mutants have growth defects at 0.1% and 1% oxygen. The above results suggest that *actSR* mutants should have the same defects. Therefore, growth of the *actSR* mutant was analyzed at various oxygen concentrations in TY medium. The *actSR* mutant failed to grow at 0.1% oxygen and had a severe growth defect at 1.0% oxygen concentration (**Fig 14a,b**). Addition of the wild-type *actSR* operon (pZL51) restored growth similar to that of the wild type. In high oxygen conditions (21%) the mutant had a slight growth defect (**Fig. 14c**).

D. *cyo* expression in varying pH conditions

Given ActSR's role as a global regulator in acidic conditions (O'Hara *et al*., 1989; Tiwari *et al*., 1996), *cyo* promoter activity was measured in various pH conditions. As pH was incrementally lowered from 7.5 to 4.8, *cyo* promoter activity began to increase (**Fig 15a**). *cyo* expression was investigated more closely at pH 4.8 vs. 7.0, using RT-qPCR in addition to the *cyo:lacZ* fusion. Transcription activity was approximately 10-fold higher at pH 4.8 compared to pH 7.0 in the wild type (**Fig. 15b,c**). In the *actSR* mutant, *cyo* transcript levels and promoter activity were lower compared to wild-type levels in any pH condition. *cyo* expression was increased after transferring the wild-type

copy of the *actSR* operon, pZL51, into the *actSR* background but was still lower compared to wild type at low pH (**Fig. 15c**).

A. ***Rhizobium etli*** **CFN42**

TGCGTCGCGTTCAAGCGACGACGACGACGGTCCGTAATGCGATGTTGTTGCCATAAAACGCCTCC
TCGTTAAGGCGCTTGCGGCAAGGCGCCTCAAGTCTGATCTTGATCAAACCTGCAGGCTTATCAAG
GCTCCGTAAGACCGAAATAGTTCATCATCACGGCTCAAATGAAGCGCAGATGGAAAAAATTGCGT
GATCCGGACGGTGATTTTCCCCTGCAAATGCTGGCCTGACCGGCAGTTGCGGATATATTGGACTG
AACATGCGCAGGGGCTAAAATCCTTCTATATTCCATCAGGATTTCAAAGCACTAGCGCCCGATGA
TTTTTGCCGCAGTGCGGCATGTTTGCTGCACTGCGACCTTCCGCCTCATGTCGCTATCCGGTTCA
GTGCTTTAGTCGCGGACAAAACGAAACAACAAGAGCTTAGAGACGTGCCAAAACTCATGAAGTTT
TCCCGCCTTCTATCCGTCTTGCCTCGCTGCTTTTCCTGGCAGGATGCAACATGGTGGTCATGGCG

B. ***S. meliloti*** **1021**

TGGCGATATTGCCGGCGGATACGGGCGTGTCGTCGTGAATGCGCCGCGCGTCGCGCTCCATCGAAGAGGAC
GACGGTCCCAGGGACTGTTGCATTGCACTGCTCATCAAACGCCTCCCGCGCTCGCACGGGGGCTAAGAACA
TGCGGTGTTCCGCCGCACCCGCTCGTACTCTCAAGATGAGAGCGCAAGGCTCCCTTGGAGGGATCTTGACC
AATCAACCGTTCATATCAAGGGGAGAAACGCGAAATAATGCGTTTCACGTCCTCACTGTCTGCAAGCGGCG
GAAGATGCTGCGTCGCAAAACGACTGCGGCGGATTGCTGCAGTGCGACCATCGACCTCATACCTTTCCCAT
CCACTCTACTTTAGTCGCAGGGCCGTCGAAACAAAATAGAGCTCCGAGCCGTGCCAGAACTGTTGAAGTTT
TCCCGCCGCCTCGCCGTTTTGCCGCTTTTCCTCGTGATGGCGGGATGCGACATGGTGGTGATGTCGCCATC

C. ***R. leguminosarum*** **bv** ***viciae*** **3841**

GCGATACTACCCGGCGAAACCGGCTTGTCGTCGTGAATGCGCCGCGCGTCGCGTTCCAGCGACGACGATGA
CGGTCCGTAATGCGATGTTGTAGCCATGAAACGCCTCCCTCGTTGAGGCGCTTTCGGCAAGGCGCCTCAAC
CTGATCTTGATCAAACCTGCAGGCTTATCAAGTCCGTAAGACGCAAATAGTTCATCATCACGGCTCAAAAT
GAGGCGTAGACGGAAAAAATAGCGTGATCCGGAGCGCGATTTTTCCCGGGGACGCTGGCTTGGCCGGCCCT
TGCGGATATATTGGAACAAAACATGCGCTGGCGAAAGAATCCTTCTTGATTTCATCAGGATTCCAAAGCTG
TAGTGCACCATCATTTGTGCCGCAGTGCGGCATGATTGCTGCACTGCGACCAAACACCTCATGTCGCTATC
GGGTTCAGTGCGTTAGTCGCGGAACGAACGAAACAACAAGAGCTTAGAGACGTGCTAAAACTGGTGAAGTT

D)

```
B. japonicum        NGNGNCNNNNN------GNNNC--
R. etli 1           TGCGGCAA------GGCGCCTC—
R. etli 2           AGCGCCCGATGATTTTTGCCGC--
R. etli 3           TGCGGCAT----G-TTTGCTGC--
R. etli 4           TGCGACCT------TCCGCCTC--
S. meliloti 1       TGCGCCGCG--------CGTCGCGC
S. meliloti 2       AGCGGCGG----AAGATGCTGC--
S. meliloti 3       TGCGGCG-----G-ATTGCTGC--
S. meliloti 4       TGCGACCA------TCGACCTC--
                     * * *           .   *
```

Figure 12: The 5' upstream promoter region of *cyo*. The sequences contain 500 BP upstream of the *cyo* orf in **(A)** *R. etli* CFN42 (RHE_PE00030), **(B)** *S. meliloti* 1021 (SMb21487), and **(C)** *R. leguminosarum* bv *vicae* 3841 (pRL110042). Putative ActR DNA binding sites are double-underlined (__). A putative CRP-FNR anaerobox is dashed-underline (_ _). A putative sigma70 promoter, was predicted using Softberry and PePPER software, and is underlined with dots (….). The potential translational start sites are highlighted in gray. **D)** Multiple sequence alignment of the putative ActR DNA binding sites in *S. meliloti*, *R. etli* and consensus RegR binding site in *B. japonicum* binding site using ClustalW2 software.

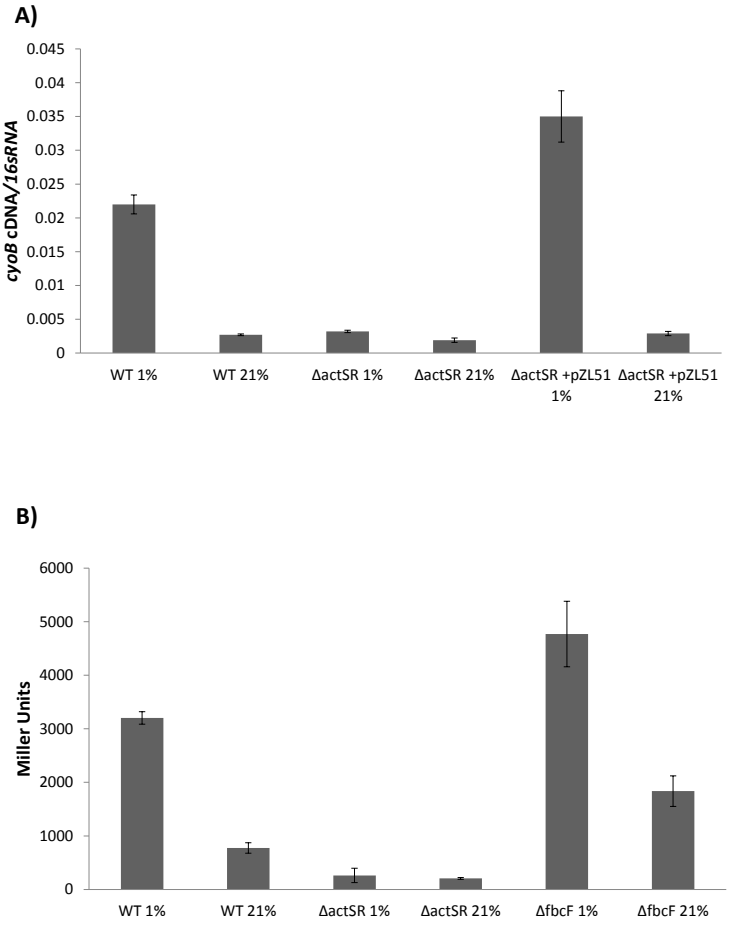

Figure 13: *cyo* expression at 1% and 21% oxygen in *actSR* mutant. Strains were grown either in 21% or at 1% oxygen conditions. Protein or RNA was extracted from cells in exponential phase. **A)** q-RT-PCR of *cyoB*. RNA was extracted and converted into cDNA using the reverse gene-specific primer. cDNA was then quantified by qPCR and then normalized to the *16sRNA* cDNA from the original RNA sample. Means ± SD values were calculated from three separate qPCR assays. **B)** Beta-galactosidase activity of the strains carrying the transcriptional fusion plasmid, pZL73 (*cyoA:lacZ*). Mean ± SD values were calculated from three or more separate lacZ assays from two different cultures.

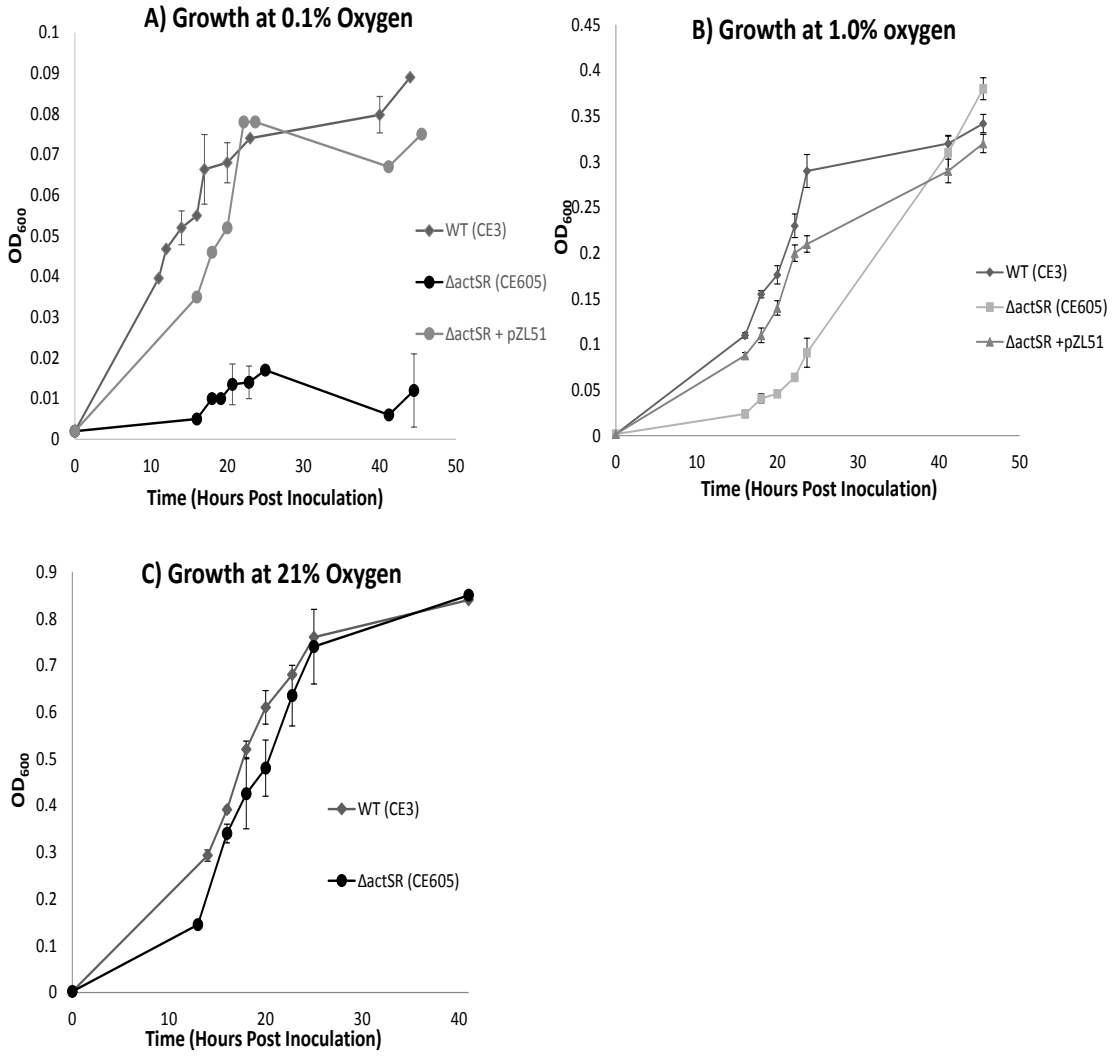

Figure 14: Growth curves of *actSR* mutant at 0.1% (A), 1.0% (B) and 21% oxygen (C). Strains were initially grown in TY liquid under a gas phase with 21% oxygen. At full growth they were sub-cultured 1:200 into 5 ml of TY liquid in 60 ml serum vials. As described in Methods, nitrogen and air were added to the headspaces in the vials above the liquid to give the indicated concentrations of oxygen. Growth was followed by measuring the optical density (OD) at 600 nm. Error bars indicate SD from at least three separate cultures

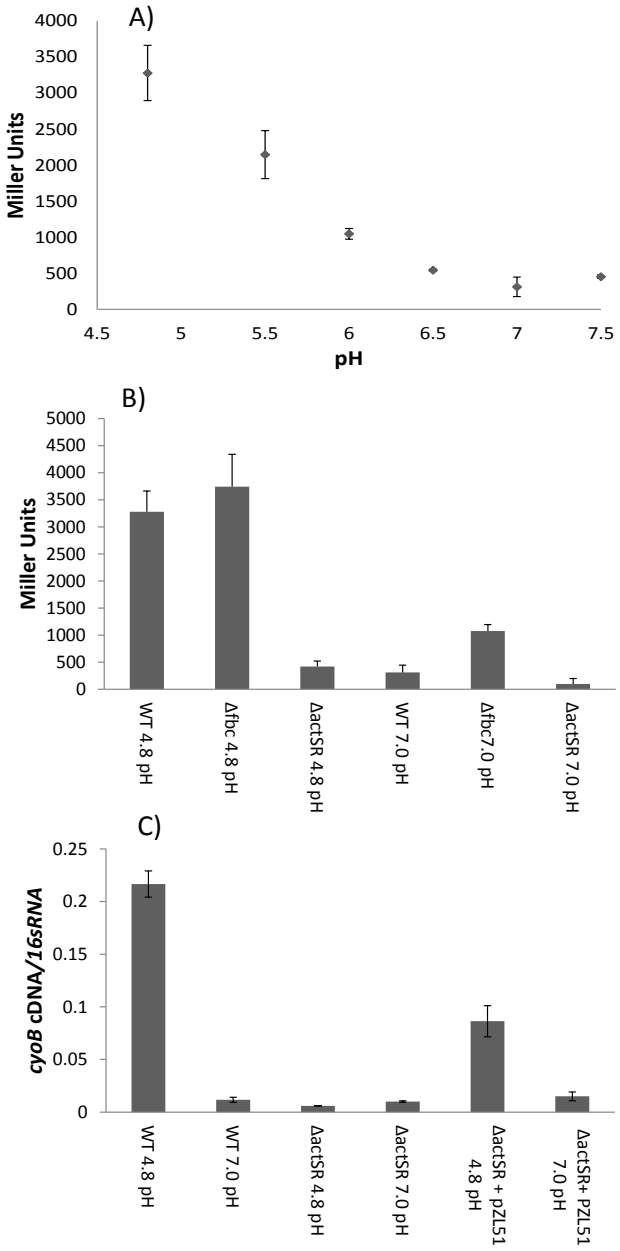

Figure 15: *cyo* expression in varying pH conditions. Strains were grown in YGM media buffered with MES. **A)** Wild type cells, carrying pZL73 (*cyo:lacZ*), were harvested from exponentially growing cultures at different pH conditions (4.8-7.5). Specific activity is given in Miller Units. Mean±SD values were calculated from three or more separate *lacZ* assays from two different cultures. **B)** Cells, carrying pZL73 (*cyo:lacZ*), were harvested in exponential phase and the beta-galactosidase activity (Miller Units) was determined. Mean ± SD values were calculated from three or more separate assays from two different cultures. **C)** RNA was extracted from strains in exponential phase and *cyoB* transcript levels were determined and normalized to the *16sRNA* levels. Means ± SD values were calculated from three separate qPCR assays.

E. Growth analysis at low pH

To determine if Cyo and ActSR had a significant physiological role at low pH, the growth of *cyo* and *actSR* mutants were analyzed at 4.8 and 7.0 pH in the defined minimal medium, YGM (**Fig. 16a,b**). Both the mutants had prolonged lag phases when grown at low pH. These growth defects were also observed in TY (tryptone, yeast extract) media adjusted to 4.8 pH (**Fig. 16d**). The growth defects were alleviated after transferring the wild-type copies of *cyoA* (pZL34) and *actSR* (pZL51) in their respected mutant backgrounds (**Fig. 16c,d**). When the pH conditions were adjusted to 7.0, the growth of the *cyo* mutant was comparable to the wild type, whereas the *actSR* mutant had a slight growth defects in neutral pH conditions.

When streaked on low pH YGM plates (4.8 pH), the *actSR* mutant did not start to form colonies until 7 days after streaking (**Fig. 17a**). The wild type consistently formed isolated colonies 2-3 days after streaking on low pH plates. Isolated colonies were consistently observed in the *cyo* mutant 4 days after streaking (**Fig. 17b**). After transferring the wild-type copies of *cyoA* and *actSR* in their respected mutant backgrounds, the onset of isolated colonies were observed similar to that of the wild type.

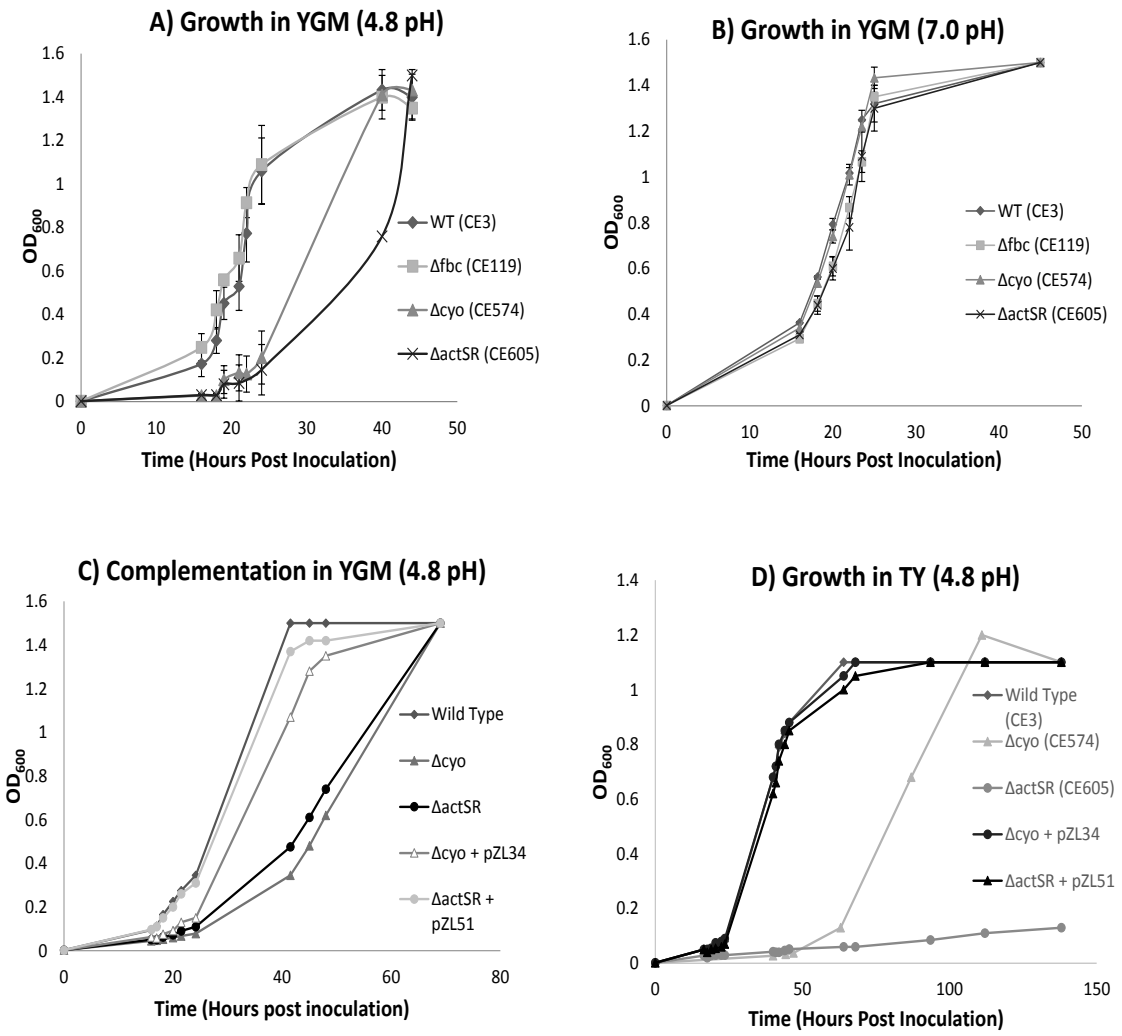

Figure 16: **Growth curves at neutral and acidic pH.** Strains were grown aerobically in YGM media buffered with MES at either 4.8 pH (**A,C**) or 7.0 pH (**B**). For (**D**) TY media was buffered with MES to 4.8 pH. Growth was followed by measuring the O.D. at 600 nm. After growth, the pH was measured to ensure the pH of the culture was maintained ± 0.2 pH of the un-inoculated cultures. Error bars, when present, indicate standard deviation from at least three separate experiments.

Δ*actSR*

Δ*cyoA*

Figure 17: Growth on low pH YGM plates. Colonies were picked from TY plates and streaked on YGM agar buffered with MES at 4.8 pH. At least three different colonies for each strain was tested. Below the plates is indicated the day after the original streaking. The strain is indicated in the triangle on the plates. The upper triangle is the wild type, lower left triangle is the mutant, and lower right is the mutant carrying the complemented plasmid. The upper panel of plates is the *actSR* analysis (**A**), and the lower panel (**B**) is the *cyo* analysis.

F. Growth analysis and *cyo* expression in low iron

To determine if Cyo had a role in low iron condititions, growth of the mutants and *cyo* expression was analyzed in cells grown in TY treated with an iron chelator, 2-2-dipyridyl. Both *cyo* and *actSR* mutants had severe growth defects in this condition (**Fig. 18a**). Addition of the wild-type copies of *cyoA* and *actSR* into their respective mutant backgrounds alleviated the observed growth defects. In the wild type, the expression of *cyo* was approximately 5-fold higher in this low iron condition (**Fig. 18b**). Conversely, *cyo* expression was not induced in the low iron conditions in the *actSR* mutant and was greatly decreased compared to the wild type.

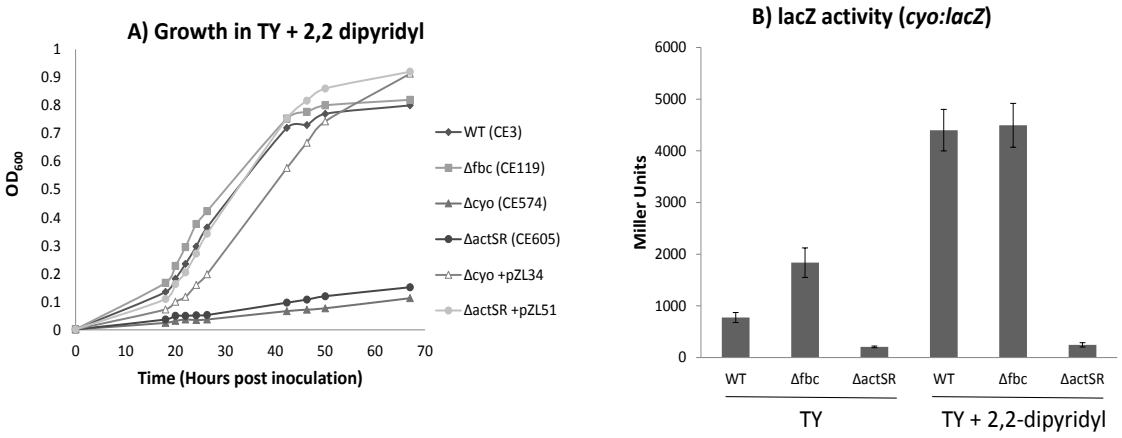

Figure 18: Growth and *cyo* expression in low iron. A)Strains were grown aerobically in TY treated with 200 µM of 2,2-dipyridyl. Growth was followed by measuring the O.D. at 600 nm. Error bars indicate S.D. from three separate cultures. **B)** Strains carrying pZL73 were grown in 2,2-dipyridyl treated and untreated TY media. Beta-galactosidase activities were determined from cells in exponential phase. Mean ± SD values were calculated from three or more separate lacZ assays from two different cultures.

G. *cyo* expression and growth analysis of the *fbc* mutant

The promoter activity of *cyo* under different conditions, using the *cyo*:*lacZ* fusion (pZL73), was also analyzed in the *fbc* mutant under the different conditions. As indicated

in the previous chapter, this mutant can only aerobically respire via Cyo. Expression was approximately 2.5 fold higher at 1% compared to 21% oxygen conditions in this mutant (**Fig. 13b**). At 21% oxygen, the *fbc* mutant had almost 3-fold higher *cyo* expression levels compared to the wild type. At 1% oxygen, *cyo* expression was approximately 1.5 fold higher in the Δ*fbcF* mutant compared to the wild type.

At lower pH (4.8), *cyo* expression was up-regulated approximately 3-fold compared to neutral pH conditions (**Fig 15b**). Compared to the wild-type, the *fbc* mutant had approximately 3-fold higher *cyo* expression at neutral pH. However, the expression levels of *cyo* were similar between the wild type and *fbc* mutant at low pH. The results were similar in regards to the varying iron conditions. *cyo* was upregulated approximately 2.5 fold in the *fbc* mutant compared to high iron conditions (**Fig. 18b**). In high iron conditions, the mutant had approximately 2-fold higher levels of *cyo* expression compared to the wild type but levels were similar between the two strains in low iron conditions.

The *fbc* mutant grew comparably to the wild type at low pH, but had a slight growth defect at neutral pH (**Fig 16a,b**). Similarly, in low iron conditions, the mutant grew similar to the wild type (**Fig. 18a**) but had a slight growth defect in high iron conditions (data not shown).

H. Deletion of the predicted ActR sites in the 5' promoter region of *cyo*

To begin to understand whether the predicted promoter elements (defined in **Fig. 19a**) were necessary for optimal *cyo* expression, the putative ActR binding sites (R1-4) and predicted Sigma70 promoter were deleted from the promoter region and fused with

lacZ. When grown at low pH, only the deletion of R4 showed a significant decrease in expression similar to that of the *actSR* mutant, indicating that R4 is necessary for optimal expression (**Fig. 19b**). Deletion of the putative Sigma70 promoter did not have an effect on *cyo* expression. However, residual *cyo* expression observed in the *actSR* mutant was abolished when the Sigma70 promoter was deleted.

A)

```
  1    TAAAACGCCTCCTCGTTAAGGCGCTTGCGGCAAGGCGCCTCAAGTCTGATCTT
 54    GATCAAACCTGCAGGCTTATCAAGGCTCCGTAAGACCGAAATAGTTCATCATC
107    ACGGCTCAAATGAAGCGCAGATGGAAAAAATTGCGTGATCCGGACGGTGATTT
160    TCCCCTGCAAATGCTGGCCTGACCGGCAGTTGCGGATATATTGGACTGAACAT
213    GCGCAGGGGCTAAAATCCTTCTATATTCCATCAGGATTTCAAAGCACTAGCGC
266    CCGATGATTTTTGCCGCAGTGCGGCATGTTTGCTGCACTGCGACCTTCCGCCT
319   CATGTCGCTATCCGGTTCAGTGCTTTAGTCGCGGACAAAACGAAACAACAAGA
372    GCTTAGAGACGTGCCAAAACTCATGAAGTTTTCCCGCCTTCTATCCGTCTTGC
425    CTCGCTGCTTTTCCTGGCAGGATGCAACATGGTGGTCATGGCGCCCTCCGGCG
```

R1: 26-41 R2: 262-282 R3:284-300 R4: 302-317 σ70: 196-228

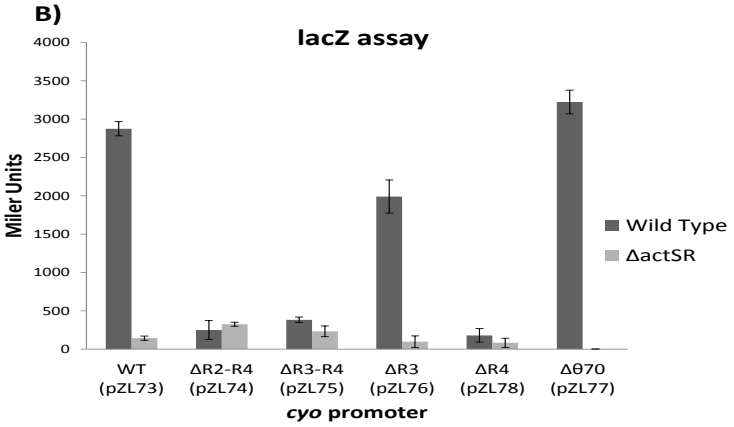

Figure 19: Impact of deleted promoter elements on *cyo* expression. A) Defined predicted ActR sites and Sigma70 region. The ActR sites are double underlined and the Sigma70 region is dotted underline. Below are the defined sites indicating the nucleotide sequences. B) *cyo* promoter regions with various deletions that were fused with lacZ. pZL73, the plasmid containing the wild type *cyo* promoter fused with *lacZ*, was used as a template for deletion mutagenesis. The mutated plasmids (pZL74-78) were then introduced into wild type (CE3) or the *actSR* mutant (CE605). Cells were grown in YGM media (pH 4.8), and beta-galactosidase activity was determined. Means and ±SD were determined from 2 separate cultures and at least 3 separate experiments.

I. Discussion

To gain additional insight into the physiology of Cyo, this study sought to determine how Cyo was transcriptionally regulated in *R. etli* CFN42. The upstream promoter region of *cyo* had several putative ActR DNA binding sites that aligned with the homologous RegR DNA binding sites of *B. japonicum*. The organization of ActR DNA binding sites in the 5' promoter region is similar with *R. leguminosarum* and *S. meliloti* indicating a possible common regulatory mechanism for these species. Based on the deletion analysis, only the last ActR site (R4) was necessary for optimal *cyo* expression. Deletion of the putative Sigma70 promoter did not have an effect on expression. However, it may serve as a weak secondary promoter independent of ActR because the residual expression seen in the *actSR* mutant is undetectable when the Sigma70 promoter is deleted. Nevertheless, this indicates that other sigma factors (RpoN, RpoE, RpoH) promoters may be involved in the transcription of *cyo*. In addition, other transcription factors may also contribute to the regulation *cyo*. For instance, each of the upstream regions examined contained an anaerobox suggesting a role for Crp-Fnr regulation. However, considering there are several Fnr-type proteins in *R. etli* (Granados-Baeza *et al*., 2007), the primary focus of this study was the impact of ActSR on *cyo* expression.

The constructed *actSR* mutant had a significant growth defect at low oxygen (0.1% and 1.0%) concentrations. This is consistent with other findings in *B. japonicum* where it is considered a global regulator for adaptation to low oxygen conditions (Bauer *et al*., 1998; Torres *et al.*, 2014). Despite its importance for growth at low oxygen, the *actSR* mutant did not have an obvious effect on the symbiosis between *R. etli* and *Phaseolus vulgaris* (data not shown).

In low or high oxygen, *cyo* expression was down-regulated in the Δ*actSR* mutant compared to the wild type. However, the expression was more affected in the low oxygen condition, because Cyo is up-regulated in these conditions in the wild type (shown in chapter 2). This result correlates with a recent microarray study in *B. japonicum*, where *cyo* genes were decreased in anoxic conditions in a mutant of the ActSR homologue, RegSR (Torres *et al*., 2014). ActSR probably is responsible for *cyo* upregulation at low oxygen in *S. meliloti* as well. It is known that *cyo* is regulated independently of FixJ in that bacterium (Bobik *et al*., 2006).

The ActSR two-component system is an important global regulator in acidic conditions in *S. meliloti* (O'Hara *et al*., 1989; Tiwari *et al*., 1996). Therefore, *R. etli cyo* regulation according to pH seemed likely. The expression of *cyo* remained at a basal-level in neutral pH but as pH was lowered below 6.5 the expression of *cyo* began to increase. As with up-regulation at low oxygen concentrations, up-regulation of *cyo* at low pH was eliminated in the *actSR* mutant. The increase of *cyo* expression in response to acidic conditions has been observed in a microarray study in *S. meliloti*, but it has yet to be linked to ActSR in this organism (Hellweg *et al*., 2009).

In an *fbc* mutant, Cyo is the only viable aerobic respiratory option thus it can reveal the capability of Cyo to function in various conditions. For instance, this mutant was able to grow effectively at either low or neutral pH conditions, indicating Cyo can be used at a wide-range of pH conditions. Moreover, the *fbc* mutant was able to grow in both low and high iron conditions tested. In conditions where *cyo* is marginally expressed in the wild type, such as high oxygen or neutral conditions, the *fbc* mutant had approximately 3-fold higher levels of *cyo* expression compared to the wild type.

However, in conditions where Cyo is upregulated in the wild type (low oxygen, low pH and low iron) the differences in *cyo* expression are minimal between the *fbc* mutant and the wild type.

How ActSR becomes active has been characterized in vitro in the homologous RegBA system in *Rhodobacter capsulatus*. One study indicated that RegB auto-phosphorylation activity can be influenced by the redox state of quinone (Wu & Bauer, 2010). Although both quinone (oxidized) and quinol (reduced) can bind to RegB with equal affinity, only quinone will promote an inactive conformation. Thus, a higher quinol:quinone ratio in the cell will lead to a more active RegBA. This may explain *fbc* mutation leads to up-regulation of *cyo* in both aerobic and neutral pH conditions. In this mutant, the Fbc pathway is non-functional which would presumably cause a build-up of quinol causing the quinol:quinone ratio to increase. The increase of quinol would further activate ActSR and consequently increase *cyo* expression.

The quinol:quinone ratio may also be affected at low pH. It is known in the alpha-proteobacterium, *Rhodobacter sphaeroides*, that the Fbc's optimum pH is approximately 8.0 for both quinol oxidation and cytochrome *c* reduction activity (Crofts *et al*., 1999; Guergova-Kuras *et al*., 2000; Zhou *et al*., 2012 Lhee *et al.,* 2010). Whereas, the optimum pH for Cyo in *E. coli* is approximately between 6.0 - 7.0 (Verkhovskaya *et al*., 1992; Thomas *et al.,* 1993). Therefore, lowering the pH would cause lower Fbc activity leading to a higher quinol:quinone ratio, consequently leading to greater ActSR activity and higher levels of *cyo* expression (see chapter 5).

Previous work has shown *cyo* to be up-regulated in response to low iron conditions in *S. meliloti* and *P. aeruginosa* (Chao *et al.*, 2005; Kawakami *et al*., 2010).

This study indicates *cyo* is not only up-regulated in *R. etli* but also necessary for efficient growth in low iron conditions as the *cyo* mutant had a severe growth defect. The results indicate ActSR is necessary for *cyo* induction in low iron similar to the other conditions tested. To our knowledge, ActSR has yet to be linked to low iron conditions. Its requirement may be that it is necessary for any high-level of expression of *cyo*. On the other hand, common iron regulatory elements (rirA, Irr, Fur) were not identified in the 5' promoter region of *cyo* (Rudolph *et al.*, 2006). As a hint of rationale for regulation by ActSR, it has been established in *B. japonicum* that cytochrome c_1 levels are vastly decreased in low iron conditions (Gao & O'Brian, 2005). Theoretically, this would cause a build-up of quinol similar to the *fbc* mutant described above and consequently cause an increase of ActSR activity leading to higher *cyo* levels (see chapter 5).

J. Summary

This work indicates a functional ActSR two-component system is needed for optimal expression of *cyo* in varying physiological conditions. The results suggest ActSR is a potent positive transcriptionally activator of Cyo. It is suspected that ActR directly regulates *cyo* but this has not been confirmed. Nevertheless, it can be concluded that *cyo* is part of the ActSR regulon. This observation led to discovering other physiological roles for this oxidase, as the *cyo* mutant also had severe growth defects in low pH and low iron conditions. Given that *cyo* was also upregulated in these conditions, it suggests that Cyo is the preferred oxidase at low pH and low iron in *R. etli* CFN42.

CHAPTER FOUR: THE EXPRESSION AND UTILIZATION OF CYO IS SHUT-OFF IN AEROBICALLY SLOW-GROWTH CONDITIONS

A. Introduction

The work in previous chapters has indicated Cyo is important for growth at low oxygen, low iron and acidic conditions in *R. etli*. Furthermore, *cyo* is up-regulated in these aforementioned conditions. It was concluded that the two-component system, ActSR, was necessary for optimal expression in any condition tested. The autophosphorylation activity of ActS is presumably influenced by the quinol:quinone ratio as it has been shown that the ActS homologue in *R. capsulatus*, RegB, is active when bound to quinol and inactive when bound to quinone (Wu & Bauer, 2010). Thus, higher quinol:quinone levels in the cell will presumably lead to higher ActS activity and *cyo* expression.

Thus far, the observations have been linked to disruptions in the aerobic respiratory chain downstream of the quinol branchpoint (**Fig. 5**). These perturbations, such as the *fbc* mutation or lowering the oxygen, would theoretically lead to higher levels of quinol, thus leading to higher ActS activity and *cyo* expression. However, the literature suggests metabolism upstream of the aerobic respiratory chains may have a significant effect on quinol:quinone ratio in the cell. For instance, it has been observed in *E. coli* that the quinol:quinone ratio changes throughout aerobic growth in that it gradually increases and peaks during exponential phase (Bekker *et al*., 2007). Upon entering stationary phase, the quinol:quinone ratio returned to basal levels. Based on these observations, it would be predicted that *cyo* expression would be lower in stationary phase compared to exponential phase. Previous transcriptomic studies in *P. aeruginosa*

and *P. putida* have shown that *cyo* is down-regulated in stationary phase (Morales *et al*., 2006; Kawakami *et al*., 2010).

In this chapter, the impact of growth on Cyo utilization and expression in *R. etli* was investigated. As a start, quinol oxidase activity and *cyo* expression was measured in concert with growth in both the wild type and *fbc* mutant. Next, the viability of the respiratory mutants during stationary phase was examined. Lastly, the expression of *cyo* and growth of respiratory mutants was examined in cells grown in minimal media with different sole carbon sources. These investigations have led to surprising results and novel insight into how Cyo is utilized and integrated into aerobic physiology.

B. Quinol oxidase activity and *cyo* expression in concert with growth.

The quinol oxidase activity was measured from cells grown aerobically in TY medium at various times during stationary and exponential phase (**Fig. 20a)**. In the wild type, Cyo became increasingly active during exponential phase but abruptly decreased upon entering stationary phase. On the other hand, the Fbc remained active (measured by Fbc activity assay) throughout the different growth phases (data not shown).

To determine if the quinol oxidase activity pattern was a result of transcriptional regulation, beta-galactosidase measurements of cells carrying a transcriptional fusion (*cyoA:lacZ*) were made in concert with growth (**Fig. 21a**). Similar to the quinol oxidase activity, beta-galactosidase activity gradually increased and peaked towards the end of exponential phase. As cells entered stationary phase, the promoter activity started to decrease and eventually minimal expression was observed. RT-qPCR was also utilized to measure *cyo* expression at different stages of growth (**Fig. 21c**). In the wild type, *cyo*

expression was down-regulated (approximately 5-fold) when cells entered stationary phase and remained repressed in later stationary phase.

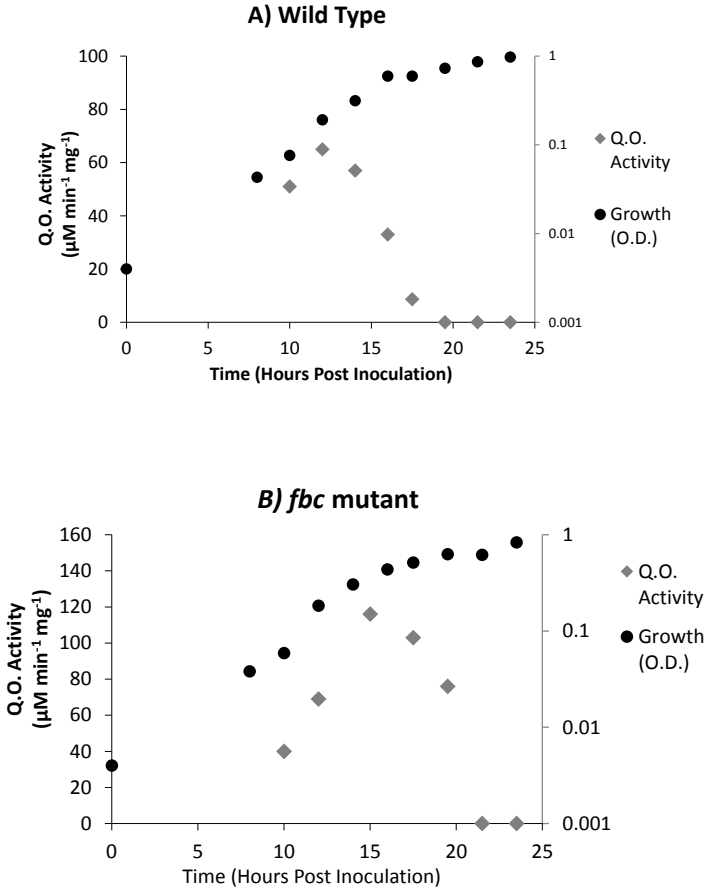

Figure 20: Quinol oxidase activity measurements in concert with growth in the (A) wild type and (B) *fbc* mutant. 10 separate 250 ml Erlenmeyer flasks containing 50 ml of TY media were inoculated and grown under aerobic conditions. At each time point, the O.D. at 600 nm (in circles) of one of the cultures was read (right axis), and the cells were harvested. The corresponding quinol oxidase activity (in diamonds) of solubilized membranes was then measured (left axis). The activity was measured by following abs 275 nm, and specific activity was calculated by using the molar absorption coefficient of quinone (12,500 M^{-1} cm^{-1}) normalized to the total protein (measured by BCA assay) used in the reaction. Note: at hour 8, there was not enough protein in the samples to measure the quinol oxidase activity.

In addition to the wild type, the *fbc* mutant was also analyzed. This mutant is able to respire only via Cyo Therefore, it was predicted that Cyo would remain active and

expressed throughout growth. The quinol oxidase activity was approximately 2-fold higher compared to the wild type during exponential growth and remained active in early stationary phase albeit at lower levels (**Fig 20b**). In later stationary phase the quinol oxidase activity was also undetectable. The pattern of *cyo* expression was similar, in that expression levels peaked in exponential phase and became vastly decreased in late stationary phase (**Fig. 21b,c**).

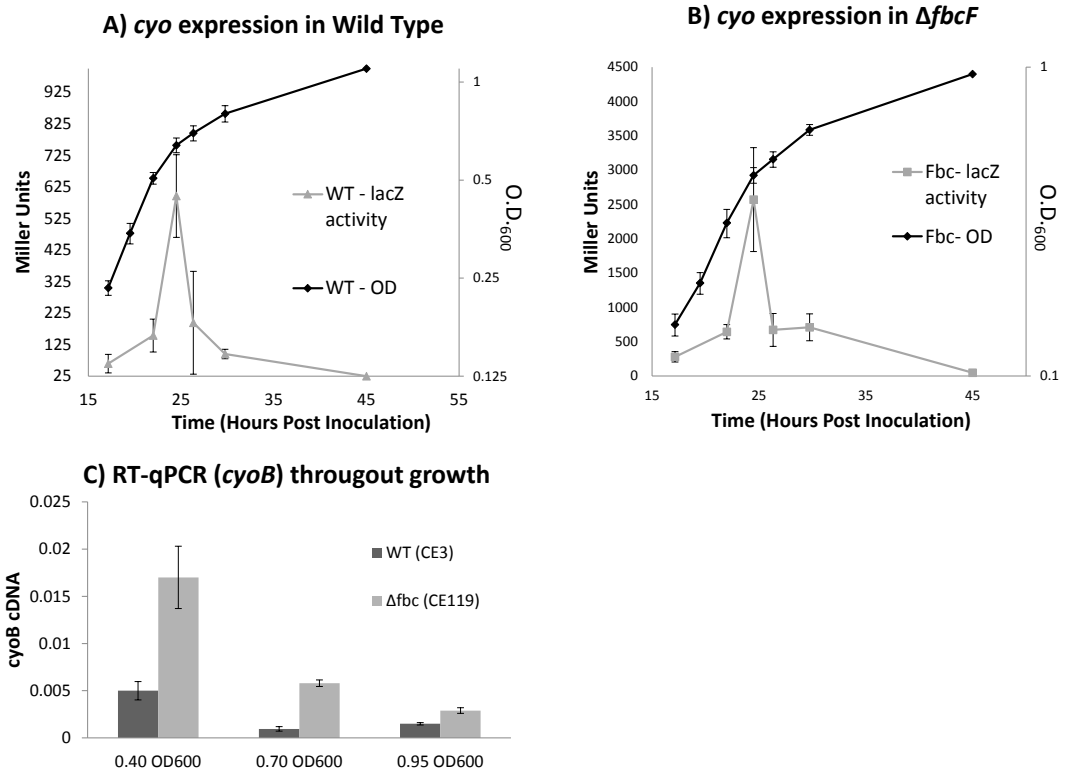

Figure 21: *cyo* expression throughout growth phases. A) Wild-type was grown in 50 ml TY liquid media in a 125 ml Erlenmeyer flask. At the given time point, 1 ml of culture was removed and the beta-galactosidase activity was measured using the fusion plasmid, pZL39. **B)** Growth and beta-galactosidase activity were measured for the *fbc* mutant as described above. Mean and S.D. for **(A)** and **(B)** were calculated from at least 3 different experiments from 2 different cultures. **C**) RT-qPCR of *cyoB* at different phases of growth. Cells were harvested at at approximately 0.40 O.D.$_{600}$, 0.70 O.D.$_{600}$ and 0.95 O.D.$_{600}$. RNA was extracted and converted into cDNA. cDNA was then quantified by qPCR. Means and standard deviations were calculated from three separate qPCR experiments. Note: (C) was performed separately from (A) and (B).

C. Viability of respiratory mutants during stationary phase

To determine if the down-regulation of Cyo during stationary phase had an effect on viability in the *fbc* mutant, the c.f.u. (colony forming units) were measured by plating on TY agar plates throughout stationary phase. The viability of the *fbc* mutant started to decrease by day 5 and eventually no c.f.u./ml were observed after 10 days (**Fig. 22a**). Conversely, the wild type and *cyo* mutant maintained 10^6 c.f.u./ml throughout the 15 days of stationary phase survival examined. The addition of the wild type *fbc* operon (pKT104) into the *fbc* mutant background, restored viability similar to that of the wild type.

To confirm that lack aerobic respiration was the cause for decreased viability in the *fbc* mutant, the cytochrome *c* oxidase mutants were also analyzed (**Fig. 22b**). The *cta* mutant started to have decreased viability by Day 5, but maintained at least 10^2 c.f.u./ml after 10 days. The double *cta*/*CoxM_P* mutant (CE602) started to decrease by day 5 and lacked any viable cells past 10 days. The single *coxM_P* mutant maintained 10^6 c.f.u./ml during stationary phase similar to the wild type.

The viability of the *actSR* mutant was also analzyed during stationary growth (**Fig. 22c**). This mutant started to have decreased viability by day 3 and only 10^1 c.f.u./ml by day 5 after inoculation. Eventually there were no viable cells that were detected by plating. The addition of the wild-type copy of *actSR* (pZl51) restored viability similar to the wild type.

D. Effect of different carbon sources on growth and *cyo* expression

Given that growth phases had a signficant impact on *cyo* expression and utilization, the growth and *cyo* expression was examined in Y* minimal medium

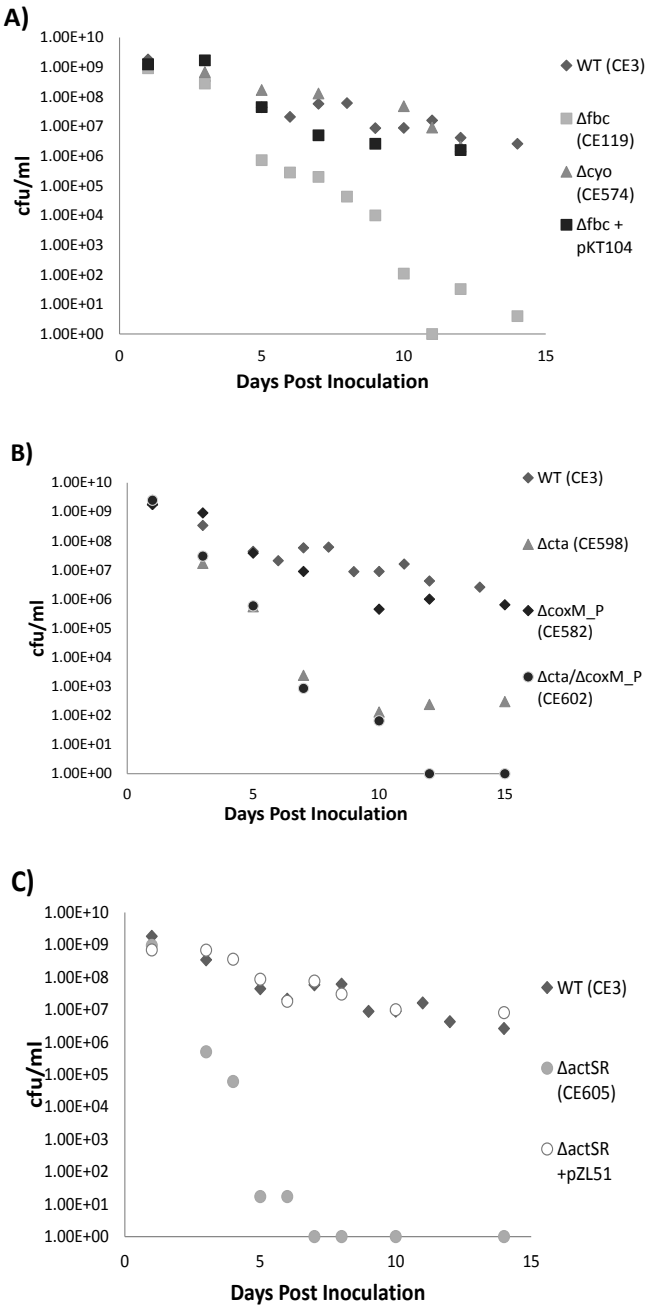

Figure 22: Viability of strains during stationary phase. 50 ml of T.Y. liquid in 125 ml Erlenmeyer flasks was inoculated with the given strain. At the days indicated, 1.5 ml of culture was removed and serial dilutions were made and plated on TY plates to determine the c.f.u./ml. Each point represents the average viability from at least two separate cultures and two separate experiments. Entry into stationary phase occurred at approximately 1 day after inoculation. **A)** Viability of *fbc* and *cyo* mutants. pKT104 is plasmid containing the wild-type *fbc* (pFAJ1700:*fbcFBC*) **B)** Viability of cytochrome *c* oxidase mutants. **C)** Viability of *actSR* mutant. pZL51 is plasmid containing the wild-type *actSR* (pFAJ1708:*actSR*)

containing a variety of sole-carbon sources (concentration at 3 mM). For the wild type, rhamnose is a relatively poor carbon source and fucose is worse compared with sucrose (**Fig 23a**). The *cyo* mutant grew similar to wild type in all the different carbon sources (**Fig. 23b,c,d**) The *fbc* mutant had a slight growth defect when grown in either sucrose or rhamnose medium. In fucose medium, the *fbc* mutant had a severe growth defect. It required over 100 hours post inoculation to observe growth, whereas in the wild type growth was observable after approximately 20 hours. The addition of the wild-type copy of *fbc* (pKT104) in the *fbc* background restored the growth in fucose similar to that of the wild type.

To confirm the lack of growth in fucose was attributed to lack of aerobic respiration, the growth of cytochrome *c* oxidase mutants was analyzed (**Fig. 23e**). The *cta* mutant had a severe growth defect, as it took approximately 50 hours to start to grow. The single *fixN_P* mutant had a slight growth defect compared to the wild type. The double *cta*/*fixN_P* mutant had a severe growth defect similar to the *fbc* mutant. The *coxM_P* mutant did not have a growth defect when grown in fucose (data not shown).

The expression of *cyo* was greater from cells grown in the sucrose minimal-medium compared to the cells grown in fucose or rhamnose minimal-medium (**Fig. 24**). The expression level of *cyo* in the *fbc* mutant was approximately 2-fold lower in fucose compared to rhamnose and sucrose medium (**Fig. 24**). Compared to the wild type, the *fbc* mutant had higher levels of *cyo* expression in all growth conditions.

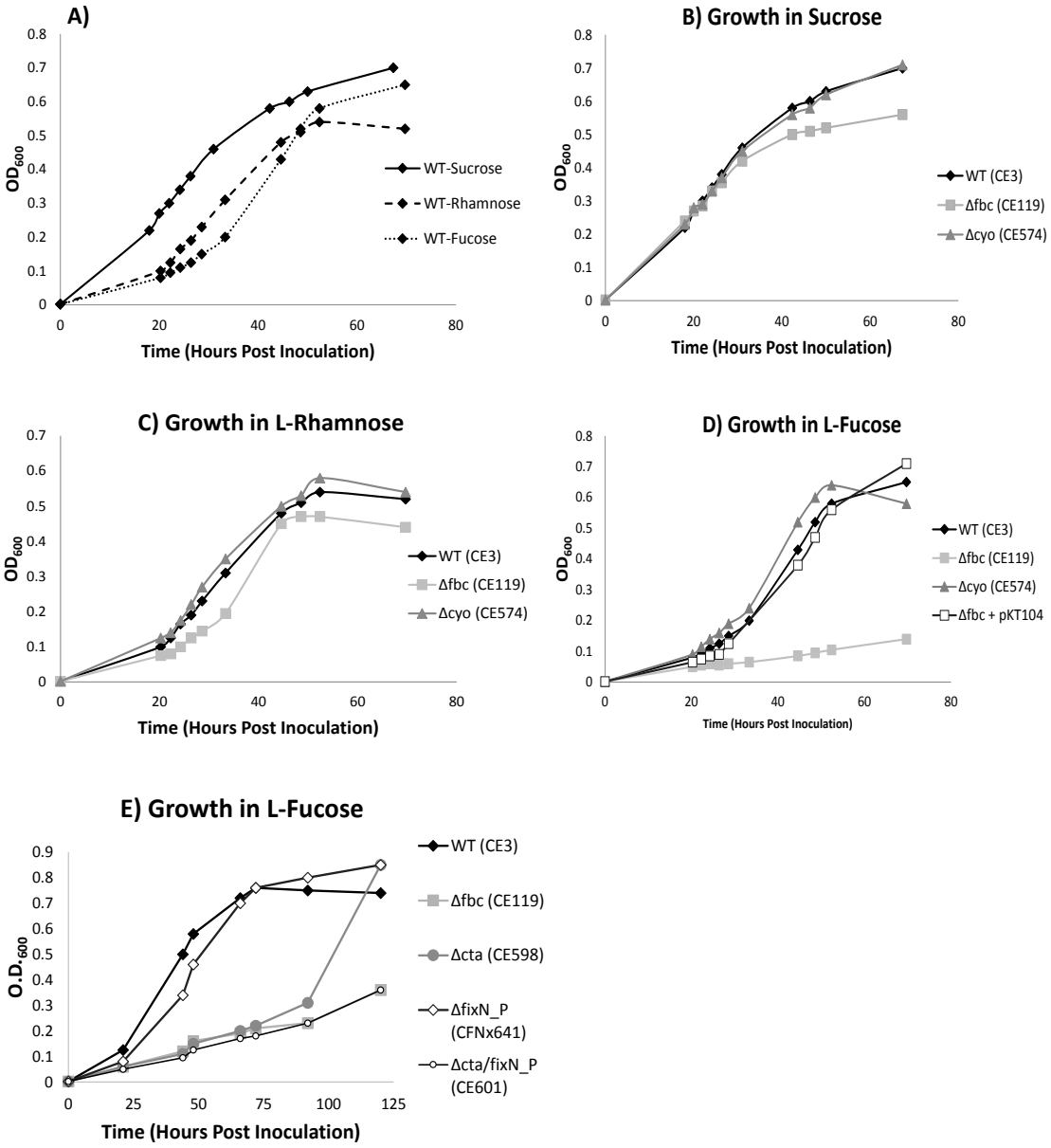

Figure 23: Growth curves in different sole-carbon sources. Strains were originally grown in TY media to full growth. The strains were then sub-cultured in to Y* minimal medium containing 3 mM of either sucrose, L-rhamnose or L-fucose. The growth was analyzed by following the O.D. at 600 nm. All data points are the means of O.D. from three separate cultures.**A)** Comparison of growth curves of the wild type in varying carbon sources. **B)** Growth curves in Sucrose. **C)** Growth curves in rhamnose. **D)** Growth curves in fucose. **E)** Growth curves of cytochrome *c* oxidase mutants in fucose. Note for graph (E), the experiment was performed independently from graphs (A) through (D).

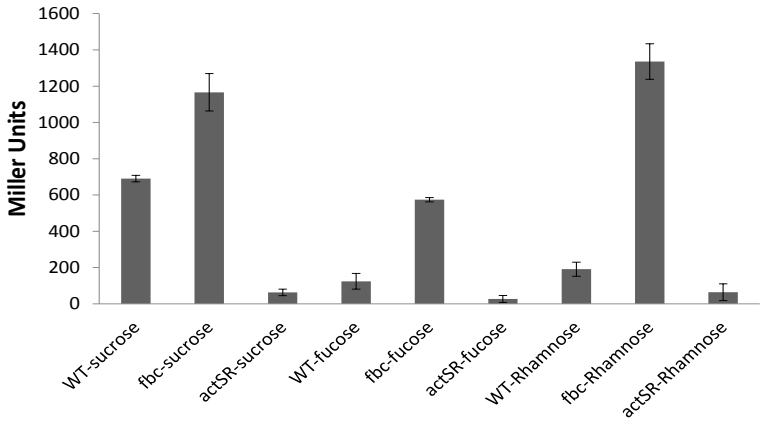

Figure 24: Expression of *cyo* from cells grown in different carbon sources. Strains carrying the *cyo:lacZ* fusion plasmid (pZL73) were grown in Y* minimal medium containing 3 mM of either sucrose, L-fucose or L-rhamnose. Cells, 1 ml, were harvested from exponential phase and the beta-galactosidase activity (calculated in Miller Units) was determined. The mean and S.D. was calculated from at least 3 different experiments from 2 separate cultures.

E. The impact of introducing a plasmid containing the *cyo* operon

The results have suggested both growth and viability defects observed in the *fbc* mutant are in part attributed to transcriptional regulation. The down-regulation of *cyo* during growth in stationary phase and fucose minimal medium has left the *fbc* mutant without a viable respiratory option. It was predicted that overexpressing the *cyo* genes in the *fbc* mutant would complement these phenotypes.

The *cyo* operon (*cyoABCD*), encoding subunits I through IV (**Fig. 4a**) was inserted into pFAJ1708 vector under the *nptII* constitutive promoter. The gene RHE_PE00026, which encodes a SURF1-like protein, was also included in this construct (**Fig. 25**). This protein may be important for Cyo biogenesis and has been shown to be necessary for optimal quinol oxidase activity in *Paracoccus denitrificans* (Bundschuh *et al., 2008*).

The resulting construct (pZL43) complements the *cyo* mutant growth phenotype in both low oxygen and low pH (**Fig. 26a,b**). Of note, in order for the operon to complement the *cyo* mutant phenotypes, an additional 122 bp upstream of the ATG translational start site needed to be included in the construct (**Fig. 25**).

The pZL43 construct was then introduced into the *fbc* mutant background. The *cyo* expression levels were 5-fold higher in this strain compared to the *fbc* mutant without the construct in exponential phase in TY medium (**Fig. 27a**). The high levels of expression was maintained in stationary phase. However, the activity levels during exponential and stationary phase were similar between the two strains (**Fig. 27b**).

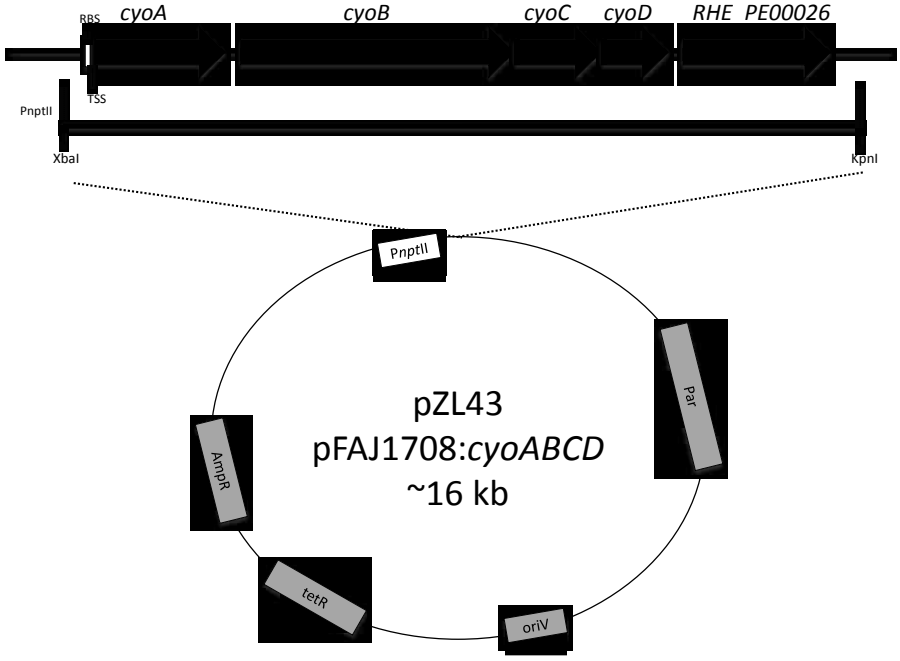

Figure 25: Construction of pZL43. A fragment containing an operon consisting of the 4 Cyo subunits (*cyoABCD*), a Surf-like protein (Rhe_PE00026) and a putative ribosome binding site (RBS) was cloned originally by PCR. In addition, this fragment included 122 bp upstream of translation start site (TSS) and 62 bp downstream of Rhe_PE00026. The *XbaI, KpnI* fragment was inserted into the MCS site of pFAJ1708 (Dombrecht *et al*., 2001) under the P*npt*II promoter. The plasmid contains genes conferring tetracycline resistance (tetR), ampicillin resistant (AmpR) and contains Par proteins for increased stability.

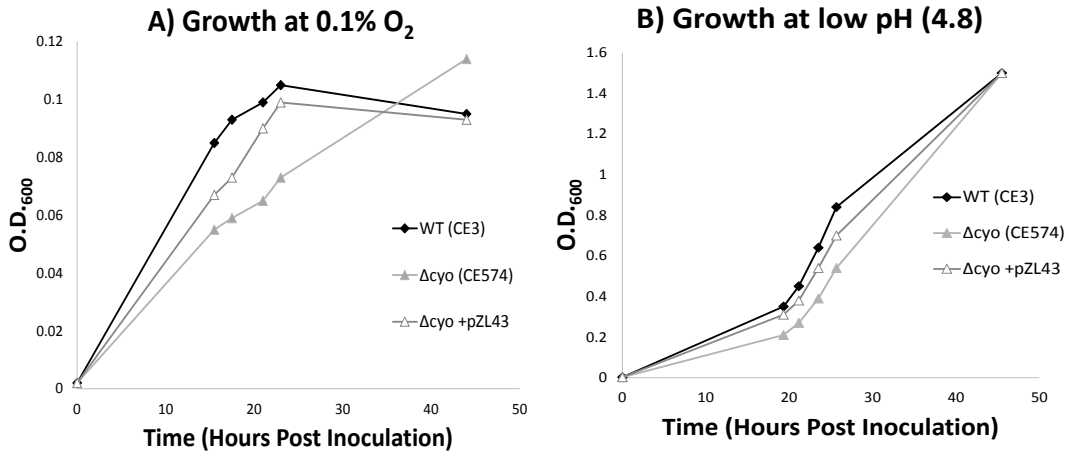

Figure 26: Complementation of *cyo* mutant with pZL43. Strains were originally grown aerobically to full-growth in TY medium and then sub-cultured in the following conditions: **A)** 0.1% oxygen in TY medium. **B)** Aerobic YGM minimal medium (4.8 pH). The data points are means from at least two separate cultures.

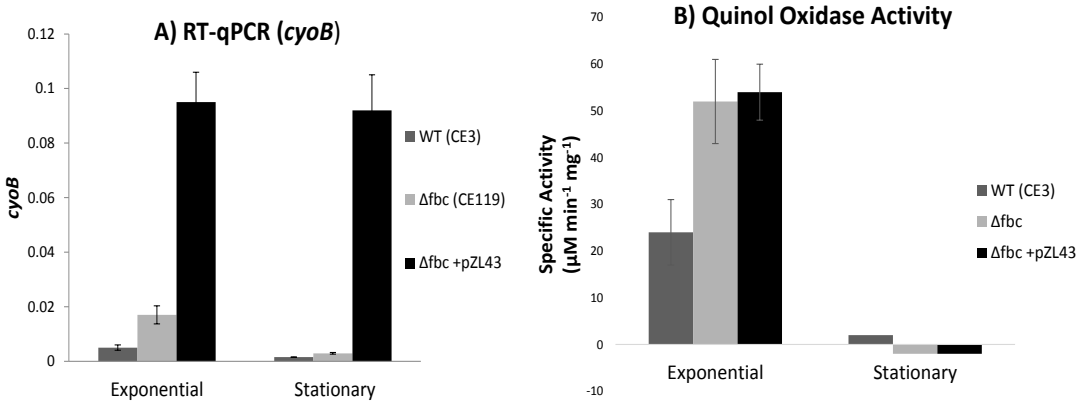

Figure 27: Expression and activity of Cyo throughout growth in aerobic TY medium in the *fbc* mutant carrying pZL43. Cells were harvested in either exponential phase (approximately 0.3-0.4 $O.D._{600}$) or in early stationary phase (0.8 $O.D._{600}$). **(A)** RNA was extracted and converted into cDNA using a specific reverse primer to *cyoB*. The cDNA was quantified by qPCR using both forward and reverese *cyoB* primers. The concentration (ng/µl) was normalized to the original RNA concentration used for the cDNA reactions. Means and S.D. are from 3 separate qPCR reactions on the same culture. (**B)** The quinol oxidase activity of solubilized membranes was measured by following the absorbance of 275 nm. The specific activity was calculated by using the molar absorption coefficient of quinone (12,500 M^{-1} cm^{-1}) and the total protein (measured by BCA Assay) used in the reaction. Means and S.D. are from 3 separate Q.O. experiments from at least 2 different cultures.

The ability of pZL43 to complement the *fbc* mutant was examined. This construct prolonged the viability of the *fbc* mutant during stationary growth (**Fig. 28a**). Viability was maintained at 10^5 C.F.U./ml (slightly less than wild type) until 11 D.P.I. where it eventually decreased to 10^2 C.F.U./ml. During growth in fucose minimal medium, pZL43 improved the lag time from approximately 100 hours seen in the *fbc* mutant to approximately 60 hours (**Fig. 28b**).

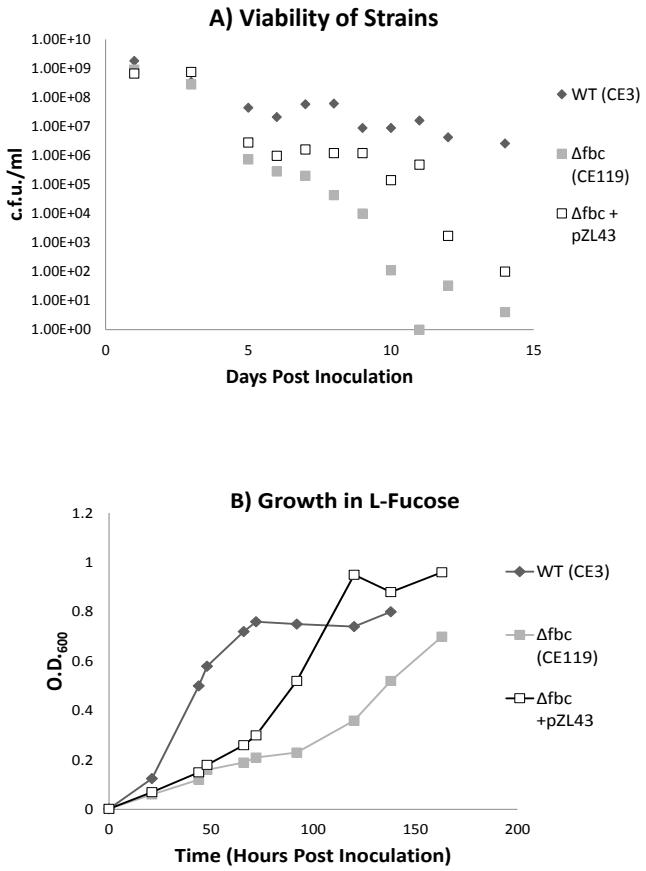

Figure 28: Impact of introducing *cyo* operon (pZL43) in the *fbc* mutant. A) Strains were grown in 50 ml of TY medium in 125 ml Erlenmeyer flasks. At each point, 1.5 ml was removed and the c.f.u./ml was determined by plating on TY agar plates. The points represent means from 3 separate cultures. **B)** Strains were originally grown to full growth in TY medium then subcultured into Y* minimal medium containing 3 mM L-fucose. The data points represent the mean from 3 separate cultures.

F. Discussion

This chapter initially investigated the impact of growth on *cyo* expression and Cyo utilization in the cell. It was determined that *cyo* transcript levels and Cyo activity gradually increased and peaked during exponential growth. Upon entering stationary phase, the *cyo* levels decreased eventually leading to undetectable activity of Cyo. The expression pattern of *cyo* during growth is similar to the quinol:quinone pattern during growth in *E. coli* (Bekker *et al*., 2007). During exponential phase, cells are dividing and are metabolically active. An active TCA cycle would lead to more reducing equivalents such as NADH which would theoretically lead to a higher quinol:quinone ratio. Consequently this would lead to an active ActSR two-component system and higher *cyo* expression at constant or decreasing oxygen. Conversely, during stationary phase, metabolism slows down and the TCA enzymes are down-regulated (Nyström, 1994; Nyström *et al*., 1996). This would lead to lower levels of reducing equivalents leading to a lower quinol:quinone ratio if oxygen is not comparably decreased and consequently lower *cyo* transcript levels. However, the *actSR* mutant is necessary for stationary phase viability. Therefore, it must be at least basally active during stationary phase. This suggests that something independent of ActSR is contributing to the vastly decreased *cyo* transcript levels and Cyo activity during later stationary phase.

Surprisingly the *fbc* mutant had the same *cyo* expression pattern as the wild type albeit had 2-3 fold higher levels during aerobic growth. Similar to the wild type, *cyo* levels in this mutant are down-regulated during stationary phase compared to exponential phase and eventually the Cyo activity is undetectable in stationary phase. It was expected

that *cyo* levels would be maintained at high levels in the *fbc* mutant considering Cyo is the only viable aerobic respiratory option in this mutant.

The results suggest the cells have evolved to depend on the Fbc pathway for survival and particularly the Cta oxidase. In addition, the CoxM_P may have a minor role in stationary phase survival as the *cta* mutant maintained 10^2 c.f.u../ml whereas the double *coxM_P/cta* mutant became completely non-viable similar to the *fbc* mutant.

Many bacteria can utilize a variety of carbon sources, however their growth rate can vary depending on the carbon source being utilized. Because growth metabolism had a great impact on Cyo expression and utilization, the ability of the strains to grow in varying carbon sources was examined. Based on the growth curves, *R. etli* has a slower growth rate while utilizing the deoxy sugars, fucose and rhamnose, as sole carbon sources. Expression of *cyo* from cells grown in the medium containing either deoxy sugar as a sole carbon source was lower (approximately 5-fold) compared to cells grown in sucrose. This is consistent with the previous observation in that slower growth during stationary phase led to lower *cyo* expression. In the *fbc* mutant, *cyo* expression was also down-regulated from cells grown in fucose, but only about 2-fold compared to cells grown in sucrose. Despite only a 2-fold change in *cyo* expression, the *fbc* mutant had a much severe growth defect in fucose. This result suggests other modes of regulation, independent of transcriptional regulation, may be involved in prohibiting the use of Cyo in cells grown in fucose. Conversely, the *fbc* mutant was able to up-regulate *cyo* expression in rhamnose similar to the cells grown in sucrose. As opposed to fucose, the *fbc* mutant only had a slight growth defect when grown in rhamnose.

The growth defects in fucose observed in the cytochrome *c* oxidase mutants suggest the growth defect in the *fbc* mutant is due to lack of aerobic respiration. Similar to viability in stationary phase, the Cta oxidase is necessary for efficient aerobic growth in fucose given that the *cta* mutant had a severe growth defect. Surprisingly, the *fixN_P* mutant had a slight growth defect in fucose conditions even though the cells were growing in fully aerobic conditions. This suggests FixN_P may have a role in certain aerobic conditions and may be up-regulated in conditions independent of oxygen concentration. This is further supported that the double *cta*/*fixN_P* mutant had a growth defect similar to the *fbc* mutant which is more severe compared to the single *cta* mutant.

The stationary survival defect in the *fbc* mutant appeared to be in part by transcriptional regulation of *cyo*. In this chapter, a plasmid containing the *cyo* operon under a constitutive promoter (*nptII*) was constructed to see if it could help the *fbc* mutant overcome the survival defect. This plasmid, pZL43, was able to partially alleviate the viability in stationary phase in the *fbc* mutant. Furthermore, the addition of *cyo* operon partially alleviated the *fbc* mutant growth defect in fucose. Altogether, the results suggest that the inherited transcriptional regulation is trapping the mutant into these phenotypic defects.

Although the *fbc* phenotypes were partially alleviated with pZL43, the viability during stationary phase and growth in fucose was still worse compared to the wild type. The *cyo* transcript levels were approximately 5-fold higher in cells carrying this construct compared to the wild-type, yet the activity levels were similar. This may indicate unknown post-translational regulation, and may explain why this construct does not complement the *fbc* mutant to similar to wild-type levels. It is also possible that another

gene is required for optimum activity of the enzyme. For instance, *ctaB* encodes a farnesyl transferase required to convert heme B to heme O. Heme O is then what is incorporated in the Cyo oxidase. This gene has been shown to be required for Cyo activity in *Paracoccus denitrificans* (Zickermann *et al.*, 1997). A third possibility is the metabolic regulation of electron transfer between the Cyo and Fbc pathways. It has been shown, using *P. denitrificans* as a model, that the quinol:quinone ratio needs to be at least 40:60 in order for either crude membranes or whole cells to consume oxygen through the Cyo pathway (Otten *et al*., 1999), whereas the quinol:quinone ratio can be as low as 10:90 for the Fbc pathway to be functional. Based on these results, if the quinol:quinone ratio is low enough it will not make a difference if Cyo is present or not.

G. Summary/Conclusions

The work presented in this chapter indicates growth metabolism has a significant influence on oxidase expression and utilization. The results suggest that Cyo is a secondary respiratory option to the Cta oxidase in aerobic conditions and that Cyo is utilized in actively growing/dividing cells such as growth during exponential phase. In these growth conditions, the active metabolism may cause quinol:quinone ratio to increase thus leading for the need for multiple options to transfer electrons to oxygen. In response to the higher quinol:quinone ratio, the cell increases *cyo* levels and Cyo can then be used to transfer electrons to oxygen. Conversely, slower metabolism, such as growth in fucose minimal medium or growth in stationary phase, would drive the quinol:quinone ratio down. This would eliminate the need for a secondary respiratory option, and

consequently the lower quinol:quinone ratio causes *cyo* expression and utilization to decrease.

CHAPTER FIVE: DISCUSSION

A. Summary of phenotypes of terminal oxidases in *R. etli*

Based on our own BLAST searches, *R. etli* contained genes that encoded up to six different terminal oxidases: 5 cytochrome *c* oxidases and 1 quinol oxidase. The focus of this dissertation was on discovering the physiological role of the quinol oxidase, Cyo. Using a combination of genetic and molecular approaches, several phenotypes were discovered associated with this oxidase. In addition to Cyo, two cytochrome *c* oxidases, Cta and FixN_P, also had significant roles in certain conditions. The following is a description of the results and interpretations associated with each of these oxidases revealed in this work. **Table 2** also summarizes the key findings and phenotypes for each of these oxidases.

Cyo: The *cyo* mutant had a growth defect at low oxygen, low pH and low iron conditions suggesting the Cyo oxidase is important for adaptation and sustaining growth in each of these conditions. The *fbc* mutant (Cyo^+) could grow in a wide range of oxygen, pH and iron conditions, indicating Cyo is relatively versatile compared to the cytochrome *c* oxidases. Furthermore, the *cyo* genes were up-regulated in the wild type in the aforementioned conditions. The up-regulation of the *cyo* genes was dependent on the ActSR two-component system for any condition tested.

During the symbiosis, Cyo was utilized during the early stages such as infection as nodules harboring the *cyo* mutant contained less bacteria. In the mature nodule, Cyo appeared to be non-functional; the nodules harboring the *fbc* mutant were Fix^- and had undetectable levels of nitrogenase activity.

During growth, Cyo was active and functional during exponential phase, but became inactive during stationary phase. This correlated with the down-regulation of *cyo* during stationary phase in the wild type and the inability of the *fbc* mutant to maintain viability during stationary phase. Lastly, it was discovered that Cyo can be utilized in a variety of carbon sources in aerobic conditions but was down-regulated in rhamnose and fucose minimal-medium. Furthermore, the growth of the *fbc* mutant was slower compared to the wild type growth in rhamnose and fucose.

FixN_P: As expected, the high-affinity FixN_P was important for growth at low oxygen as the *fixN_P* mutant had a growth defect at low oxygen conditions, similar to the *fbc* mutant. In TY medium, it appears to be non-functional in fully aerobic conditions as a double *cta*/*cyo* mutant was unattainable. As already shown in *R. etli*, FixN_P is necessary for nitrogen fixation during the symbiosis (Girard *et al.*, 2000). The *fixN_P* mutant formed dark green nodules and contained about 8% nitrogenase activity compared to the wild type. Based on the literature, the FixN_P is regulated by Fnr proteins (Michiels *et* al., 1998; Girard *et al*., 2000; Lopez *et al.*, 2001; Moris *et* al., 2004; Granados-Baeza *et al.*, 2007;), suggesting this oxidase is exclusively utilized in low oxygen conditions. However, the *fixN_P* mutant also had a slight growth defect in fucose minimal medium in fully aerobic conditions. This result indicates FixN_P may have a role at higher oxygen concentrations in certain physiological conditions.

Cta: Similar to the *fbc* mutant, the *cta* mutant had a slight growth defect in fully aerobic conditions. It was the only oxidase mutant to exhibit a growth defect in TY aerobic conditions, indicating it is the main oxidase utilized in these conditions. In addition, Cta was also the most important oxidase during stationary phase as the *cta*

mutant had the greatest viability defect compared to the other oxidase mutants. Lastly, the Cta oxidase was important for growth in fucose as the *cta* mutant had a severe growth defect compared to the wild type. Despite being an important oxidase for each of these conditions, the transcriptional regulation of Cta is unknown.

The Cta oxidase does not appear to be utilized in low oxygen conditions in culture as the double *cyo/fixN_P* failed to grow at 0.1% oxygen. However, it appeared to be active during the symbiosis even though the oxygen levels inside the nodule are below 50 nM (Poole & Cook, 2000). The double *cta/fixN_P* mutant formed bright green nodules and had undetectable levels of nitrogenase activity, similar to the *fbc* mutant. As noted earlier, the single *fixN_P* mutant had approximately 8% residual nitrogenase activity. The *cta* mutant grew similarly to the wild type in both low pH and low iron conditions, suggesting Cta is not utilized in these conditions even in fully aerobic conditions. However, rather than the Cta itself having a defect at low pH and low iron, it is more likely the Fbc enzyme is defective in these conditions making the cell unable to transfer electrons to Cta (discussed later).

Oxidase (operon)	Conditions in which oxidase is utilized	Conditions in which oxidase is repressed	Regulator (Cue)
Cyo (*cyoABCD*)	*Intermediate O_2 (1-5%) Low pH Low Iron Symbiosis (Early Stages) Exponential Phase	Symbiosis (Mature Nodule) Fucose/Rhamnose Stationary Phase	ActSR (Quinone redox state)
Cta (*ctaCDGE*)	High O_2 (>5%) Stationary Phase Exponential Phase Fucose/Rhamnose Symbiosis	Low O_2 (<5% O_2) Low pH Low iron	Unknown
FixN_P (*fixNOQP*)	Low O_2 (<1%) Fucose/rhamnose Symbiosis	High O_2 (>5%)	Fnr (Oxygen)

Table 2: Summary of phenotypes and regulation of the terminal oxidases in this study.

*Capable of being utilized in a wide range of oxygen.

B. Properties of oxidases that influence their physiological roles

The classification and defined roles for oxidases is commonly based on their ability to bind oxygen. It is often assumed that the oxygen affinity is the major biochemical property of the oxidases that influences which oxygen concentrations the oxidases are utilized at. Based on this assumption, the growth curves of the mutants at varying oxygen concentrations suggests that Cyo has a higher affinity for oxygen compared to Cta. On the other hand, during the symbiosis the Cta seems to be more active compared to Cyo, even though the oxygen concentrations are in the nanomolar range. The conflicting results indicate other environmental factors, independent of oxygen, may influence the roles of oxidases. It is apparent from this dissertation that nutrient availability, pH and growth have a significant effect on oxidase expression and

utilization. Other properties of the oxidases, independent of oxygen affinity, need to be considered when trying to define their physiological roles.

The amount of energy generated by each of the aerobic respiratory pathways terminating at the different oxidases may influence the role of terminal oxidases. During the electron-transfer steps in each respiratory chain, protons are translocated across the membrane forming a proton gradient across the membrane. The potential energy in this proton gradient is utilized by the cell to generate ATP. Thus, the more protons that are translocated, the more energy the cell can potentially generate. It has been shown that the different respiratory pathways vary in their ability to generate a proton gradient. For instance, both Cyo and Cta translocate protons when they transfer electrons to oxygen (Puustinen *et al*., 1989; Hosler *et al*., 1992), but the Cyo pathway does not include the additional electron-transfer between quinol and cytochrome *c* catalyzed by Fbc (**Fig. 5**). Thus, there is more net protons pumped via the Cta pathway compared to the Cyo pathway, and consequently more energy is potentially generated in the Cta pathway. As opposed to Cta and Cyo, evidence in the literature suggests the FixN_P oxidase is a poor proton-pump. A recent study in *P. aeruginosa* (Arai *et al.*, 2014), showed the Cta pathway had the highest proton translocation efficiency (~6 H^+/O), whereas the FixN_P and Cyo pathways were similar (~4 H^+/O). The energy generated by the different pathways may explain why Cyo, which seems to have the capability of functioning at a wide-range of oxygen concentrations, is not the oxidase utilized in aerobic conditions. In addition, it also may explain why Cta is important during stationary phase as it may enable the cell to generate the most energy in nutrient limited conditions.

Arguably, the transcriptional regulation of the oxidases has the greatest influence on oxidase utilization. It is assumed that the bacteria have evolved their transcriptional regulation in order to express the oxidase of greatest benefit and/or turn-off other oxidases so they can efficiently adapt to different environments. For instance, FixN_P has higher affinity for oxygen but it cannot pump protons in comparison to Cta. Therefore, *R. etli* specifically regulates *fixN_P* to ensure it is only expressed in low oxygen conditions when the bacteria would preferentially deliver electrons through FixN_P as opposed to the Cta.

On the other hand, the transcriptional regulation of the oxidase could lead to certain phenotypes that mistakenly insinuate biochemical properties of that enzyme. For example, this work showed that Cyo was non-functional in stationary phase causing the *fbc* mutant to have a viability defect. By overexpressing the *cyo* operon in this mutant, the viability defect was alleviated. This result indicated the *fbc* mutant's viability was not strictly due to the inability of Cyo to function during stationary phase but rather the inherited transcriptional regulation of *cyo* prevented it from being expressed in stationary phase. As stated above, it is assumed Cyo has greater affinity for oxygen compared to the Cta based on the mutant growth curves at low oxygen. However, it is not known if this is due to Cta's affinity for oxygen and/or the down-regulation of *cta* preventing this pathway to be non-functional at low oxygen in culture.

C. Transcriptional regulatory mechanism of Cyo

This work identified the ActSR two-component system as a major transcriptional activator of Cyo based on the *actSR* mutant's inability to express *cyo* in any condition.

Initially four putative ActR sites were found in the 5' promoter region of *cyo*. Only one ActR site, the closest in proximity to the translation start site, was necessary for optimal promoter activity based on systematic deletions of the 5' promoter region. It has yet to be confirmed that ActR binds to this site and directly regulates *cyo* expression.

It was initially hypothesized that ActR was working through the housekeeping sigma70 factor based on a predicted promoter motif in the 5' region. However, the deletion of this motif did not affect *cyo* expression, indicating it is not the promoter of the *cyo* gene. In hindsight, this was not surprising because the necessary ActR DNA binding site was downstream of the predicted sigma70 promoter. To our knowledge, all of the ActR DNA binding sites in the literature have been upstream of the predicted promoter (Elsen *et al.*, 2004; Lindemann *et al.*, 2007; Torres *et a*., 2014). The result suggested that the ActR regulation of *cyo* is working through a different sigma promoter that is predicted to be downstream of the putative ActR DNA binding site.

R. etli, like many rhizobia, contain many sigma factors. In addition to the housekeeping sigma70 factor, *R. etli* contains two sigma32 (RpoH), two sigma54 (RpoN), and 18 extracellular (RpoE) factors. The NCBI database suggests a putative RpoN promoter in 5' promoter region of *cyo*. However this overlaps with the 3rd ActR site, in which the deletion did not cause an effect on *cyo* expression. RpoH is intriguing because it is necessary for growth in acidic conditions in *S. meliloti* (de Lucena *et al*., 2010). However, comparison of the microarray data at low pH in the wild type and an RpoH mutant did not indicate *cyo* to be under the RpoH regulon in this study. In addition, an RpoH promoter motif (López-Leal *et al*., 2014) is not apparent in 5' promoter region of *cyo*. There is a potential RpoE -10/-35 promoter motif that is

downstream of ActR in the *cyo* promoter region (**Fig. 29**). This promoter motif is also found in the 5' upstream region of *cyo* in both *R. leguminosarum* and *S. meliloti*. The location of the predicted RpoE promoter in relation to the ActR DNA binding site and translational start site are similar in all 3 species. All rhizobia have a plethora of RpoE sigma factors that are often involved in adaptation to various stress responses. The numerous RpoE sigma factors in rhizobia make it difficult to predict and identify which RpoE is necessary for *cyo* transcription.

A) *Rhizobium etli* CFN42

TGACCGGCAGTTGCGGATATATTTGGACTGAACATGCGCAGGGGCTAAAATCCTTCTATATTCCATCAGGAT
TTCAAAGCACTAGCGCCCGATGATTTTTGCCGCAGTGCGGCATGTTTGCTGCACTGCGACCTTCCGCCTCA
TGTCGCTATCCGGTTCAGTGCTTTAGTCGCGGACAAAACGAAACAACAAGAGCTTAGAGACGTGCCAAAAC
TCATGAAGTTTTCCCGCCTTCTATCCGTCTTGCCTCGCTGCTTTTCCTGGCAGGATGCAACATGGTGGTCA

B) *S. meliloti* 1021

GATCTTGACCAATCAACCGTTCATATCAAGGGGAGAAACGCGAAATAATGCGTTTCACGTCCTCACTGTCT
GCAAGCGGCGGAAGATGCTGCGTCGCAAAACGACTGCGGCGGATTGCTGCAGTGCGACCATCGACCTCATA
CCTTTCCCATCCACTCTACTTTAGTCGCAGGGCCGTCGAAACAAAATAGAGCTCCGAGCCGTGCCAGAACT
GTTGAAGTTTTCCCGCCGCCTCGCCGTTTTGCCGCTTTTCCTCGTGATGGCGGGATGCGACATGGTGGTGA

C) *R. leguminosarum* bv *viciae* 3841

TGGCTTGGCCGGCCCTTGCGGATATATTGGAACAAAACATGCGCTGGCGAAAGAATCCTTCTTGATTTCAT
CAGGATTCCAAAGCTGTAGTGCACCATCATTTGTGCCGCAGTGCGGCATGATTGCTGCACTGCGACCAAAC
ACCTCATGTCGCTATCGGGTTCAGTGCGTTAGTCGCGGAACGAACGAAACAACAAGAGCTTAGAGACGTGC
TAAAACTGGTGAAGTTTTCCCGCCTTCTATCCGTCTTGCCGCTGCTTTTCCTGGCAGGATGCAACATGGTG

Figure 29: Conserved RpoE-like motif in 5' *cyo* promoter region. The sequences contain approximately 275 BP upstream of the *cyo* orf in **(A)** *R. etli* CFN42 (RHE_PE00030), **(B)** *S. meliloti* 1021 (SMb21487), and **(C)** *R. leguminosarum* bv *vicae* 3841 (pRL110042). The putative ActR site is boldy underlined (___). The predicted sigma70 promoter, using Softberry and PePPER software (Soloyvev & Salomov, 2011; de Jong *et al*., 2012), is highlighted in light gray. The RpoE-like promoter is underlined with dots (….). The possible translation start sites are highlighted in black.

D. The quinol:quinone ratio may be a major cue for Cyo utilization

It is predicted that ActSR is more active in the presence of a higher quinol:quinone ratio in the cell based on the biochemical studies performed on the homologous RegBA two-component system in *Rhodobacter capsulatus* (Wu and Bauer, 2010). Thus, a higher ratio of quinol:quinone would theoretically lead to higher levels of *cyo* since ActSR is a transcriptional activator of *cyo*. The quinol:quinone ratio remains to be determined in *R. etli*, but, in many of the conditions tested, the level of *cyo* transcript can be theoretically linked to the quinol:quinone ratio. This regulation is well-suited for Cyo given that quinol is one of its substrates. The following is a list of phenotypes associated with Cyo and a description of how the quinol:quinone ratio may be impacted in these physiological conditions.

The upregulation of cyo upon the lowering of oxygen: At intermediate oxygen concentrations, the oxygen may be low enough for Cta to be non-functional but not low enough for FixN_P to be fully induced leading to an inefficient Fbc pathway. The inability of the cell to transfer electrons via Fbc would drive the quinol:quinone ratio up presumably leading to higher levels of *cyo* expression. Further lowering the oxygen concentration would fully induce FixN_P and electrons could be passed through the Fbc pathway again. As a consequence, the quinol:quinone ratio would decrease. This would explain why *cyo* expression starts to increase as the oxygen concentration is lowered below 5%, but then falls back to basal levels at 0.1%. Depicted in **Figure 30** is the proposed impact of low oxygen on the aerobic respiratory chains.

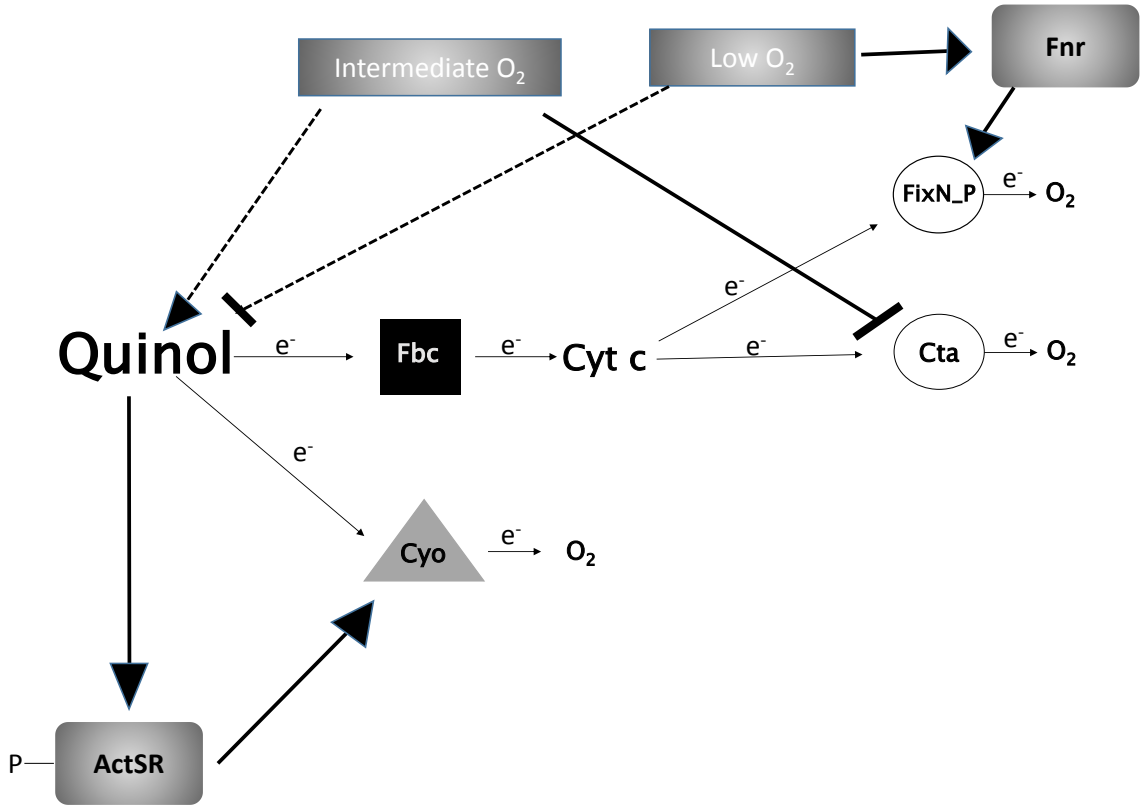

Figure 30: Predicted effects and mechanism of low oxygen on the aerobic respiratory chains in *R. etli*. Solid thick lines indicate direct regulatory effect, whereas the dashed lines indicate an indirect effect. The large arrows indicate induction or activation. Arrows are replaced by a bar when repression or inactivation is proposed. Proposed mechanism: The lowering of oxygen causes the Cta enzyme to be inactive. This causes a temporary build-up of quinol, increasing the quinol:quinone ratio. The increased quinol:quinone ratio promotes an active ActSR two component system leading to higher levels of *cyo* expression. As oxygen is further depleted, Fnr proteins will be active leading to higher levels of FixN_P. The FixN_P may cause the quinol:quinone ratio to return back to basal levels leading to lower levels of Cyo.

The upregulation of cyo at low pH: In both bacteria and eukaryotes, the optimum pH for cytochrome *c* and quinol oxidases is between 6.0 - 7.0 (Kitada & Krulwich, 1984; Fetter *et al.*, 1995; Verkhovskaya *et al.*, 1992; Thomas *et al.*, 1993). On the other hand, it has been shown in the alpha-proteobacterium, *Rhodobacter sphaeroides*, that the Fbc's optimum pH is approximately 8.0 for both quinol oxidation and cytochrome *c* reduction activity (Crofts *et al.*, 1999; Guergova-Kuras *et al.*, 2000; Zhou *et al.*, 2012). Lowering

the pH to 5.5 decreased the Fbc activity 9-fold in one study (Lhee *et al.*, 2010). Therefore, lowering the pH would cause an ineffective Fbc pathway leading to a higher quinol:quinone ratio, consequently leading to greater ActSR activity and higher levels of *cyo* expression (**Fig. 31**). The original hypothesis was the lower pH would keep the Cys residue of ActS in a reduced state promoting an active ActSR leading to higher levels of *cyo* expression. However, the cytoplasm is likely buffered in that it remains at neutral pH even in external acidic conditions (Wilks & Slonczewski, 2007). Conversely, the periplasm is not buffered. Therefore, the reaction between Fbc and cytochrome *c* likely happens at a pH similar to that of the external environment.

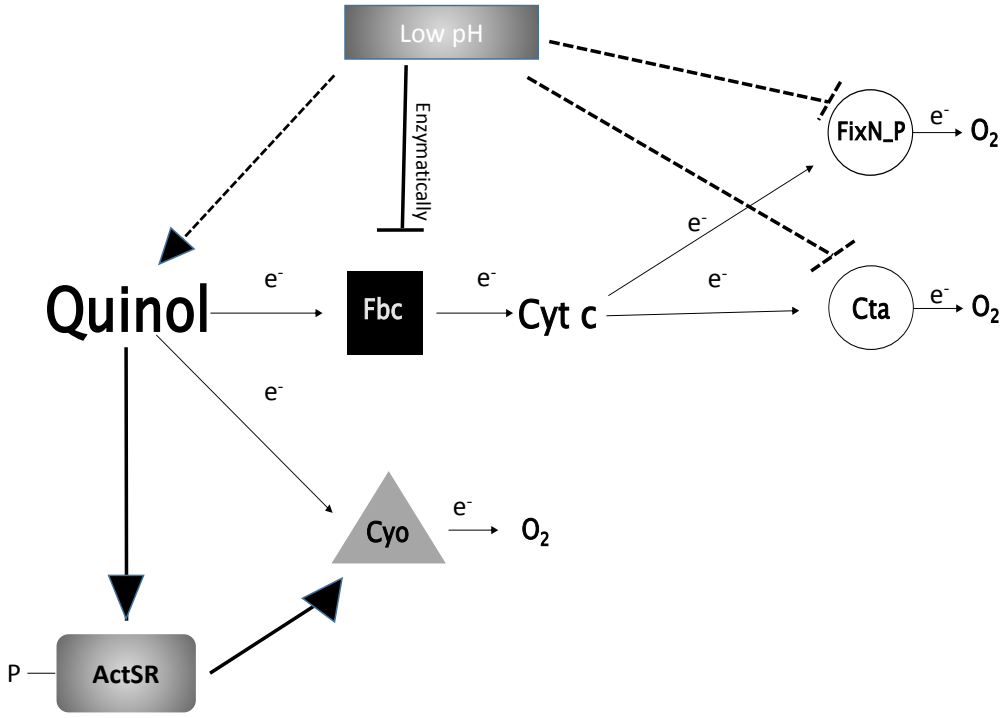

Figure 31: Predicted effects and mechanism of low pH on aerobic respiratory chains in *R. etli.* Solid thick lines indicate direct regulatory effect, whereas the dashed lines indicate an indirect effect. The large arrows indicate induction or activation. Arrows are replaced by a bar when repression or inactivation is proposed. At low pH, the Fbc enzymatic activity decreases, thus leading to a higher quinol:quinone ratio. The higher quinol:quinone ratio will promote an active ActSR leading to higher levels of *cyo*.

The upregulation of cyo in low iron: In *B. japonicum*, depleted iron levels cause a depletion of cytochrome c_1 levels (Gao & Brian, 2005). The depletion of cytochrome c_1 would consequently decrease the synthesis of Fbc (bc_1 complex). Thus, not only would Cyo be necessary for aerobic respiration in depleted iron conditions, but *cyo* would also be up-regulated via ActSR as a result from the indirect increase of the quinol:quinone (**Fig. 32**).

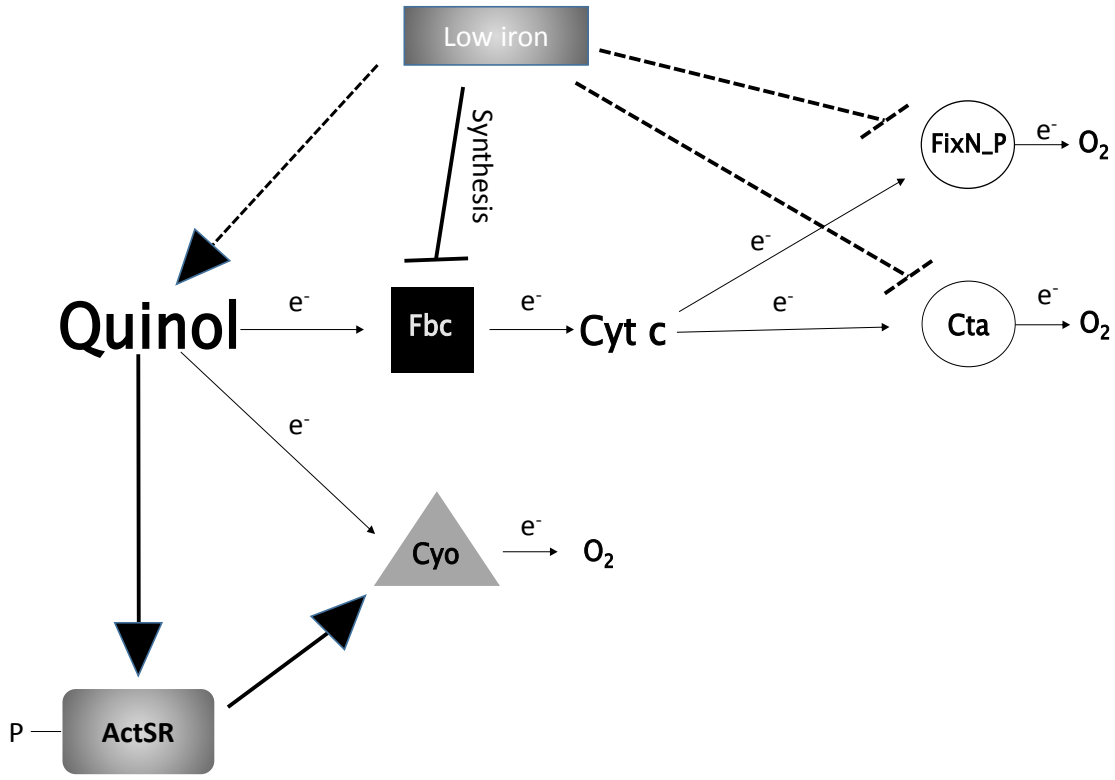

Figure 32: Predicted effects and mechanism of low iron on aerobic respiratory chains in *R. etli*. Solid thick lines indicate direct regulatory effect, whereas the dashed lines indicate an indirect effect. The large arrows indicate induction or activation. Arrows are replaced by a bar when repression or inactivation is proposed. At low iron, the depletion of cytochrome c_1 is leads to impaired synthesis of Fbc. As a result there would be a higher quinol:quinone ratio will promoting an active ActSR leading to higher levels of *cyo*.

The down-regulation of cyo in stationary phase (slow growth): During stationary phase, cells are in a non-growth state and in response the TCA enzymes are down-regulated and metabolism slows down (Vercruysse *et* al., 2011; Nyström, 1994; Nyström *et al*., 1996). Consequently less reducing equivalents (NADH) would be fed into the electron transport chain leading to a lower quinol:quinone ratio (**Fig. 33**). In *E. coli*, the quinol:quinone ratio is approximately .8 at mid-late exponential phase, whereas in stationary phase the ratio is near 0.3 (Bekker *et al.*, 2007). The lower quinol:quinone ratio would promote an inactive ActSR leading to lower levels of *cyo* expression.

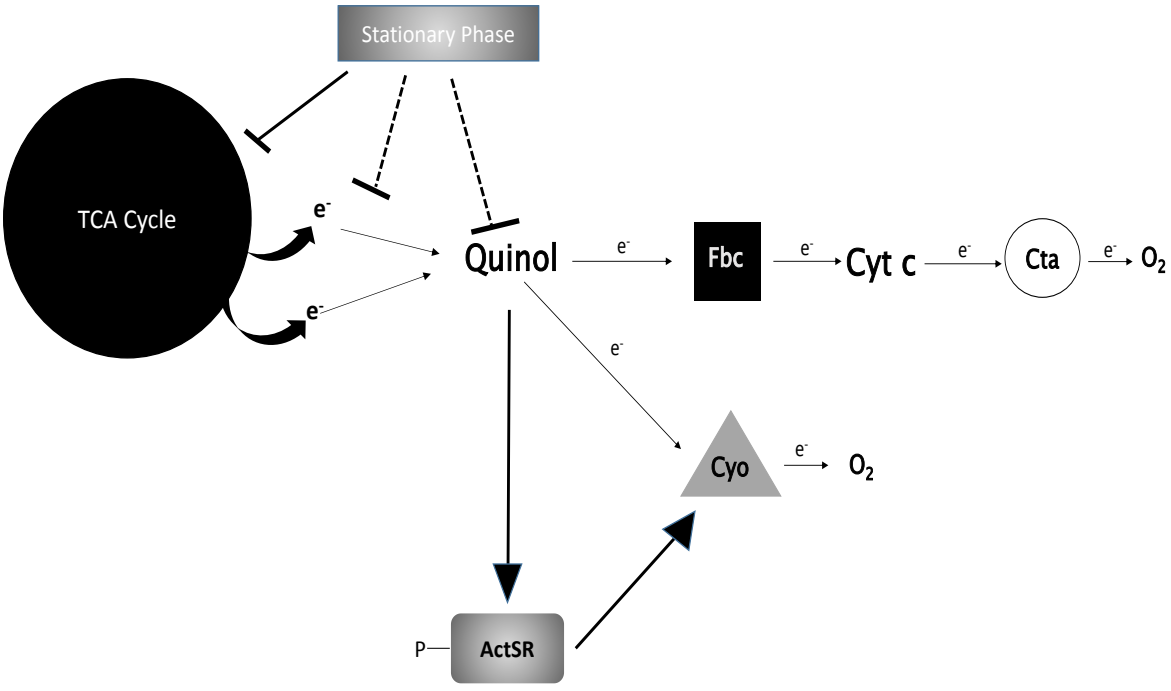

Figure 33: Predicted effects and mechanism of stationary phase on aerobic respiratory chains in *R. etli.* Solid thick lines indicate direct regulatory effect, whereas the dashed lines indicate an indirect effect. The large arrows indicate induction or activation. Arrows are replaced by a bar when repression or inactivation is proposed. During stationary phase, TCA enzymes are down-regulated and growth metabolism slows down. This would decrease the reducing equivalents being fed into the electron transport chain, thus leading to a lower quinol:quinone ratio. The lower quinol:quinone ratio would promote an inactive ActSR and lower *cyo* levels.

E. The conundrum of the *fbc* mutant

In the previous section, it is predicted that the quinol:quinone ratio is an important cue for Cyo regulation and utilization. Based on the models (**Fig. 30-33**), an *fbc* mutant would lead to a higher quinol:quinone ratio leading to higher levels of *cyo* expression. For many of the conditions tested this was the case, as the *fbc* mutant consistently had approximately 2-3 fold higher levels of *cyo* expression. However, Cyo activity and *cyo* expression was not sustained at a high level during stationary phase where *cyo* was down-regulated in both the wild type and *fbc* mutant. This suggests there may be additional transcriptional regulation independent of ActSR during stationary phase. Supporting this hypothesis is that the *actSR* mutant is necessary for stationary phase, indicating it does have at least some basal activity. Therefore, it is likely that the inability of the *fbc* mutant to upregulate *cyo* during stationary phase is not due to the inactivity of ActSR. One possible explanation is that the sigma factor (predicted to be RpoE) is not present during stationary phase, causing the lack of *cyo* expression. Alternatively, there may be an additional transcriptional regulator that shuts off *cyo* transcription.

The inability for the *fbc* mutant to fix nitrogen during symbiosis is also a conundrum. Despite Cyo being important for growth in low oxygen, low pH, and low iron, Cyo utilization is limited to the early developmental stages of the symbiosis. The original hypothesis was that ATP generation may be the problem, as the Fbc pathway has more electron-transfer steps in comparison to the Cyo pathway. However, recent data suggests the FixN_P pathway generates equal amounts of energy compared to the Cyo pathway because the FixN_P oxidase may be a poor proton-pump (Arai *et al.,* 2014).

Similar to stationary phase, other transcriptional regulatory factors may be involved during the symbiosis that prevent *cyo* from being turned on.

F. Overall ecological role for Cyo in *R. etli*

Overall, the Cyo pathway can be considered versatile compared to the cytochrome *c* oxidase pathways in that it is utilized at a wide-range of oxygen, pH and iron conditions. On the other hand, Cyo is restrictive in that it only seems to be utilized in cells that are actively dividing or growing. Therefore, we propose Cyo may be an important enzyme to help bacteria establish microbial communities in the soil ex planta while responding to varying environmental conditions.

CHAPTER SIX: METHODS

A. Bacterial strains and growth conditions

The bacterial strains utilized in the study are listed **Table 3**. For general growth of cultures, *R. etli* strains were grown at 30°C on a rotating shaker in TY liquid medium (0.5% tryptone [Difco Laboratories], 0.3% yeast extract [Difco], and 10mM $CaCl_2$). To follow the growth, the optical density (O.D.) at 600 nm was measured or for some cultures the c.f.u./ml was measured. *E. coli* strains were grown in LB liquid medium (1.0% tryptone, 0.5% yeast extract, and 0.5% NaCl) at 37°C on a rotating shaker (Sambrook *et al.*, 1989). Agar medium contained 1.5% Bacto agar (Difco).

Growth at various oxygen – Strains were originally grown in 3 ml of TY medium in 18 x 150 mm culture tubes and incubated in aerobic conditions. After 24 hours, cultures were diluted 1:200 in 5 ml of TY medium in 18 x 150 mm culture tubes. The diluted cultures were grown to stationary growth (between 24-48 hours) and diluted once again 1:200 into 5 ml of TY medium resting in 60 ml serum vials. The serum vials were then capped and the headspace was flushed with nitrogen gas. Using a sterile syringe needle, ambient air (assumed 21% O_2) was injected back into the headspace to make it 1% and 0.1% oxygen. For growth at 21% O_2, the vials were covered with aluminum foil. Cultures were then grown at 30°C on a rotating shaker. To follow growth, 400 µl was removed from the cultures using a sterile syringe needle and the (O.D.) at 600 nm was analyzed or the c.f.u./ml was measured. To ensure oxygen wouldn't be re-introduced into the cultures while sampling for growth, nitrogen gas was aspirated from a separate vial prior to sampling.

Growth at various pH - Strains were originally grown and subcultured in TY medium as described for growth at low oxygen. Fully grown cultures were diluted 1:100 in 3 ml of TY medium or YGM minimal medium (0.4 mM $MgSO_4$, 1.25 mM K_2HPO_4, 0.11% Na-glutamate, 0.4% glucose, 4 mM NH_4Cl, 1 mM $CaCl_2$, 0.15 mM $FeCl_3$, 1 µg biotin per ml, 1 µg thiamine per ml, 1 µg pantothenic acid per ml) in 13 x 100 mM culture tubes. 40 mM MES was added to the medium to buffer the pH to approximately 4.8. For growth at neutral pH in YGM medium, the pH was adjusted to 7.0 by titration with NaOH. The pH of the medium was tested after growth to ensure the pH was maintained at ± 0.2 pH unit of the un-inoculated medium. To follow growth, the O.D. at 600 nm was directly measured from the grown culture in the 13 x 100 mm tube.

Growth in various carbon sources – Strains were originally grown and subcultured as described for growth at low oxygen. Fully grown cultures were diluted 1:100 in 3 ml of minimal Y* medium (0.4 mM $MgSO_4$, 1,25 mM K_2HPO_4, 12.5 mM NH_4NO_3, 140 µM $FeCl_3$, 1 mM $CaCl_2$) with 3 mM of fucose, rhamnose, sucrose, glucose, succinate or malate as the sole carbon source in 13 x 100 mm culture tubes. To follow growth, the O.D. was directly measured from the culture in the 13 x 100 mm tube.

Growth at low iron – Strains were originally grown and subcultured to fully growth in TY medium as described above for growth at low oxygen. Fully grown cultures were diluted 1:150 in 3 ml of TY medium treated with 200 µM of the iron chelator, 2,2-dipyridl in 13 x 100 mm tubes. To follow growth, the O.D. was measured directly from the culture in the 13 x 100 mm tube.

B. Viability in stationary phase

Strains were originally grown in T.Y. medium to full growth in 3 ml of TY liquid medium in disposable 18 x 150 mm culture tubes. 250 µl of fully grown culture was used to inoculate 50 ml of T.Y. liquid medium in 125 ml Erlenmeyer flasks. Plating on T.Y. plates was used for determining viability in stationary phase. Each day after inoculation, 1 ml of culture was removed and serial diluted 10-fold from 10^{-1} to 10^{-5}. 100 µl of serial dilutions was plated on TY plates and the colonies were counted after 3 days of incubation at 30°C.

C. Materials and techniques for DNA isolation

Genomic DNA was isolated from *R. etli* strains using the GenElute™ Bacterial Genomic DNA Kit (Sigma) for use in cloning. *E. coli* NEB-5α (Invitrogen) competent cells were transformed (Hanahan, 1983), and plasmids were isolated using QIAprep spin miniprep kit (Qiagen). DNA was recovered from agarose gels using Gel/PCR DNA Fragments Extraction Kit (IBI Scientific) and modified with restriction enzymes purchased from New England BioLabs (NEB). Custom primers were synthesized by Eurofins MWG Operon (Huntsville, AL). DNA sequencing was performed by Functional Biosciences.

Table 3: Bacterial strains used in study

Strain	Description	Source[a]	Location
R. etli strains			
CE3	Wild-type strain, *str-1*	Noel *et al.*, 1984	C7 (A2)
CE3/pZL39	CE3 carrying pZL39, Tc^r	This Work	C37 (E7)
CE3/pZL73	CE3 carrying pZL73; Tc^r	This Work	C38 (B8)
CE3/pZL74	CE3 carrying pZL74; Tc^r	This Work	C38 (C1)
CE3/pZL75	CE3 carrying pZL75; Tc^r	This Work	C38 (C7)
CE3/pZL76	CE3 carrying pZL76; Tc^r	This Work	C38 (C8)
CE3/pZL77	CE3 carrying pZL77; Tc^r	This Work	C38 (C9)
CE3/pZL78	CE3 carrying pZL78; Tc^r	This Work	C38 (C10)
CE119	CE3 derivative; *str-1 fbcF::*Tn5	This Work	C25 (A4)
CE119/pKT104	CE119 carrying pKT104; Tc^r	KO, unpublished	C32 (C1)
CE119/pZL39	CE119 carrying pZL39; Tc^r	This Work	C37 (E8)
CE119/pZL43	CE119 carrying pZL43; Tc^r	This Work	C37 (H5)
CE119/pZL73	CE119 carrying pZL73; Tc^r	This Work	C38 (B10)
CE426	CE3 with mTn*5*SS*gusA11* at unknown site; *str-1* Sp^r	Duelli *et al.*, 2001	C13 (A4)
CE574	CE3 derivative; *str-1 cyoA*::Km	This Work	C34 (F6)
CE574/pZL34	CE574 carrying pZL34, Tc^r	This Work	C37 (C3)
CE574/pZL43	CE574 carrying pZL43; Tc^r	This Work	C37 (H2)
CE576	CE3 derivative; *str-1 cyoA*::Gm	This Work	C34 (G5)
CE579	CE3 derivative; *str-1 cyoB*::Gm	This Work	C35 (C3)
CE580	CE574 derivative; *str-1 cyoB*::Gm *cyoA*::Km	This Work	C35 (C4)
CE581	CE3 derivative; *str-1 fbcB*::Gm	This Work	C35 (D7)
CE582	CE3 derivative; *str-1 coxN*::CmΩ	This Work	C35 (E4)
CE583	CFNX641 derivative; *str-1 cyoB*::Gm *fixNf*::Sp *fixNd*::Km	This Work	C35 (E5)
CE584	CE582 derivative; *str-1 coxN*::CmΩ *cyoA*::Km	This Work	C35 (F2)
CE597	CE3 derivative; *str-1 ctaD*::Gm	This Work	C36 (I7)

Table 3 cont.

CE598	CE3 derivative; *str-1 ctaC*::Gm	This Work	C36 (I8)
CE599	CE3 derivative; *str-1 ctaC*::Km	This Work	C36 (I9)
CE601	CFNX641 derivative; *str-1 fixNf*::Sp *fixNd*::Km *ctaC*::Gm	This Work	C37 (B9)
CE602	CE598 derivative; *str-1 ctaC*::Gm *coxN*::CmΩ	This Work	C37 (B10)
CE603	CFNX641 derivative: *str-1 fixNf*::Sp *fixNd*::Km *coxN*::CmΩ	This Work	C37 (C1)
CE604	CE601 derivative: *str-1 fixNf*::Sp *fixNd*::Km *coxN*::CmΩ *ctaC*::Gm	This Work	C37 (C2)
CE605	CE3 derivative; *str-1 actSR*::Km	This Work	C37 (F8)
CE605/pZL39	CE605 carrying pZL39; Tc^r	This Work	C37 (H6)
CE605/pZL51	CE605 carrying pZL51; Tc^r	This Work	C37 (I2)
CE605/pZL54	CE605 carrying pZL54; Cm^r	This Work	C39 (J1)
CE605/pZL73	CE605 carrying pZL73; Tc^r	This Work	C38 (B9)
CE605/pZL74	CE605 carrying pZL74; Tc^r	This Work	C38 (C2)
CE605/pZL75	CE605 carrying pZL75; Tc^r	This Work	C38 (D1)
CE605/pZL76	CE605 carrying pZL76; Tc^r	This Work	C38 (D2)
CE605/pZL77	CE605 carrying pZL77; Tc^r	This Work	C38 (D3)
CE605/pZL78	CE605 carrying pZL78; Tc^r	This Work	C38 (D4)
C606	CE3 derivative; *str-1 actSR*::Gm	This Work	C37 (F9)
CE607	CE574 with mTn*5*SS*gusA11* at unknown site; *str-1 cyoA*::Km; Sp^r	This Work	C37 (J4)
CE608	CE3 derivative; *str-1 actS*::Km	This Work	C38 (A5)
CE609	CE3 derivative; *str-1 actS*::Gm	This Work	C38 (A6)
CFNX641	CE3 derivative; *str-1 fixNf*::Sp *fixNd*::Km	Girard *et al*., 2000	C30 (H5)
E. coli strains			
NEB-5α	Competent strain used for cloning	New England Biolabs	NA
MT616	*pro thi endA hsdR supE44 recA-J6* pRK2013Km::Tn*9*	Finan *et al*, 1986	C20 (A3)

a. KO, Kristylea Ojeda

D. Mutant Construction

Using the designed primers listed in **Table 4**, the gene and approximately 500 bp of flanking sequence was amplified by PCR. The PCR products were inserted into the TA cloning vector, pCR2.1. Plasmids were then digested using the restriction enzymes (that were tagged on the 5' end of the designed primers) and then inserted into plasmid pEX18Tc (Hoang *et al.*, 1998). Either the gentamicin resistant cassette (Gm) from plasmid pUCGm, the kanamycin resistant cassette (Km) from plasmid pBSL86, or the omega chloramphenicol resistant cassette (Cm) from pBSL119 was inserted (Schweizer, 1993; Alexeyev, 1995, Alexeyev *et al*.,1995). The plasmids used for cloning and mutagenesis are listed in **Table 5.**

Plasmids carrying the mutated ORFs were transferred into *R. etli* CE3 by using the plasmid-mobilizer strain MT616 on TY agar plates (Glazebrook and Walker, 1991; Finan *et al*.,1986). 200 µl of MT616, 200 µl of plasmid and 800 µl of *R. etli* was mixed in a tube and spread on TY plates. After 24-hour incubation, cells were scraped, diluted (1:100, 1:1000, 1:10,000) and spread on TY agar plates including the selected antibiotic resistant marker. Double-crossover recombinants were screened on TY agar plates supplemented with 1 µg of tetracycline/ml and on TY agar plates with 8% sucrose. Of the recombinants that were sensitive to 1 µg tetracycline/ml and resistant to 8% sucrose on TY agar, it was then verified by PCR that the colonies contained only the mutant allele and the wild-type allele was absent. The mutant constructs are included in **Table 3.** The *fbcF* mutant (CE119) was isolated previously in the lab via transposon mutagenesis. The *fixN_P* mutant was generously provided by L. Girard (Girard *et al.*, 2000).

cyoA cloning and mutagenesis – The *cyoA* mutant (CE574) was designed to insert a non-polar antibiotic cassette into the *SalI* site (nucleotides 39576-39581 of the *R. etli* CFN42 genome) of *cyoA*. The *cyoA* orf and flanking sequence (nucleotides 38,357-40,666) was amplified by PCR using cyoA-XbaI and cyoA-HndIII primers (Table 4). The PCR product was ligated into pCR2.1 creating plasmid pZL1. pZL1 was then digested with *XbaI* and *HndIII* to release the 2.3 kb fragment and ligated into pEX18Tc to create plasmid pZL2. pZL2 was then digested with *SalI* and a Km cassette was inserted at this stie to create plasmid pSY6. pSY6 was transferred to *R. etli* CE3 by triparental mating to create *R. etli* CE574.

cyoB cloning and mutagenesis – The *cyoB* mutant (CE579) was designed to delete 1058 bp of *cyoB* orf. The *cyoB* orf and flanking sequence (nucleotides 36,347 – 39,314) was amplified by PCR using cyoB-XbaI and cyoB-HndIII primers (Table 4). The PCR product was ligated into pCR2.1, creating plasmid pZL4. pZL4 was digested with *XbaI* and *HndIII* to release 3.0 kb fragment and ligated into pEX18Tc creating pZL5. pZL5 was digested with *SalI,* which cut at nucleotides 38,252-38,247 and 37,188-37,183 removing 1,058 bp of *cyoB,* and a Gm cassette was inserted at the *SalI* sites creating pZL6. pZL6 was transferred to *R. etli* CE3 by triparental mating, creating CE579.

actSR cloning and mutagenesis - The *actSR* mutant (CE605) was designed to delete 1148 bp of *actS* and additionally 511 bp of actR. The initial 181 bp of *actSR* together with 566 bp of 5' upstream sequence (nucleotides 59,093 to 58,347 of the *R. etli* CFN42 genome) was amplified by PCR using ActSup-EcoRI and ActSup-XbaI primers (listed in Table S1). The PCR product was then ligated into PCR2.1, creating pZL45. In addition, the last 65 bp of *actR* together with 586 bp of 3' downstream sequence

(nucleotides 56,614 to 55,964 of the *R. etli* CFN42 genome) was amplified by PCR using ActRdwn-XbaI and ActRdwn-HndIII primers (Table 4) and ligated into PCR2.1 creating pZL46. pZL45 was then digested with *EcoRI* and *XbaI* to release 747 bp fragment and pZL46 was digested with *XbaI* and *HndIII* to release 651 bp fragment. Both of these fragments were ligated into pEX18Tc ((Hoang *et al*.,1998), creating plasmid pZL47. pZL47 was then digested with *XbaI* and a Km resistance cassette (Alexeyev, 1995) was inserted into this site to create plasmid pZL48. pZL48 was transferred into *R. etli* CE3 by tri-parental mating to construct *R. etli* CE605.

ctaC cloning and mutagenesis – The *ctaC* mutant (CE598) was designed to delete 754 bp of *ctaC*. The initial 74 bp of *ctaC* together with 545 bp of 5' upstream sequence (nucleotides 1,000,120 – 1,000,738 of the *R. etli* CFN42 genome) was amplified by PCR using CtaCup-EcoRI and CtaCup-XbaI primers (listed in Table 4). The PCR product was then ligated into pCR2.1, creating pZL27. In addition, the last 54 bp of *ctaC* together with 643 bp of 3' downstream sequence (nucleotides 1,001,496 - 1,002,192 of the *R. etli* CFN42 genome) was amplified by PCR using CtaCdwn-XbaI and CtaCdwn-HndIII primers (Table 4) and ligated into pCR2.1 creating pZL28. pZL27 was then digested with *EcoRI* and *XbaI* to release 635 bp fragment and pZL28 was digested with *XbaI* and *HndIII* to release 713 bp fragment. Both of these fragments were ligated into pEX18Tc, creating plasmid pZL29. pZL29 was then digested with *XbaI* and a Gm resistance cassette was inserted into this site to create plasmid pZL31. pZL31 was transferred into *R. etli* CE3 by tri-parental mating to construct *R. etli* CE598.

coxN cloning and mutagenesis - The *coxM_P* mutant (CE582) was designed to insert a polar antibiotic cassette into the *PstI* site (nucleotides 2,730,029-2,730,024 of the

R. etli CFN42 genome) of *coxN*. The *coxN* orf and flanking sequence (nucleotides 2,728,717-2,730,971) was amplified by PCR using coxN-XbaI and coxN-HndIII primers (Table 4). The PCR product was ligated into pCR2.1 creating plasmid pZL9. pZL9 was then digested with *XbaI* and *HndIII* to release the 2.2 kb fragment and ligated into pEX18Tc to create plasmid pZL11. pZL11 was then digested with *PstI* and a Cm cassette was inserted at this site to create plasmid pZL12. pZL12 was transferred to *R. etli* CE3 by triparental mating to create *R. etli* CE582.

Construction of double/triple mutants – Plasmid pZL6 (*cyoB*::Gm) was transferred into *R. etli* CFNX641 to create *R. etli* CE583 (*cyo/fixN_P* mutant). Plasmid pSY6 (*cyoA*::Km) was transferred into *R. etli* CE582 to create *R. etli* CE584 (*cyo/coxM_P* mutant). Plasmid pZL31 (*ctaC*::GM) was transferred into *R. etli* CFNX641 to create *R. etli* CE601 (*cta/fixN_P* mutant). Plasmid pZL12 (*coxN*:Cm) was transferred into *R. etli* CE598 and *R. etli* CFNX641 to create CE602 (*cta*/*coxM_P*) and CE603 (*coxM_P/fixN_P)* respectively. Plasmid pZL12 was also transferred into *R. etli* CE601 to create CE604 (*coxM_P*/*fixN_P/cta* mutant). Double mutants of *cta*/*cyo* and *cyo*/*fbc* were unattainable aerobic conditions.

E. Expression Constructs

Using designed primers listed in **Table 4,** *cyoA* and the *actSR* operon containing their ribosome binding site and promoter regions were amplified by PCR. The PCR products were then digested using restriction enzymes and inserted into pFAJ1708 (Dombrecht *et al*., 2001). The *fbc* mutant was complemented previously in the lab using

the expression vector pFAJ1700 (without *nptII* promoter) instead of pFAJ1708 (Ojeda and Noel unpublished). The expression constructs are included in **Table 5.**

Construction of pZL34 for complementation of cyo mutant (CE574) – To complement the *cyoA* mutant (CE574), the *cyoA* orf including flanking sequence (nucleotides 38,815-40,110) was amplified by PCR using cyoA-BamHI and cyoA-PstI primers (Table 4). The DNA PCR product was ligated into pCR2.1, creating plasmid pZL23. pZL23 was then digested with *BamHI* and *XbaI* to release 1.3kb fragment and ligated into pFAJ1708 creating plasmid pZL34. pZL34 was then introduced to *R. etli* CE574 by triparental mating.

Construction of pZL51 for complementation of actSR mutant (CE605) - The entire *actSR* operon including flanking sequence (nucleotides 59,093 to 55,964 of the *R. etli* CFN42 genome) was amplified using the primers, ActSR-XbaI and ActSR-BamHI (Table 4). The DNA PCR product was ligated into pCR2.1, creating pZL50. pZL50 was then digested with restriction enzymes, *XbaI* and *BamHI*, to release the 3.2 kb fragment containing *actSR* and was ligated to pFAJ1708. The resulting plasmid, pZL51, was transferred into *R. etli* CE605 (*actSR* mutant) by triparental mating as described above.

Construction of pKT104 for complementation of fbc mutant (CE119) – pKT104 was constructed previously in the lab (Noel and Ojeda, unpublished). The *fbc* operon including flanking sequence (nucleotides 3,179,479-3,175,379) was amplified by PCR and cloned into pCR2.1 creating pKT103. pKT was then digested with restriction enzymes, *PstI* and *SacI*, to release a 3.9 kb fragment (nucleotides 3,179,479 – 3,175,633 of *R. etli* CFN42 genome) and ligated into pJB21 (pFAJ700 derivative). The resulting plasmid, pKT104, was transferred into *R. etli* CE119 by triparental mating.

Construction of pZL43 for overexpression of cyo operon – The *cyo* operon (*cyoABCD*) including RHE_PE00026 (nucleotides 40,126-34,933) was amplified by PCR using primers, CyoOperon-XbaI and CyoOperon-KpnI (**Table 4).** The PCR product was ligated into pCR2.1, creating plasmid pZL38. pZL38 was digested with *XbaI* and *KpnI* to release 5.1 kb fragment and was ligated to pFAJ1708. The resulting plasmid, pZL43, was transferred into *R. etli* CE119 (*fbc* mutant) and *R. etli* CE574 (*cyo* mutant).

F. Promoter P*cyo*::*lacZ* transcriptional fusion

In this study, two transcriptional fusions were constructed. Originally, a fragment containing 331 bp of 5' upstream sequence of *cyoA* (nucleotides 40,020 – 40, 351) was amplified from *R. etli* CE3 genomic DNA by PCR, using PCyoA-KpnI and PCyoA-XbaI primers (**Table 4**). The PCR product was then inserted into the TA cloning vector, PCR 2.1 creating pZL36. pZL36 was cut with *XbaI* and *KpnI* restriction enzymes to release fragment and insert into the pMP220 plasmid (Spaink *et al*., 1987) resulting in pZL39. The same approach was used to construct pZL73, which contains an additional 125 bp (nucleotides 40,020 – 40,490) upstream of *cyoA* open reading frame. DNA was amplified by PCR using PcyoA-KpnI-2 and PcyoA-XbaI primers (**Tabl**e **4**), and then ligated into pCR2.1 creating pZL67. pZL67 was then cut with *XbaI* and *KpnI* to release fragment and ligate into pMP220 to create pZL73. pZL39 or pZL73 was transferred into CE3, CE605 and CE119 using the MT616 plasmid-mobilizer strain. The plasmids used for cloning and fusing the P*cyoA* with *lacZ* are included in **Table 5**.

G. Deletion of putative regulatory elements in *cyo* promoter

The Q5 Site-Directed Mutagenesis Kit (New England BioLabs) was used to delete the various regulatory elements. Plasmid pZL73 (p*cyoA:lacZ*) was used as a template. The amplification reaction mixture (25 µl) contained:1x Q5 Hot Start 2x Master Mix, 0.5 µM forward primer, 0.5 µM reverse primer, and 25 ng of template DNA. The primers used for each of the deletions are listed in **Table 4**. Reactions were initially incubated at 98^{o}C for 30 sec, followed by a 25-cycle protocol (98^{o}C for 10 sec, 50-72^{o}C for 30 sec (annealing temperature of primers), 72^{o}C for 5.5 min), followed by 72^{o}C for 2 min. After amplication, the PCR reaction was treated with a mutienzyme solution, KLD (kinase, ligase, DpnI) for 5 minutes at room temperature. The 10µl reaction mixture for the step was: 1 µl of PCR product, 5 µl 2X KLD reaction buffer (1x final conc), 1 µl 10X KLD enzyme mix (1x final conc), and 3 µl nuclease free water. 5 µl of this reaction was then used to transform NEB-5α competent cells. Colony PCR was used to initially screen for deletions, and then confirmed by sequencing. The resulting constructs (pZL74-pZL78) are listed in **Table 5.**

H . Beta-galactosidase measurements

The beta-galactosidase activity was measured essentially as previously described (Sambrook *et al.*, 1989). Prior to harvesting the cells, the O.D.$_{600}$ was determined. 1 ml of culture was harvested and washed twice with cold Z-buffer (0.06M Na_2HPO_4, 0.04M NaH_2PO_4, 0.01M KCl, 0.001M $MgSO_4$, and 0.05M β-mercaptoethanol). After washing, cell pellets were stored immediately at -20^{o}C until testing. Cells were thawed on ice and re-suspended in 300 µl of Z-buffer and added to 2.7 ml of Z-buffer in a 13x100 mm

culture tube. 6 drops of chloroform and 3 drops of 0.1% SDS were added to the tubes and vortexed for 10 seconds. The tubes were then stored at 30°C for 10 minutes. After 10 minutes, 600 µl of *o*-nitrophenyl-β-D-galactopyranoside (ONPG) at 4 mg/ml concentration was added to the tube. The absorbance at 420 nm and 550 nm was recorded at different time points (min). Based on these absorbance readings (420 and 550 nm), the original $O.D._{600}$ of the culture, and the time (*t*) after ONPG was added the activity was calculated in Miller Units: $1000 \times (A_{420} - (1.75 \times A_{550}))/ (t \text{ (min)} \times 0.1 \times O.D._{600})$. The wild type (CE3) carrying the empty vector, pMP220, was tested as a negative control.

I. RT-qPCR

RNA extraction - Cultures were pelleted and immediately frozen in dry ice and stored at -80 °C. Typically, 3 ml of cells pelleted for RNA extraction. When ready for testing, cells were thawed on ice and RNA was extracted using NucleoSpin® RNA II kit (Macherey Nagel). For the final step, the RNA was eluted with 40 µl of RNase free water. To further purify the RNA from DNA contamination, the RNA was further treated with rDNase, following the protocol provided by Macherey Nagel (pages 40-41, Feb 2013 Revision)

cDNA synthesis (Reverse transcription reaction) - The RNA was converted into cDNA using an EasyScript™ cDNA synthesis kit (MidSci) with the specific reverse primer for the gene of interest. Each 20 µl reaction contained 4 µl of RNA (0.8-2.0 µg total), 1 µl of dNTP (500 µM final) , 4 µl of 5x RT buffer (1x final), 0.5 µl of RNasin (20U final), 0.3 µl of gene specific reverse primer (0.15 µM final) and 1 µl of reverse

transcriptase (200U final). As a negative control, water was added instead of the reverse-transcriptase for each RNA sample. The reactions were incubated at 42°C for 60 minutes, followed by 85°C for 5 min, and then at 4°C until taken out of the PCR machine. cDNA samples were stored at -20°C until further testing.

qPCR - cDNA products were quantified by real-time PCR using EvaGreen qPCR Mastermix (MidSci), gene specific primers and the BioRad iCycler®. Reactions were carried out using a semi-skirted thin wall plate (MidSci). Each well contained a 25 µl reaction consisting of 12.5 µl of Evagreen mastermix, 0.5 µl of each gene specific primer (0.2 µM final), 9 µl of water (GDW) and 2.5 µl of sample (cDNA or standard plasmid). For analyzing *cyo* expression, cyoBRT-Forward and cyoBRT-Reverse primers were designed to detect a 118 bp fragment in *cyoB* (**Table 4**). This 118 bp fragment was cloned into pCR2.1 creating plasmid pZL22. pZL22 was serial diluted 10^{1} to 10^{-6} and used to determine a standard curve. Samples were initially denatured at 95° for 10 minutes followed by a 40-cycle amplification protocol (95° for 15 sec, 60° for 60 sec). After the PCR, a melt curve was performed to ensure only one amplification product was present. The amount of cDNA present in the sample was calculated using the standard curve generated from the pZL22 plasmid.

The expression of the *16sRNA* gene was analyzed using 16sRNART-Forward and 16sRNART-Reverse primers (**Table 4**) that detected a 101 bp fragment in the *16sRNA* gene. The 101 bp fragment was cloned into pCR2.1 resulting in pZL35, which was used to generate a standard curve. The PCR protocol and reaction mixtures were identical to that to analyze *cyoB* expression. *cyoB* expression was normalized to the expression of the *16sRNA* gene or to the original RNA concentration used in the cDNA reaction.

Table 4: Primers used in study

Gene(s) (Purpose)	Forward Primer[a]	Reverse Primer[a]
actS –up (Mutagenesis)	ActSup-EcoRI (ActSup.fwd) GCGAATTCAGGAGGTACTGCAGCTT	ActSup-XbaI (ActSup.rev) GTTCTAGATAGCGATCAGCGGCAAC
actR-down (Mutagenesis)	ActRdwn-XbaI (ActRdwn.fwd) GCTCTAGACACGCCGGCTCAATATG	ActRdwn-HndIII (ActRdwn.rev) GTAAGCTTGCGAGGAATCCGTCTGC
cyoA (Mutagenesis)	cyoA-XbaI (cyoA up) GATCTAGAAGCGTGCCGGTCAGCCT	cyoA-HndIII (cyoAdwn) GTAAGCTTCGGCGGTCGTCATCCAG
cyoB (Mutagenesis)	cyoB-XbaI (cyoBup) GCTCTAGACGCGACGCTTATCTGAA	cyoB-HndIII (cyoBup) GCAAGCTTATCAGCGTGATCAGCCA
ctaC –up (Mutagenesis)	ctaCup-EcoRI (ctaC2upfragup) GCGAATTCATGCTGGCAGTCACGAG	ctaCup-XbaI (ctaC2upfragdwn) GTTCTAGAGGCTGGTCGGCATATGT
ctaC-down (Mutagenesis)	ctaCdwn-XbaI (ctaC2dwnfragup) GCTCTAGAATGGCCGCAACCGATGG	ctaCdwn-HndIII (ctaC2dwnfragdn) GTAAGCTTGAGGCGCCGGCAATGTG
ctaD (Mutagenesis)	ctaD-XbaI (ctaD2up) GCTCTAGATCCGCTCGCCTTCGATT	ctaD-HndIII (ctaD2dwn) GTAAGCTTCACCGCCGATGACGATG
coxN (Mutagenesis)	coxN-XbaI (coxNup) GCTCTAGATATTGCTGCGTTCCGTC	coxN-HndIII (coxNdwn) GCAAGCTTCCGCTCAATGCCAAGAT
fbcB (Mutagenesis)	fbcB-XbaI (fbcBup) GCTCTAGATGATCGGCACCTGCACC	fbcB-HndIII (fbcBdwn) GCAAGCTTCCGAGTTCGTCGAGCGT
actSR (comp.)	ActSR-XBAI (ActSup.fwd) GCTCTAGAAGGAGGTACTGCAGTT	ActSR-BamHI (ActRdwn.rev) GTGGATCCGCGAGGAATCCGTCTGC
cyoA (Comp.)	cyoA-BamHI GCGGATCCCGGTTCAGTGCTTTAGT	cyoA-PstI TGCTGCAGTTCAGGAGGTCAGGATT
cyoABCD (*cyo* operon)	CyoOperon-XbaI (CyoOP.Fwd2) GCTCTAGATCGCTATCCGGTTCAGT	CyoOperon-KpnI (CyoOP.Rev) GAGGTACCAGCAGTAGCGGACATCA
P*cyoA*1 (*lacZ* fusion)	PCyoA-KpnI (cyoprom2up) GCGGTACCTTCATCATCACGGCTCA	PCyoA-XbaI (cyoprom2dwn) GATCTAGACAGCGGCAAGACGGATA
P*cyoA*2 (*lacZ* fusion)	PCyoA-KpnI-2 (CyoP3up) GCGGTACCTTCAAGCGACGACGA	PCyoA-XbaI (cyoprom2dwn) GATCTAGACAGCGGCAAGACGGATA
cyoB (q-RT-PCR)	cyoBRT-Forward (cyoBRT1up) TGTTCGGCTATGCCTCAATG	cyoBRT-Reverse (cyoBRT1dwn) CCGAAGAAGGAATTGACGCT
16sRNA (q-RT-PCR)	16sRNART-Forward (16S.RNA2up) TGGAGTATGGAAGAGGTGAG	16sRNART-Reverse (16SRNA2dwn) TCAGTAATGGACCAGTGAGC
P*cyoA* (R2-R4 deletion)	ΔR2-R4 Forward (CyoPDelFwd) ATGTCGTATCCGGTTCAGTGCTTT	ΔR2-R4 Reverse (CyoPDelRev) TAGTGCTTTGAAATCCTGATGGAAT
P*cyoA* (R3 deletion)	ΔR3 Forward (CyoPdelA3.Fwd) ACTGCGACCTTCCGCCTCATGTCGC	ΔR3 Reverse (CyoPdelA3-4.Rev) CTGCGGCAAAAATCATCGGGCGCTA
P*cyoA* (R4 deletion)	ΔR4 Forward (CyoPdelA3-4.Fwd) ATGTCGCTATCCGGTTCAGTGCTTT	ΔR4 Reverse (CyoPdelA4.Rev) GTGCAGCAAACATGCCGCACTGCGG
P*cyoA* (R3-R4 deletion)	ΔR3-R4 Fwd (CyoPdelA3-4.Fwd) ATGTCGCTATCCGGTTCAGTGCTTT	ΔR3-R4 Rev(CyoPdelA3-4.Rev) CTGCGGCAAAAATCATCGGGCGCTA

Table 4 Cont.

P*cyoA* (σ70 deletion)	Δσ70 Forward (CyoPdel70.Fwd) CCATCAGGATTTCAAAGCACTAGCG	Δσ70 Reverse (CyoPdel70.Rev) TCCGCAACTGCCGGTCAGGCCAGCA

a. In parentheses is the actual name that was given to the primer when ordered by the lab.

Table 5: Plasmids used in study

Plasmid	Description	Source[a]	Location
pBSL86	*nptII* (Km) gene cassette, Km^r	Alexeyev, 1995	C21 (D5)
pBSL119	Cm omega cassette; Cm^r	Alexeyev *et al.*, 1995	C18 (E4)
pCAM111	Carries mTn*5SSgusA11*; Sp^r Amp^r	Wilson *et al*., 1995	C20 (D4)
pCR2.1	TA cloning vector for PCR products; Amp^r Km^r	Invitrogen	
pEX18Tc	Suicide plasmid; Tc^r	Hoang *et al*., 1998	C21 (F2)
pFAJ1700	Expression vector; Tc^r	Dombrecht *et al*., 2001	C19 (C3)
pFAJ1708	Expression vector with *nptII* promoter; Tc^r	Dombrecht *et al*., 2001	C19 (C7)
pJBC1	Expression vector; Cm^r	Bouhenni *et al*., 2010	C36 (C1)
pKT104	3.9 kb *PstI, SacI* fragment of *fbc* operon in pFAJ1700.	KT	C32 (A6)
pMP220	*lacZ* fusion vector; Tc^r	Spaink *et al*., 1987	C18 (G1)
pSY6	Km cassette inserted in *SalI* site of *cyoA* in pEX18Tc	SY	C34 (C7)
pUCGm	*aaC1* gene cassette (Gm); Gm^r	Schweizer, 1993	
pZL1	2.3 Kb PCR product of *cyoA* in pCR2.1	ZL	C34 (C6)
pZL2	2.3 Kb *XbaI, HndIII* fragment of *cyoA* in pEX18Tc	ZL	C34 (F5)
pZL3	Gm cassette inserted in *SalI* site of *cyoA* in pEX18Tc	ZL	C34 (G4)
pZL4	3.0 Kb PCR product of *cyoB* in pCR2.1	ZL	C34 (G6)
pZL5	3.0 Kb *XbaI, HndIII* fragment of *cyoB* in pEX18Tc	ZL	C35 (A4)
pZL6	Gm cassette inserted in *SalI* site of *cyoB* in pEX18Tc	ZL	C35 (A5)
pZL7	1.8 Kb PCR product of *fbcB* in pCR2.1	ZL	C35 (C2)
pZL8	1.8 Kb *XbaI, HndIII* fragment of *fbcB* in pEX18Tc	ZL	C35 (D1)
pZL9	2.2 Kb PCR product of *coxN* in pCR2.1	ZL	C35 (D2)
pZL10	Gm cassette inserted into *SphI* site of *fbcB* in pEX18Tc.	ZL	C35 (D3)

Table 5 cont.

pZL11	2.2 Kb *XbaI, HndIII* fragment of *coxN* in pEX18Tc	ZL	C35 (D4)
pZL12	Cm omega cassette inserted into *PstI* site of *coxN* in pEX18Tc	ZL	C35 (D5)
pZL17	2.7 Kb PCR product of *ctaD* in pCR2.1	ZL	C36 (C1)
pZL18	2.7 Kb *XbaI, HndIII* fragment of *ctaD* in pEX18Tc	ZL	C36 (C2)
pZL19	Gm cassette inserted into *PstI* site of *ctaD* in pEX18Tc	ZL	C36 (C4)
pZL22	120 bp PCR product of *cyoB* in pCR2.1 (standard for qPCR	ZL	C36 (C8)
pZL23	1.3 Kb PCR product of *cyoA* in pCR2.1	ZL	C36 (D4)
pZL27	635 bp PCR product of upstream region of *ctaC* in pCR2.1	ZL	C36 (F7)
pZL28	713 bp PCR product of downstream region of *ctaC* in pCR2.1	ZL	C36 (F8)
pZL29	635 bp *EcoRI, XbaI* fragment of *ctaC* upstream region and 713 bp *XbaI, HndIII* fragment of *ctaC* downstream region in *EcoRI, HndIII* pEX18Tc	ZL	C36 (F9)
pZL30	Gm cassette inserted into *PstI, SphI* site of *ctaD* in pEX18Tc	ZL	C36 (G3)
pZL31	Gm cassette inserted into *XbaI* site of *ctaC* (pZL29) in pEX18Tc	ZL	C36 (G4)
pZL32	Km cassette inserted into *XbaI* site of *ctaC* (pZL29) in pEX18Tc	ZL	C36 (G5)
pZL34	1.3 kb *BamHI, PstI* fragment of *cyoA* in pFAJ1708	ZL	C36 (H2)
pZL35	101 bp PCR product of *16sRNA* in pCR2.1	ZL	C37 (B6)
pZL36	348 bp PCR product of *cyoA* promoter region in pCR2.1	ZL	C37 (B7)
pZL37	5.0 kb PCR product of *cyo* operon in pCR2.1	ZL	C37 (C5)
pZL38	5.1 kb PCR product of *cyo* operon and additional 130 bp upstream sequence in pCR2.1	ZL	C37 (C6)
pZL39	348 bp *XbaI, KpnI* fragment of *cyoA* promoter region in pMP220	ZL	C37 (C7)
pZL40	5.0 kb *XbaI, KpnI* fragment of *cyo* operon in pFAJ1700	ZL	C37 (C8)
pZL41	5.1 kb *XbaI, KpnI* fragment of *cyo* operon in pFAJ1700	ZL	C37 (C9)

Table 5 cont.

pZL42	5.0 kb *XbaI, KpnI* fragment of *cyo* operon in pFAJ1708	ZL	C37 (C10)
pZL43	5.1 kb *XbaI, KpnI* fragment of *cyo* operon in pFAJ1708	ZL	C37 (D1)
pZL45	747 bp PCR product of 5' upstream region of *actS*	ZL	C37 (F3)
pZL46	650 bp PCR product of 3' downstream region of *actR*	ZL	C37 (F4)
pZL47	747 bp *EcoRI,XbaI* fragment of *actS* upstream region and 650 bp *XbaI, HndIII* fragment of *actR* downstream region in *EcoRI, HndIII* pEX18Tc	ZL	C37 (F5)
pZL48	Km inserted into *XbaI* site of *actSR* (pZL47) in pEX18Tc	ZL	C37 (F6)
pZL49	Gm inserted into *XbaI* site of *actSR* (pZL47) in pEX18Tc	ZL	C37 (F7)
pZL50	3.2 kb PCR product of *actSR* in pCR2.1	ZL	C37 (H10)
pZL51	3.2 kb *XbaI,BamHI* fragment of *actSR* in pFAJ1708	ZL	C37 (I1)
pZL54	3.2 kb *XbaI, BamHI* fragment of *actSR* in pJBC1	ZL	C37 (I7)
pZL61	1.0 kb PCR product of downstream of *actS* in pCR2.1	ZL	C37 (J8)
pZL62	650 bp *XbaI, HndIII actR* down fragment (pZL47) replaced with 1.0 kb *XbaI, HndIII actS* down fragment.	ZL	C37 (J9)
pZL63	Gm cassette inserted into *XbaI* site of *actS* (pZL62)	ZL	C37 (J10)
pZL64	Km cassette inserted into *XbaI* site of *actS* (pZL62)	ZL	C38 (A1)
pZL67	485 bp PCR product of the *cyo* promoter region in pCR2.1	ZL	C38 (A7)
pZL73	485 bp *XbaI, KpnI* fragment of *cyo* promoter region in pMP220	ZL	C38 (B4)
pZL74	*cyo* promoter region with deleted putative ActR sites 2 through 4 (ΔR2-4) in pMP220.	ZL	C38 (B5)
pZL75	*cyo* promoter region with deleted putative ActR sites 3 and 4 (ΔR3-4) in pMP220.	ZL	C38 (C3)
pZL76	*cyo* promoter region with deleted putative ActR sites #3 (ΔR3) in pMP220.	ZL	C38 (C4)
pZL77	*cyo* promoter region with deleted sigma70 region in pMP220.	ZL	C38 (C5)
pZL78	*cyo* promoter region with deleted putative ActR site #4 (ΔR4) in pMP220.	ZL	C38 (C6)

a. KT, Kristylea Ojeda (Thompson); SY, Sihui Yang; ZL, Zac Lunak

J. Quinol Oxidase Activity

Membranes were prepared and solubilized by modifying a protocol previously described (Ludwig, 1986). Cells were either grown in 500 ml Erlenmeyer flasks containing 250 ml of TY media or 120 ml serum vials containing 10 ml of TY media. Cells in exponential growth phase in 250 ml of TY medium were harvested and washed with 50 mM K-phosphate buffer (7.5 pH). The washed cells were suspended in 15 ml of buffer and broken by sonication. Crude extracts were obtained by centrifuging the sonicate for 15 min at 6,000 x g. The supernatant (crude extract) was removed and centrifuged at 75,000 x g for 2 hr 15 min. The pellet (membranes) was suspended in 3 ml of buffer. Triton-X was added to the membranes at a final concentration of 2% and allowed to incubate on a rotator for 2 hrs at 4 ^{o}C to solubilize the membranes. The solubilized membranes were kept at -80 ^{o}C until tested.

Measurements of quinol oxidase activity were essentially performed as previously described (Richter *et al*.,1994). The activity of solubilized membranes was determined by measuring the change of absorbance at 275 nm. The membranes were incubated in a 1 ml reaction containing 50 mM of K-phosphate buffer (pH 7.5) and 30 µM of antimycin A. The addition of anitmycin A, an fbc inhibitor, gave approximately 2-fold higher quinol oxidase activity. The substrate, 75 µM quinol (reduced according to Rieske,1967), was added to the mixture and the absorbance was immediately detected. The specific activity was then calculated by using the molar extinction coefficient of quinone (12,500) and the total protein (measured by BCA assay, Thermo Scientific) used in the reaction. To inhibit quinol oxidase activity, 1 mM potassium cyanide (KCN) was added to the reaction prior to the addition of quinol.

K. Western Blotting of BacS

1 ml of cells were pelleted and re-suspended in 100 µl of 1x SDS buffer. The sample was then boiled for 6 min and then stored at -20°C until testing. The extracts were separated by SDS-PAGE (Laemmli, 1970) with 15% acrylamide in the separating gel. The gel was either stained with Coomassie blue (Dzandu *et al*., 1984) to visualize protein amount in each sample or the contents were electroblotted onto nitrocellulose. The blot was incubated with rabbit polyclonal antiserum against BacS protein (Jahn *et al*., 2003), and bound antibodies were detected with goat alkaline-phosphatase-conjugated anti-rabbit immunoglobulin G (Sigma) that was developed with 5-bromo-4-chloro-3-indolyl phosphate.

L. Nodule Assays

Inoculation of bean seeds (*P. vulgaris*) with *R. etli* was performed as described previously (Box and Noel, 2011). Bean seeds were disinfected with 6% sodium hypochlorite solution for 15 min and then rinsed with deionized water 5 times. The washed seeds were then germinated in the dark on sterilized water-saturated filter paper for 48 hours at 30°C. The germinated seeds were then planted in plastic growth pouches containing 40 ml of nitrogen-free salts solution (0.6x RBN) inoculated with 0.5 ml of fully grown bacterial culture in TY liquid. Inoculated plants were then grown at 27°C with a cycle of 14 hour light and 10 hour darkness. The plants were watered with sterilized deionized water to maintain approximately 40 ml of liquid in each of the pouches.

GUS staining of nodules - For nodule staining, the wild type and the *cyo* mutant were tagged with beta-glucuronidase (GUS) by introducing pCAM111 via mating (Wilson *et al*., 1995; Duelli *et al.*, 2001). Slicing and staining of the nodules were performed as previously described (Box and Noel, 2011). The nodules were sliced longitudinally with a sterilized double-edged razor blade (approximately 15 slices per nodule). Slices were then put into an X-GlcA staining solution (X-GlcA at 0.5 mg/ml, 0.02% sodium azide, 1 mM potassium ferrocyanide, 1 mM potassium ferricyanide, Sarkosyl at 0.1g/ml, Triton X-100 at 0.1g/ml, 1 mM EDTA, and 50 mM sodium phosphate pH 7.0) for 15 minutes and then placed in storage solution (0.02% sodium azide, Sarkosyl at 0.1g/ml, Triton X-100 at 0.1g/ml, 1 mM EDTA, and 50 mM sodium phosphate pH 7.0) until viewing under a microscope.

GUS activity of cultures - Cells (1 ml of culture) were harvested and washed with 50 mM sodium phosphate buffer (pH 7.0). Washed cells were immediately frozen at -20^{o}C until testing. Cells were re-suspended in 500 µl of buffer and extracts were prepared by adding 7.5 µl of 0.1% SDS and 23.5 µl of chloroform. To determine GUS activity, the absorbance at 405 nm was followed of 1 ml reactions containing 800 µl of gus assay buffer (50 mM Na-Phos (pH 7.0), 50 mM DTT, 10 mM EDTA (pH8.0), and 4 mg PNPG) and 200 µl of cell extract. The activity (ΔAbs_{405}) was normalized to protein concentration (measured by the BCA assay, Thermo Scientific).

Nitrogenase Activity of Nodules - Nitrogenase activity of nodules was measured as acetylene reduction. Shoots were removed, and intact roots were placed in 60 ml serum vials and capped. 3 ml of acetylene gas was added to the serum vials and followed by a one hour incubation at room temperature. After one hour, 0.3 ml of the gas phase

was injected into a gas chromotatraph using a Porapak N column (Noel *et al*., 1982). The ratio of ethylene:acetylene (area of ethylene peak/area of acetylene peak) was normalized to the collective weight of the nodules (g) on the root to give an overall specific activity.

M. Prediction of regulatory elements in 5' promoter sequences

The genomes of *R. etli* CFN42, *S. meliloti* 1021, and *R. leguminosarum* bv *viciae* 3841 have been determined (Gonzalez *et al*., 2006; Finan *et al*., 2001; Young *et al*., 2006). Putative promoters in the 5' upstream sequence were predicted using Softberry and PePPER software (Soloyvev & Salomov, 2011; de Jong *et al*., 2012). To identify possible ActR DNA binding sites, various parts of the promoter region were aligned with known RegR DNA binding sites in *B. japonicum* (Lindemann *et al*., 2007; Torres *et al*., 2014) using ClustalW2 software.

REFERENCES

Alexeyev, M.F. (1995). Three kanamycin resistance gene cassettes with different polylinkers. *Biotechniques* **18**, 52-56.

Alexeyev, M.F., Shokolenko, I.N. & Croughan, T.P. (1995). Improved antibiotic-resistance gene cassettes and omega elements for *Escherichia coli* vector construction and in vitro deletion/insertion mutagenesis. *Gene* **160**, 63-67.

Altschul, S.F., Gish, W., Miller, W., Myers, E.W. & Lipman DJ. (1990). Basic Local Alignment Search Tool. *J Mol Bio* **215**, 403-410.

Arai, H. (2011). Regulation and function of versatile aerobic and anaerobic respiratory metabolism in *Pseudomonas aeruginosa. Front Microbiol* **2**, 103.

Arai, H., Kawakami, T., Osamura, T., Hirai, T., Sakai, Y. & Ishii, M. (2014). Enzymatic characterization *in vivo* function of five terminal oxidases in *Pseudomonas aeruginosa*. *J Bacteriol* **196**, 4206-4215.

Balleza, E., López-Bojorquez, L.N., Martínez-Antonio, A., Resendis-Antonio, O., Lozada-Chávez, I., Balderas-Martínez, Y.I., Encarnación, S. & Collado-Vides, J. (2009). Regulation by transcription factors in bacteria: beyond description. *FEMS Microbiol Rev* **33**, 133-151.

Bauer, E., Kaspar, T., Fischer H.M. & Hennecke, H. (1998). Expression of the *fixR-nifA* operon in *Bradyrhizobium japonicum* depends on a new response regulator, RegR. *J Bacteriol* **180**, 3853-3863.

Bekker, M., Kramer, G., Hartog, A.F., Wagner, M.J., de Koster, C.G., Hellingwerf, K.J. & de Mattos, M.J. (2007). Changes in the redox state and composition of the quinone pool in *Escherichia coli* during aerobic batch-culture growth. *Microbiology* **153**, 1974-1980.

Bobik, C., Meilhoc, E. & Batut, J. (2006). FixJ: a Major Regulator of the Oxygen Limitation Response and Late Symbiotic Functions of *Sinorhizobium meliloti*. *J Bacteriol* **188**, 4890-4902.

Bott, M., Bolliger, M. & Hennecke, H. (1990) Genetic analysis of the cytochrome c-aa3 branch of the *Bradyrhizobium japonicum* respiratory chain. *Mol Microbiol* **4**, 2147-2157.

Bouhenni, R.A., Vora, G.J., Biffinger, J.C., Shirodkar, S. *et al*. (2010) The role of *Shewanella oneidensis* MR-1 outer surface membrane surface structures in extracellular electron transfer. *Electroanalysis* **22**, 856-864.

Box, J. & Noel, K.D. (2011). Controlling the expression of rhizobial genes during nodule development with elements and aniInducer of the *lac* operon. *Mol Plant Microbe Interact* **24**, 478-486.

Bueno, E., Mesa, S., Bedmar, E.J., Richardson, D.J. & Delgado, M.J. (2012). Bacterial adaptation from oxic to microoxic and anoxic conditions: redox control. *Antioxid Redox Signal* **16**, 819-852.

Bundschuh, F.A., Hoffmeier, K. & Ludwig, B. (2008). Two variants of the assembly factor Surf1 target specific terminal oxidases in *Paracoccus denitrificans*. *Biochim Biophys Acta* **1777,** 1336-1343.

Chao, T.C., Buhrmester, J., Hansmeier, N., Pühler, A. & Weidner, S. (2005). Role of the regulatory gene *rirA* in the transcriptional response of *Sinorhizobium meliloti* to iron limitation. *App Environ Microbiol* **71**, 5969-5982.

Crofts, A.R., Hong, S, Ugulava, N., Barquera, B., Gennis, R., Guergova-Kuras, M.A. & Berry E.A. (1999). Pathways for proton release during ubihydroquinone oxidation by the bc(1) complex. *Proc Natl Acad Sci USA* **96**, 10021-10026.

D'Mello, R., Hill, S. & Poole, R.K. (1995). The oxygen affinity of cytochrome bo' in *Escherichia coli* determined by the deoxygenation of oxyleghemoglobin and oxymyoglobin: K_m values for oxygen are in the submicromolar range. *J Bacteriol* **177**, 867-870.

D'Mello, R., Hill, S. & Poole, R.K. **(1996).** The cytochrome bd oxidase in *Escherichia coli* has extremely high oxygen affinity and two oxygen-binding hemes: implications for regulation of activity in vivo by oxygen inhibitor. *Microbiology* **142**, 755-763.

de Jong, A., Pietersma, H., Cordes, M., Kuipers, O.P. & Kok, J. (2012). PePPER: a webserver for prediction of prokaryotic elements and regulons. *BMC Genomics* **13**, 299.

de Lucena, **D.K.C., Pühler, A. & Weidner,S. (2010).** The role of sigma factor RpoH1 in the pH stress response of *Sinorhizobium meliloti*. *BMC Microbiol* **10**, 265.

Delgado, M.J., Bedmar, E.J. & Downie, J.A. (1998). Genes involved in the formation and assembly of rhizobial cytochromes and their role in symbiotic nitrogen fixation. *Adv Microb Physiol* **40**, 193-231.

Dombrecht, B., Vanderleyden, J. & Michiels, J. (2001). Stable RK2-derived cloning vectors for the analysis of rhizobial cytochromes and their role in symbiotic nitrogen fixation. *Mol Plant Microbe Interact* **14,** 426-430.

Duelli D.M., Tobin A., Box J.M., Kolli V.S.K., Carlson R.W. & Noel K.D. (2001). Genetic locus required for antigenic determination of *Rhizobium etli* CE3 polysaccharide. *J Bacteriol* **183,** 6054-6064.

Dzandu, J.K., Deh, M.E., Barratt, D.L. & Wise, G.E. (1984). Detection of erythrocyte membrane proteins, sialoglycoproteins, and lipids in the same polyacrylamide gel using a double-staining technique. *Proc Natl Acad Sci USA* **81**, 1733-1737.

Elsen, S., Swem, L.R., Swem, D.L. & Bauer C.E. (2004). RegB/RegA, a highly conserved redox-responding global two-component regulatory system. *Microbiol Mol Biol Rev* **68**, 263-279.

Emmerich, R., Hennecke, H. & Fischer, H.M. (2000). Evidence for a functional similarity between the two-component regulatory system RegSR, ActSR, and RegBA (PrrBA) in α-Proteobacteria. *Arch Microbiol* **174**, 307-313.

Emmerich, R., Strehler, P., Hennecke, H. & Fischer, H.M. (2000). An imperfect inverted repeat is critical for DNA binding of the response regulator RegR of *Bradyrhizobium japonicum*. *Nucleic Acids Res* **28**, 4166-4171.

Fetter, J.R., Qian, J., Shapleigh, J., Thomas, J.W., García-Horsman, A., Schmidt, E., Hosler, J., Babcock, G.T., Gennis, R.B. & Ferguson-Miller, S.. (1995). Possible proton relays in cytochrome *c* oxidase. *Proc Natl Acad Sci USA* **92,** 1604-1608.

Finan, T.M., Kunkel, B., De Vos G.F. & Signer, E.R. (1986). Second symbiotic megaplasmid in *Rhizobium meliloti* carrying exopolysaccharide and thiamine synthesis genes. *J Bacteriol* **167**, 66-72.

Gao, T. & O'Brian, M.R. (2005). Iron-dependent cytochrome c_1 expression is mediated by the status of heme in *Bradyrhizobium japonicum. J Bacteriol* **187**, 5084-5089.

García-Horsman, J.A., Barquera, B., Rumbley, J., Ma, J. & Gennis R.B. (1994). The superfamily of heme-copper respiratory oxidases. *J Bacteriol* **176**, 5587-5600.

Girard, L., Brom, S., Dávalos, A., López, O., Soberón, M. & Romero, D. **(2000).** Differential regulation of fixN-reiterated genes in Rhizobium etli by a novel fixL-fixK cascade. *Mol Plant Microbe Interact* **13**, 1283-1292.

González, V., Santamaría, R.I., Bustos, P., Hernández-González, I., Medrano-Soto, A., Moreno-Hagelsieb, G., Janga, S.C., Ramírez, M.A., Jiménez-Jacinto, V., Collado-Vides, J. & Dávila, G. (2006). The partitioned *Rhizobium etli* genome: genetic and metabolic redundancy in seven interacting replicons. *Proc Natl Acad Sci USA* **103**, 3834-3839.

Granados-Baeza, M.J., Gómez-Hernández, N., Mora, Y., Delgado, M.J., Romero, D. & Girard, L. (2007). Novel reiterated Fnr-type proteins control the production of the symbiotic terminal oxidase cbb3 in *Rhizobium etli* CFN42. *Mol Plant Microbe Interact* **20**, 1241-1249.

Guergova-Kuras, M., Kuras, R., Ugulava, N., Hadad, I. & Crofts, R. (2000). Specific mutagenesis of the Rieske iron-sulfur protein in *Rhodobacter sphaeroides* shows that both the thermodynamic gradient and pK of the oxidized form determine the rate of quinol oxidation by the bc(1) complex. *Biochemistry* **39**, 7436-7444.

Hellweg, C., Pühler, A. & Weidner, S. (2009). The time course of the transcriptomic response of *Sinorhizobium meliloti* 1021 following a shift to acidic pH. *BMC Microbiol* **9**, 37.

Hoang, T.T., Karkahoff-Schweizer, R.R., Kutchma, A.J. & Schweizer, H.P. (1998). A broad-host-range Flp-FRT recombination system for site-specific excision of chromosomally-located DNA sequences: application for isolation of unmarked *Pseudomonas aeruginosa* mutants. *Gene* **212**, 77-89.

Hosler, J.P., Fetter, J., Tecklenberg, M.M.J., Espe, M., Lerma, C. & Ferguson-Miller S. (1992). Cytochrome aa_3 of *Rhodobacter sphaeroides* as a model for mitochondrial cytochrome *c* oxidase: purification, kinetics, proton pumping and spectral analysis. *J Biol Chem* **267**, 24264-24272.

Jahn, O., Davila, G., Romero, D. & Noel, K.D. **(2003).** BacS: An abundant bacteroid protein in *Rhizobium etli* whose expression ex planta requires *nifA*. *Mol Plant Microbe Interact* **16**, 65-73.

Kawakami, T., Kuroki, M., Ishii, M., Igarashi, Y. & Arai, H. (2010). Differential expression of multiple terminal oxidases for aerobic respiration in *Pseudomonas aeruginosa*. *Environ Microbiol* **12**, 1399-1412.

Kiley, P.J. & Beinert, H. (1999). Oxygen sensing by the global regulator, FNR: the role of the iron sulfur cluster. *FEMS Microbiol Rev* **22,** 341-352.

Kitada, M. & Krulwich, T.A. (1984). Purification and characterization of cytochrome oxidase from alkalophilic *Bacillus firmus* RAB. *J Bacteriol* **158**, 963-966.

Körner, H., Sofia, H.J. & Zumft, W.J. (2003). Phylogeny of the bacterial superfamily Crp-Fnr transcription regulators: exploiting the metabolic spectrum by controlling alternative gene programs. *FEMS Microbiol Rev* **27**, 559-592.

Laemmli, U.K. **(1970).** Cleavage of structural proteins during the assembly of the bacteriophage T4. *Nature* **277**, 680-685

Landeta, C., Dávalos, A., Cevallos, M.Á., Geiger, O., Brom, S. C. & Romero, D. **(2011).** Plasmids with a chromosome-like role in rhizobia. *J. Bacteriol* **193**, 1317-1326.

Lhee, S., Kolling, D.R., Nair, S.K., Dikanov, S.A. & Crofts, A.R. (2010). Modifications of protein environment of the (2Fe-S) cluster of the bc_1 complex: effects on the biophysical properties of the rieske iron-sulfur protein and on the kinetics of the complex. *J Biol Chem* **285**, 9233-9248.

Lindemann A., Moser A., Pessi, G., Hauser, F., Friberg, M., Hennecke, H. & Fischer, H.M. (2007). New target genes controlled by the *Bradyrhizobium japonicum* two-component regulatory system RegSR. *J Bacteriol* **189**, 8928-8943.

Lopez, O., Morera, C., Miranda-Rios, J., Girard, L., Romero, D. & Soberón, M. **(2001).** Regulation of gene expression in response to oxygen in *Rhizobium etli*: role of FnrN in *fixNOQP* expression and in symbiotic nitrogen fixation. *J Bacteriol* **183**, 6999-7006.

López-Leal, G., Tabche, M.L., Castillo-Ramírez, S., Mendoza-Vargas, A., Ramírez-Romero, M.A. & Dávila, G. (2014). RNA-seq analysis of the multipartite genome of *Rhizobium etli* CE3 shows different replicon contributions under heat and saline shock. *BMC Genomics* **15,** 770.

Ludwig, B. **(1986).** Cytochrome *c* oxidase from *Paracoccus denitrificans*. *Methods Enzymol* **126**, 153-159.

Michiels, J., Moris, M., Dombrecht, B., Verreth, C. & Vanderyleyden, J. **(1998).** Differential regulation of *Rhizobium etli rpoN2* gene expression during symbiosis and Free-living growth. *J Bacteriol* **180**, 3620-3628.

Morales, G., Ugidos, A. & Rojo, F. (2006) Inactivation of the *Pseudomonas putida* cytochrome O ubiquinol oxidase leads to a significant change in the transcriptome and to increased expression of the CIO and *cbb3-1* terminal oxidases. *Environ Microbiol* **8**, 1764-1774.

Moris, M., Dombrecht, B., Xi, C., Vanderleyden, J. & Michiels, J. **(2004).** Regulatory role of *Rhizobium etli* CNPAF512 *fnrN* during symbiosis. *Appl Environ Microbiol* **70**, 1286-1297.

Morris, R.L. & Schmidt, T.M. (2013). Shallow breathing: bacterial life at low O_2. *Nat Rev Microbiol* **11**, 205-212.

Noel, K.D., Carneol, M. & Brill, W.J. (1982). Nodule protein synthesis and nitrogenase activity of soybeans exposed to fixed nitrogen. *Plant Physiol* **70**, 1236-1241.

Nyström, T. (1994). The glucose starvation stimulon in *Escherichia coli*: induced and repressed synthesis of enzymes of central metabolic pathways and the role of acetyl phosphate in gene expression and starvation survival. *Mol Microbiol* **12**, 833-843.

Nyström, T., Larsson, C. & Gustafsson, L. (1996). Bacterial defense against aging: role of *Escherichia coli* ArcA regulator of gene expression, readjusted energy flux, and survival during stasis. *EMBO J* **15**, 3219-3228.

O'Hara, G.W., Goss, T.J., Dilworth, M.J. & Glenn, A.R. (1989). Maintenance of intracellular pH and acid tolerance in *Rhizobium meliloti*. *J Bacteriol* **55**, 1870-1876.

Otten, M.F., Rijnders, W.N., Bedaux, J.J., Westerhoff, H.V., Krab, K. & Van Spanning, R.J. (1999). The reduction state of the Q-pool regulates the electron flux through the branched respiratory network of *Paracoccus denitrificans*. *Eur J Biochem* **261**, 767-774.

Poole, R.K. & Cook, G.M. **(2000).** Redundancy of aerobic respiratory chains in bacteria? Routes, reasons and regulation. *Adv Microb Physiol* **43**, 167-224.

Puustinen, A., Finel, M., Virkki, M. & Wikström. (1989). Cytochrome *o* (*bo*) is a proton pump in *Paracoccus denitrificans* and *Escherichia coli*. *FEBS Lett* **249**, 163-167.

Qian, Y. & Tabita, F.R. (1996). A global signal transduction system regulates aerobic and anaerobic CO_2 fixation in *Rhodobacter sphaeroides*. *J Bacteriol* **178**, 12-18.

Ramírez-Romero, M.A., Masulis, I., Cevallos, M.A., González V. & Dávila G. (2006). The *Rhizobium etli* σ^{70} (SigA) factor recognizes a lax consensus promoter. *Nucleic Acid Res* **34**, 1470-1480.

Richhardt J., **Luchterhand B., Bringer S., Büchs J. & Bott M. (2013).** Evidence for a key role of cytochrome bo_3 oxidase in respiratory energy metabolism of *Gluconobacter oxydans*. *J Bacteriol* **195**, 4210-4220.

Richter, O.M.H., Tao, J., Turba, A. & Ludwig, B. (1994). A cytochrome *ba3* functions as a quinol oxidase in *Paracoccus denitrificans. J Biol Chem* **269**, 23079-23086.

Rieske, J.S. **(1967).** Preparation and properties of reduced coenzyme Q-cytochrome c reductase (complex III of the respiratory chain). *Methods Enzymol* **10**, 239-245.

Rudolph, G., Hennecke, H. & Fischer, H.M. (2006). Beyond the Fur paradigm: iron-controlled gene expression in rhizobia. *FEMS Microbiol Rev* **30**, 631-648.

Sambrook, J., Fritsch, E.F. & Maniatis, T. (1989). *Molecular cloning: a laboratory manual*, 2nd edn. Cold Spring Harbor, N.Y: Cold Spring Harbor Laboratory.

Schweizer, H.P. (1993). Small broad-host-range gentamycin resistance gene cassettes for site-specific insertion and deletion mutagenesis. *Biotechniques* **15**, 831-833.

Soloyvev, V. & Salamov, A. (2011). Automatic Annotation of Microbial Genomes and Metagenomic Sequences. In Metagenomics and its Applications in Agriculture, Biomedicine and Environmental Studies (Ed. R.W. Li), Nova Science Publishers, p. 61-78.

Surpin, M.A., Lübben, M. & Maier, R.J. (1996). The *Bradyrhizobium japonicum coxWXYZ* gene cluster encodes a *bb3*-type ubiquinol oxidase. *Gene* **183**, 201-206.

Surpin, M.A. & Maier, R.J. (1998). Roles of the *Bradyrhizobium japonicum* terminal oxidase complexes in microaerobic H_2-dependent growth. *Biochim Biophys Acta* 1364, 37-45.

Surpin, M.A. & Maier, R.J. (1999). Symbiotic deficiencies associated with a *coxWXYZ* mutant of *Bradyrhizobium japonicum*. *Appl Environ Microbiol* **65,** 339-341.

Spaink, H.P., Okker, R.J.H., Wijffelman, C.A., Pees, E. & Lugtenberg, B.J.J. (1987). Promoters in the nodulation region of *Rhizobium leguminosarum* Sym plasmid pRL1J1. *Plant Mol Biol* **9**, 27-39.

Thomas J.W., Puustinen, A., Alben, J.O., Gennis, R.B. & Wikström, M. (1993). Substitution of asparagine for aspartate-135 in subunit I of the cytochrome bo ubiquinol oxidase of E*scherichia coli* eliminates proton-pumping activity. *Biochemistry* **32**, 10923-10928.

Thöny-Meyer, L., Stax, D. & Hennecke, H. 1989. An unusual gene cluster for the cytochrome *bc1* complex in *Bradyrhizobium japonicum* and its requirement for effective root nodule symbiosis. *Cell* **57**, 683-697.

Tiwari, R.P., Reeve W.G., Dilworth, M.J. & Glenn, A.R. (1996). Acid tolerance in *Rhizobium meliloti* strain WSM419 involves a two-component sensor-regulator system. *Microbiology* **142**, 1693-1704.

Torres M.J., Argandoña M., Vargas C., Bedmar E.J., Fischer H.M., Mesa S. & Delgado M.J. (2014). The global response regulator RegR controls expression of denitrification genes in *Bradyrhizobium japonicum*. *PLoS One* **9**, 6.

Trzebiatowski, J.R., Ragatz, D.M. & de Bruijn, F.J. (2001). Isolation and regulation of *Sinorhizobium meliloti* 1021 loci induced by oxygen limitation. *Appl Environ Microbiol* **67**, 3728-3731.

Tseng, C.P., Albrecht, J. & Gunsalus, R.P. (1996). Effect of microaerophilic cell growth conditions on expression of the aerobic (*cyoABCDE* and *cydAB*) and anaerobic (*narGHJI*, *frdABCD*, and *dmsABC*) respiratory pathway genes in *Escherichia coli*. *J Bacteriol* **178**, 1094.

Vercruysse, M., Fauvart, M., Beullens, S., Braeken, K., Cloots, L., Engelen, K., Marchal, K. & Michiels, J. (2011). A comparative transcriptome analysis of *Rhizobium etli* bacteroids: specific gene expression during symbiotic nongrowth. *Mol Plant Microbe Interact* **24**, 1553-1561.

Verkhovskaya, M., Verkhovsky, M. & Wikström. (1992). pH dependence of proton translocation by E*scherichia coli*. *J Biol Chem* **267**, 14559-14562.

Wilks, J.C. & Slonczewski, J.L. (2007). pH of the cytoplasm and periplasm of *Escherichia coli*: rapid measurement by green fluorescent protein fluorimetry. *J Bacteriol* **189**, 5601-5607.

Wilson, K.J., Sessitsch, A., **Corbo, J.C., Giller, K.E., Akkermans, A.D.L. & Jefferson, R.A. (1995).** beta-Glucuronidase (GUS) transposons for ecological and genetic studies of rhizobia and other Gram-negative bacteria. *Microbiology* 141, 1691-1705.

Wu, G, Delgado, M.J., Vargas, C., Davies, A.E., Poole, R.K. & Downie, J.A. (1996). The cytochrome bc1 complex but not CycM is necessary for symbiotic nitrogen fixation by Rhizobium leguminosarum. *Microbiology* **142**, 3381-3388.

Wu, J. & Bauer, C.E. (2008). RegB/RegA, a global redox-responding two-component system. *Adv Exp Med Biol* **631,** 131-148.

Wu, J. & Bauer, C.E. (2010). RegB kinase activity is controlled in part by monitoring the ratio of oxidized to reduced ubiquinones in the ubiquinone pool. *mBio* **1**, e00272-10.

Wu, J., Cheng, Z., Reddie, K., Carroll, K., Hammad, L.A., Karty, J.A. & Bauer C.E. (2013). RegB kinase activity is repressed by oxidative formation of cysteine sulfenic acid. *J Biol Chem* **288**, 4755-4762.

Zhou, F., Yin, Y., Su, T., Yu, L. & Yu C.A. (2012). Oxygen dependent electron transfer in the cytochrome bc(1) complex. *Biochimica et Biophysics Acta* **1817**, 2103-2109.

Zickermann, I., Tautu, O.S., Link, T.A., Korn, M., Ludwig, B. & Richter, O.M. (1997). Expression studies on the ba_3 quinol oxidase from *Paracoccus denitrificans*: A bb_3 variant is inactive. *Eur J Biochem* **246**, 618-624.